Structural and functional relationship between the basal forebrain and the medial prefrontal cortex

Thesis of PhD

Biology graduate program

Dr. Anna Erdei, D. Sc.

Neurosciences and human biology

Supervisor:

Dr. László Détári, D.Sc.

Eötvös Loránd University,

Pázmány P. Stny. 1/C

Budapest, 1117

TABLE OF CONTENT

Abbreviations

ACh – acetylcholine

AChE - acetylcholine esterase

AD – Alzheimer disease

ADHD - attention-deficit hyperactivity disorder

BDA – biotynilated dextran amine

BF – basal forebrain

BFC – basal forebrain cholinergic system

BST – bed nucleus of stria terminalis

CB - calbindin

CBP – calcium binding protein

ChAT – choline acetyltransferase

CoA – acetyl coenzyme A

CR - calretinin

ECoG - electrocorticogram

EEG – electroencephalogram

GABA – γ – amino-butyric acid

GAD – glutamic acid decarboxylase

GP – globus pallidus

HDB – horizontal diagonal band

LDT - nucleus laterodorsalis tegmentalis

LVFA – low voltage fast activity

mAChR – muscarinic acetyl choline receptor

MBN - magnocellular nucleus basalis

MD - mediodorsal thalamic nucleus

mPFC – medial prefrontal cortex

MS – medial septum

nAChR - nicotinergic acetyl choline receptor

NPY – neuropeptide-Y

OF – orbito frontal cortex

PAG - phosphate-activated glutaminase

PFC – prefrontal cortex

PHA-L - Phaseolus Vulgaris-leucoagglutinin

PPT - nucleus pedunculopontinus tegmentalis

PV - parvalbumin

RE – nucleus reuniens

SI – substantia innominata

SPT - nucleus subpeduncularis tegmentalis

SS – somatostatin

SWA – slow wave activity

TH – tyrosine hydroxylase

VDB – ventral diagonal band

VGlut – vesicular glutamate transporter

VP – ventral pallidum

VTA – ventral tegmental area

1 Introduction

The basal forebrain (BF) has been intensively studied for decades in relation to many physiological processes such as the sleep-wake cycle regulation, attention, learning and memory consolidation. It also has a considerable role in the progress of degenerative diseases, such as Alzheimer's disease (AD), Huntington disease, and Parkinson disease. For developing possible treatments for these and many other neurological disorders it is crucial to understand the exact function and structure of the circuitry that involves the basal forebrain, the neocortex and other connected areas.

The BF sends abundant innervations to many parts of the brain, including the neocortex and receives numerous inputs from other brain areas; however the prefrontal cortex (PFC) is the only cortical area that sends direct projections back to the BF from higher cortical regions. The prefrontal cortex is associated with higher cognitive functions, such as attention, planning, working memory and other phenomena like behavioral inhibition, cognitive flexibility, and goal directed control. Consequently, the prefrontal cortical input to the BF represents an extraordinary and influential link that has not been extensively studied yet.

Hence, this thesis is aimed to examine the functional and anatomical connection between PFC and the BF using electrophysiological and anatomical methods. In the followings, I would like to provide a detailed description about what is already known about the anatomy of the basal forebrain and the prefrontal cortical areas in terms of their neuronal subpopulations, afferent and efferent connections, their possible interconnection, and then I will overview their functional relationship.

1.1 Neurons in the basal forebrain

1.1.1 Cholinergic neurons

The BF is located at the medial and ventral part of the cerebral hemispheres, below the anterior commissure and lateral to the hypothalamus. In the human brain, the BF area contains a group of diverse structures, including the diagonal band of Broca, the basal

nucleus of Meynert, the ventral striatum, and also cell groups underneath the globus pallidus that bridge the centromedial amygdala to the bed nucleus of the stria terminalis (Prensa et al., 2003;Zaborszky et al., 2008)(Fig 1A). These areas are also identified in rats and are well characterized by various cell types that differ in transmitter content, morphology, and projection pattern (Woolf and Butcher, 1985; Zaborszky et al., 1997; Zaborszky et al., 1999) (Fig 1B).

Among the different neuronal populations, the cholinergic corticopetal projection neurons have received particular emphasis due to their prominent loss in Alzheimer's and related neurodegenerative diseases (Hall et al., 2008; Perry, 1993; Tsuboi and Dickson, 2005). However, cholinergic projection neurons represent only about 20% of the total cell population in the BF areas.

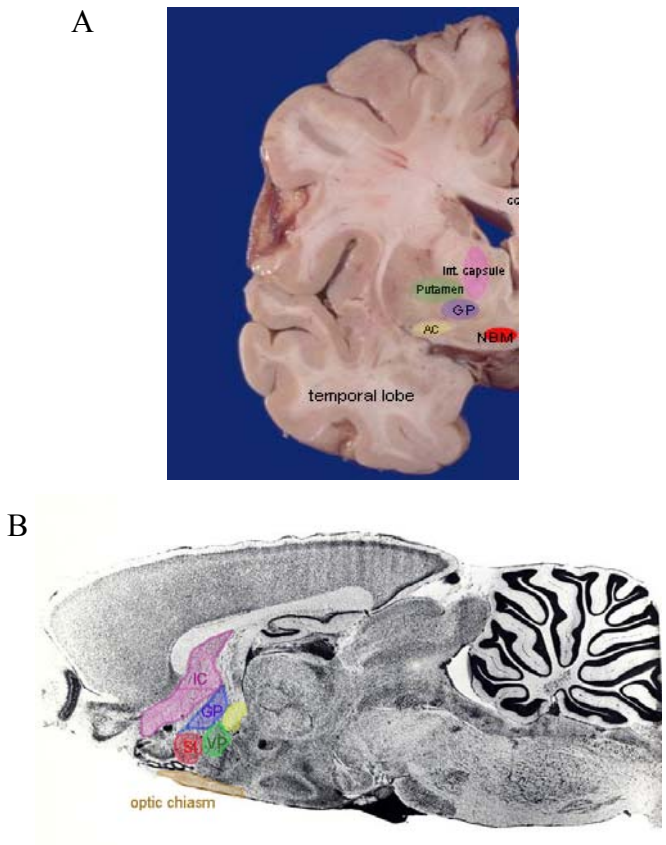

Figure 1. Location of the basal forebrain in the human (A) and rat (B) brain on coronal and sagittal sections. A) The nucleus basalis of Meynert (NBM) is marked with red and located on the medial ventral part of the human brain. B) Sagittal section of the rat brain. Note that the size of the area of the BF compared to the whole brain is relatively small in humans (modified from Paxinos and Watson (Paxinos et al., 1980).

1.1.1.1 Acetylcholine as a neurotransmitter

Acetylcholine (ACh) is extensively distributed in the central nervous system. Neurons that use acetylcholine as a neurotransmitter in the BF were in the center of attention because of their role in cortical activation, sleep-wake cycle, cognitive performances and memory processes.

Synthesis of acetylcholine (ACh) is facilitated by choline acetyltransferase (ChAT). This enzyme combines choline with acetate derived from acetyl coenzyme A (CoA). Choline is taken up into cholinergic axon terminals by a high affinity transport process (sodium-choline co transport) that is indirectly coupled to the energy stored in the strong Na gradient by the Na/K pump ATPase (Hassel et al., 2008;Rylett and Schmidt, 1993;Tucek, 1990;Tucek, 1985). Inactivation of ACh in the synaptic cleft occurs by hydrolysis, which is greatly accelerated by cholinesterase enzymes, mainly by acetyl cholinesterase (AChE) that is presented in high concentration in cholinergic synapses. It catalyzes a chemical reaction that forms two products (choline and acetate) that are essentially inactive. Diffusion of ACh from the synaptic region plays a minor role because AChE is highly active.

ACh has diverse actions on a number of cell types mediated by two major classes of receptors categorized by the affinity to their agonists: nicotine and muscarine.

Nicotinic receptors (nAChR) are ligand-gated ion channels with the strongest affinity for nicotine as a ligand. They are composed of five symmetrically arranged protein subunits. The subunit composition is highly variable across different tissues. These subunits span across the membrane and consist of approximately 20 amino acids. Outside of the brain, nACh receptors are found at the edges of the neuromuscular junction on the postsynaptic side, and are activated by acetylcholine release across the synapse. The diffusion of Na^+ across the receptor causes depolarization in the neurons leading to increased firing rate and potentially muscular contraction.

Muscarinic acetylcholine (mAChR) receptors are part of the 7TM (seven transmembrane) G-protein coupled receptor family. G-protein-coupled receptors are present in a large number in connection with various neurotransmitters, hormones, and

other substances (Brann et al., 1993;Peralta et al., 1987;Venter, 1983). In G-protein-coupled receptors, the signaling molecule binds to a receptor which has seven transmembrane regions. In the case of the mAChR, the ligand is ACh and its binding initiates the signalization cascade within the cell. This cascade reaction takes more time to complete than the opening of the voltage gated ion channel (nAChR), which means that mAChR represents a slow type of signalization.

By the use of selective radioactively-labeled agonist and antagonist substances, five subtypes of muscarinic receptors have been described, named M_1-M_5 (Caulfield and Birdsall, 1998) G proteins contain an alpha-subunit, which is critical to the functioning of receptors. There are four different forms of G-proteins, G_s, G_i, G_q and $G_{12/13}$ (Simon et al., 1991). Muscarinic receptors differ in the G protein to which they are bound to, G proteins are classified according to their susceptibility to cholera toxin (CTX) and pertussis toxin (PTX). G_s and some subtypes of G_i ($G_{\alpha t}$ and $G_{\alpha g}$) are susceptible to CTX (Dell'Acqua et al., 1993). Based on their effects G-proteins can be classified as stimulative or inhibitory regulative G-proteins. In the simulative regulative G-proteins the α-subunit of the receptor would stimulate the activity of an enzyme or other intracellular metabolism (through for example cAMP activation). On the contrary, the inhibitory regulative G-protein receptor type would inhibit the activity of the cell (Chen-Izu et al., 2000).

1.1.1.2 Localization of cholinergic neurons in the rat brain

Based on choline acetyltransferase (ChAT) immunostaining, cholinergic neurons were found throughout the rat brain in the following areas: (1) the striatum, (2) the basal forebrain, (3) the pontine tegmentum, including the nucleus laterodorsalis tegmentalis (LDT), the nucleus subpeduncularis tegmentalis (SPT) and nucleus pedunculopontinus tegmentalis (PPT), and (4) the cranial nerve motor nuclei (Armstrong et al. 1983; Mesulam et al. 1984a) (Fig. 2). However, in the following, I will focus on the basal forebrain cholinergic system that is present in the area of interest during my experiments. Further I would like to focus on the neuroanatomical distribution of the cholinergic neurons in the BF.

Cholinergic (Ch) neurons form a relatively continuous chain of somas from the rostral to the caudal part of the rat basal forebrain defining the cholinergic basal forebrain

areas (Zaborszky et al., 1999;Zaborszky, 1989). Cholinergic neurons in the BF provide the major extrinsic source of Ach to the cerebral cortex (Pang et al., 1998;Rasmusson et al., 1994;Zaborszky et al., 1999). Maximal release of ACh occurs in the cortex in association with cortical activation during states of waking and paradoxical sleep, suggesting that this projection is critically involved in the maintenance of cortical activation and in the process of normal wakefulness. Applying a 3-dimensional-sampling design, Vogels et al (1990) estimated the total number of neurons within the human Ch complex to be 1.2 million in each hemisphere (Vogels et al., 1990). In contrast, the number of cholinergic neurons in one hemisphere of the rat brain has been estimated to be around 22,000-26,000 (Gritti et al., 2006;Miettinen et al., 2002).

Mesulam (1983) proposed the Ch nomenclature to designate different groups of cholinergic neurons in rat brain (Mesulam et al., 1983). The constituent neurons of the BF-Ch complex can be subdivided into six regions: the Ch1 and Ch2 regions, including the medial septum (MS) and ventral diagonal band (VDB) complex, respectively; the Ch3 region, which is the lateral portion of the horizontal limb nucleus of the diagonal band (HDB); the Ch4 region, that includes the nucleus basalis; Ch5-Ch6 sectors are located mostly within the pedunculopontine nucleus of the pontomesencephalic reticular formation (Ch5) and within the laterodorsal tegmental gray of the periventricular area (Ch6) (Mesulam et al., 1983). The Ch4 region, also termed the nucleus basalis of Meynert in humans, can be further subdivided into six sectors that occupy its anteromedial, anterolateral, anterointermediate, intermediodorsal, intermedioventral and posterior regions (Varga et al., 2003;Wu et al., 2000).

The middle territories of the rat cholinergic basal forebrain include the HDB nucleus and magnocellular preoptic nucleus. These cholinergic neurons innervate the olfactory bulb, the amygdala and the cingulate, retrosplenial, entorhinal, perirhinal, insular cortices, as well as parts of the frontal cortex. Cholinergic terminals are especially dense in the basolateral and lateral amygdala. These medial cholinergic pathways exhibit considerable plasticity following axotomy, even in the adult organism, that can be modified by trophic factors (Farris et al., 1993;Farris et al., 1995). It has been reported that removal of the olfactory bulbs produces spatial memory deficits and disruption of cholinergic indexes in the HDB and magnocellular preoptic nuclei (Bobkova et al., 2001).

The caudal part of the cholinergic basal forebrain pathway is composed of the basal nucleus and substantia innominata (SI). These structures contain neurons that project cholinergic axons to all of the neocortex: frontal, parietal, temporal, and visual. Two exceptions to this rule in rat brain are the medial part of the visual cortex that receives input from the VDB nucleus (Carey and Rieck, 1987), similar to that of the retrosplenial cortex, which lies adjacent, and the limbic regions of frontal cortex that receive afferents from the HDB and magnocellular preoptic nuclei (Fig 2).

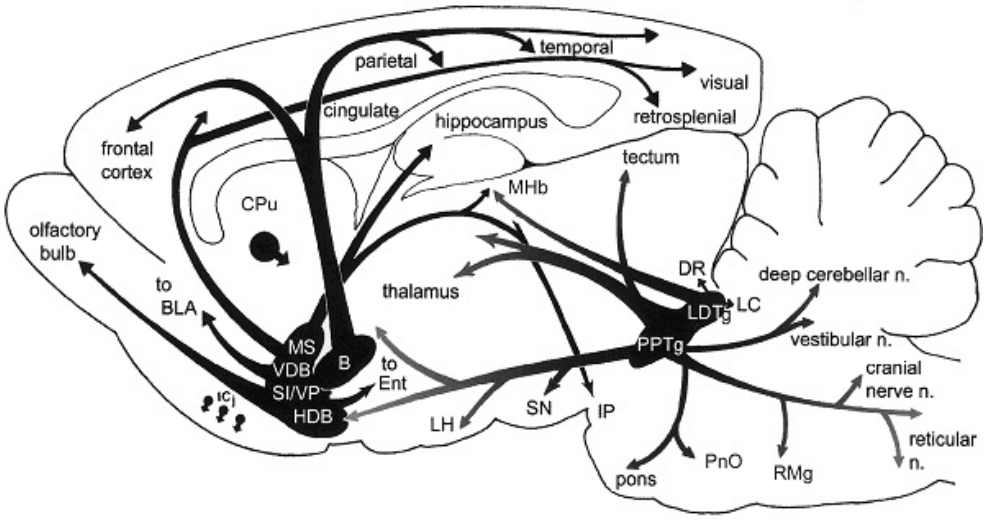

Figure 2. Schematic representation in the rat brain of telencephalic local-circuit cholinergic neurons and projections of the basal forebrain and mesopontine cholinergic systems (Woolf et al. 1983).

1.1.1.3 Cholinergic system in Alzheimer's disease

The cholinergic cell population undergoes moderate degenerative changes during aging under non pathological circumstances that result in loss of the cholinergic function. These processes are responsible for the increasing memory deficits during aging (Yufu et al., 1994). Besides their role in non pathological functions, cholinergic corticopetal projection neurons have received enormous attention due to their loss in AD and in related disorders that cause cognitive deficits. This discovery led to the cholinergic hypothesis of memory dysfunction (Averback, 1981;Geula and Mesulam, 1994;Jellinger, 1996;Perry, 1993).

In most regions of the world, AD is the most common cause of dementia among the elderly (Launer et al., 1999). The occurrence of the disease is about 5% among people aged 65 or older, and the prevalence rises sharply to 19% after 75 years and to 30% after 85 years. The 85 and older age group is one of the fastest growing population segments diagnosed with AD in industrialized countries and all together the disease is affecting over 25 million people all over the world (Qiu et al., 2009; Xie et al., 2009).

More than one hundred years ago, in 1906, the German neuropathologist and psychiatrist Alois Alzheimer first described cerebral atrophy, presence of extracellular neuritic plaques and intracellular neurofibrillary tangles as neuropathological characteristics in the brain of a demented patient. The pathological features of AD are described by two major qualities: (1) degeneration of basal forebrain cholinergic neurons that results in deficiency of cholinergic functions in cortex and hippocampus; (2) extracellular protein aggregates containing beta-amyloid peptides (Aβ) in these cholinergic target areas (Yan and Feng, 2004). Further studies revealed that the neuropathological changes occur initially in the medial temporal lobe structures such as the entorhinal cortex and the hippocampus. At later stages, the pathological features extend into other cortical and subcortical regions such as the basal forebrain cholinergic system (Bondareff et al., 1994;Braak and Braak, 1991;Geula, 1998). The neurofibrillary tangles, one of the hallmarks of AD, represent intracellular inclusions formed by aggregates of hyperphosphorylated microtubule-associated tau proteins which are found in selected neuronal populations (Kosik et al., 1986). While in the brains of Alzheimer's patients no tau mutations have been described, pathogenic mutations in the tau genes cause frontotemporal dementia (Goedert and Jakes, 2005) suggesting that post-transcriptional alterations in tau gene expression may also contribute to the cognitive deficits in AD. In 1974, Drachman and Leavitt demonstrated that the blockade of the cholinergic receptors in young healthy individuals produces a memory deficit, which is similar to that seen in AD patients (Drachman and Leavitt, 1972). Other studies have revealed that activation of nAChR results in a significant increase in tau phosphorylation, whereas mAChR activation may prevent tau phosphorylation (Hellstrom-Lindahl, 2000; Rubio et al., 2006; Wang and Shyu, 2004). Smoking, in fact is a risk factor of AD and recently it has been shown that decreasing risk factors such as smoking and alcohol consumption would be associated with

slower development of dementia in AD (Deschaintre, 2009; Cataldo, 2009). Amyloid-beta peptide (Aβ) may be at the root of neurodegeneration processes. The development of Aβ induces neurotoxicity that appears to be mediated by oxidative stress (Singh et al. 2009; Zraika et al. 2009). In the familial cases, the mutation in either the APP gene or the presenilin 1 gene resulted in increased production of Aβ peptides (Shepherd et al., 2009).

In earlier studies, a severe loss (up to 95%) of cholinergic markers in the cerebral cortex in AD subjects was independently reported by two research groups (Davies and Maloney, 1976;Smith and Bowen, 1976). Later studies showed significant decreases (of varying extents, ranging between 15% and 95%) in the number of cholinergic neurons in AD patients (Arendt et al., 1985;Geula and Mesulam, 1994;Iraizoz et al., 1991;Whitehouse et al., 1982b;Whitehouse et al., 1982a). Furthermore, the severity of the cholinergic deficits in AD was found to be positively correlated with the progress and duration of the AD (Francis et al., 1999; Perry et al., 1983). This encouraged the development and introduction of pharmacotherapy that involved cholinergic system modulating agents such as inhibitors of AChE (Orgogozo et al., 2003). However, the enthusiasm that cholinergic therapy may be used to eliminate memory and cognitive deficits in demented patients soon decreased. Clinical trials using cholinergic drugs, which are in fact the only medication available, showed only modest improvements and could not restore cognitive function. There are several factors that could influence such an outcome. First, cholinergic degeneration is not apparent in cases with mild cognitive impairment (Davis et al., 1999). These individuals are the main target group for the disease prevention. Moreover, there is no general brain cholinergic system lesion in AD (Mesulam, 2004). The cholinergic nuclei in the brainstem remain relatively intact in contrast to the basal forebrain cholinergic neurons. Finally, catecholaminergic neurons show even more prominent losses in activity at early stages of the disease than cholinergic cells (Zarow et al., 2003). Therefore, the current treatment strategies that use drugs targeting the cholinergic system at preclinical or early stages of the disease might prove to be productive when combined with other therapeutic approaches than when used alone.

It has been clearly demonstrated that cortical cholinergic transmission does play a major role in the development of AD, however there is still a heated debate whether the

cholinergic deficit observed in patients with AD is a primary event or secondary to the appearance of the other pathological features (Schliebs and Arendt, 2006).

1.1.2 Non-cholinergic neurons

Cholinergic neurons are co-distributed with several other cell populations, including GABAergic neurons and various calcium binding protein containing cells (e.g. calbindin, calretinin, parvalbumin) (Gaykema and Zaborszky, 1997;Manns et al., 2000;Manns et al., 2001;Manns et al., 2003;Ribak and Roberts, 1990). Anatomical and electrophysiological studies identified a wide ranged diversity of BF neurons, including local interneurons that express NPY and somatostatin, in addition to cholinergic, GABAergic and glutamatergic projection neurons (Duque et al., 2000;Manns et al., 2003;Szymusiak et al., 2000;Zaborszky et al., 1999). Cholinergic, calbindin (CB), calretinin (CR) and parvalbumin (PV) cells represent non-overlapping populations of neurons in rat and they show specific spatial and numerical relations (Zaborszky et al., 2005). A substantial proportion of PV cells contain GABA and project to the cerebral cortex (Gritti et al. 1993). A small percentage of CB and CR cells also project to the cortex (Zaborszky et al., 1999), although their transmitter content remains to be determined.

1.1.2.1 γ – amino-butyric acid (GABA)

In a quantitative study, it was calculated that the total number of GABAergic neurons in one side of the BF is around 40,000 in the rat, as compared to 18,000 cholinergic neurons, which would suggest, on the average, a 2:1 ratio for GABAergic/cholinergic neurons (Gritti et al., 1993). Although the calcium binding protein containing cell groups are distributed in a coextensive manner with the GABAergic cells, they were collectively more numerous. Using CB, CR and PV as markers for different classes of GABAergic neurons, Zaborszky et al (1996) found a much higher GABAergic/cholinergic ratio of 3.8:1. However, different brain structures show different ratios. In the MS/VDB, HDB, ventral pallidum and the internal capsule the total GABAergic/cholinergic ratio is 3-4:1, however in the globus pallidus, the bed nucleus of

stria terminals and SI (extended amygdala) an even higher ratio of 8:1 was found. It has been suggested that at least a portion of CB, CR and PV neurons indeed project to various cortical areas (Henny and Jones, 2008;Zaborszky and Duque, 2003). Freund et al suggested that GABA containing projection neurons participate in the regulation of cortical activation via direct synaptic contacts onto GABA and somatostatin (SS) containing cortical neurons (Freund and Meskenaite 1992).

1.1.2.2 Parvalbumin

Parvalbumin, a member of the calcium-binding protein family, has been found to be widely distributed in the central nervous system. It is present in distinct subpopulations of GABAergic neurons (Cowan et al. 1990; Hironaka et al. 1990) and is thought to be associated with neurons with high firing rates and a highly active metabolism. Almost the entire basal forebrain region contains neurons showing PV immunoreactivity (Celio, 1990; Zaborszky et al., 2005).

Identified PV cells in the BF discharged at 7–15 Hz, regular or in random modes and showed positive correlation in their discharge pattern to concurrent EEG desynchronization (Duque et al., 2000). PV containing cells are distributed across the globus pallidus and ventral pallidum. Neurons with variably intense PV immunoreactivity are furthermore present in the SI, VDB/HDB nuclei and MS. The vast majority of PV-positive neurons in the MS-diagonal band have been shown to contain GABA and to innervate inhibitory interneurons in the hippocampus (Freund and Antal, 1988). PV-positive cells in the other territories of the BF are most likely GABAergic as well. PV has been found to be co-localized with GABAergic neurons in many brain areas, including GABAergic local interneurons of the cerebral cortex, the hippocampus, and the neostriatum (Mascagni and McDonald, 2003;Tamamaki et al., 2003).

1.1.2.3 Calbindin and calretinin

Another substantial proportion of corticopetal and septohippocampal neurons contain CB, however only a small proportion of CR cells projects to the cortex. In contrast to PV cells, only a small proportion of CB and CR cells contain GABA in the basal forebrain (Gritti et al., 2003).

In the BF area of the rat, neurons containing the calcium binding proteins (CBP): CB and CR are diverse in size and shape and distributed in a manner overlapping with the GABAergic neurons as well as with cholinergic cells. However, they are greater in number than the GABAergic cells within the area. CB neurons were retrogradely labeled from the cerebral cortex, just like GABAergic, PV containing neurons, but they were also larger in number than the GABAergic projection neurons. These results indicated that CBP containing neurons might comprise GABAergic and non-GABAergic neurons in the BF. This has been also supported by dual immunostaining for CBPs and enzymes involved in neurotransmitter synthesis or degradation showed that, whereas the vast majority of PV neurons contained glutamic acid decarboxylase (GAD) suggesting that they were GABAergic, the vast majority of CB and CR neurons did not. They appeared to contain phosphate-activated glutaminase (PAG) in significant proportions, which is the enzyme for the synthesis of transmitter glutamate. Accordingly, caudally or locally projecting, possibly glutamatergic, neurons would include CR and the basal cortical projection neurons would include PV, GABAergic, and CB neurons in addition to CBP cholinergic neurons (Gritti et al., 2003).

In the MS–diagonal band nuclei, CR-containing neurons appeared to correspond to locally or caudally projecting presumed GABAergic neurons (Kiss et al., 1997). CR-positive neurons were also present mainly in the proximity of the MS midline. Although CR containing cells were scattered in the VP and MBN/SI complex, numerous CR passing fibers, though with heterogeneous densities, were visualized (Varga et al., 2003).

CB cells appeared very similar in size to the CR containing neurons. In rodents, relatively few CB immunoreactive cells were localized in the midline of MS and ventral diagonal band (VDB), where they were surrounded by the cholinergic neurons or intermingled with ChAT-positive perikarya. Interestingly, CB containing cholinergic

neurons were present in the posterior magnocellular nucleus basalis (MBN) but not in the anterior or intermediate MBN subdivisions. In comparison with the distribution pattern of CB containing neurons, however, a significantly broader zone of intermingled CR and ChAT neurons was evident in the MS and VDB. The dorsal subdivision of the nucleus caudatus and putamen exhibited intense CB and CR immunoreactivity, where both cellular and neuropil labeling for these calcium-binding proteins was present, and virtually all striatal principal neurons expressed CB.

1.1.2.4 Somatostatin

Somatostatin (SS) a 14- or 28-amino acid-containing neuropeptide has been identified in synapses on cholinergic projection neurons (Zaborszky, 1989) in the BF. A portion of these SS-containing terminals may originate from local neurons distributed mainly in the ventral pallidum, SI and around the HDB (Fig 3). Little is known about the electrophysiological properties of the SS-containing neurons in the BF, but it has been shown by Momiyama et al (2006) that somatostatin presynaptically inhibits both GABA and glutamate release onto rat BF cholinergic neurons (Momiyama and Zaborszky, 2006). Neurons expressing SS constitute a peptidergic interneuronal system in the septum, striatum, hippocampus, and cerebral cortex (Chesselet and Graybiel, 1986;Forloni et al., 1990;Kohler and Eriksson, 1984;Vincent et al., 1985). In BF areas, patches of SS fibers and axons of local SS neurons were observed in close vicinity to cholinergic neurons (Zaborszky and Duque, 2000), indicating a potential effect of SS on cholinergic neurons. Cholinergic neurons receive GABAergic input in BF areas (Zaborszky, 1989) and SS have been shown to be co expressed with γ-amino butyric acid (GABA) in many perikarya in forebrain areas (Esclapez and Houser, 1995;Hendry et al., 1984;Kosaka et al., 1988;Somogyi et al., 1984).

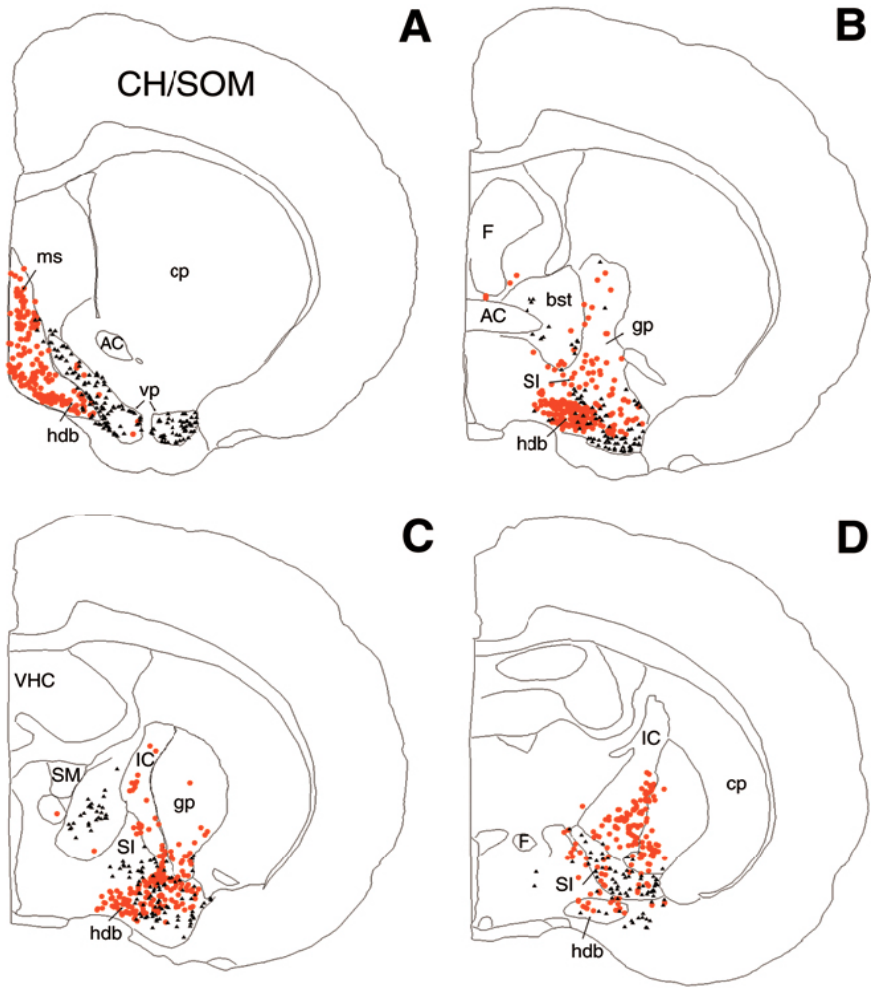

Figure 3. Distribution of cholinergic (red) and somatostatin (black) containing neurons at four rostro-caudal coronal levels plotted from a rat brain that was double stained for choline acetyltransferase and somatostatin (Zaborszky and Duque, 2000).

1.1.2.5 Neuropeptide-Y (NPY)

Several studies described the presence of BF cells that reduced their firing rate during cortical EEG activation in anesthetized rats (Duque et al., 2007). These so-called S-cells were suggested to be local GABAergic interneurons, as they could not be activated antidromically from the cortex (Detari et al., 1997a). Several functionally S type cells have been identified, some of which were stained positively for NPY (Duque et al., 2000). Although, the number of NPY neurons is relatively low, their function might be significant because they possess abundant axon collaterals. Some of the axon collaterals enter into

synaptic contacts with cholinergic profiles the possibility that they contain GABA (Aoki and Pickel, 1990). It is likely that burst firing of NPY neurons could result in a pronounced modulation of GABAergic-cholinergic transmission at least in the ventral pallidum where cholinergic cell bodies are richly innervated by GABAergic terminals (Zaborszky et al., 1986). In anaesthetized rats, significant EEG changes were found after NPY injections to BF (Toth et al., 2005) and it has been suggested that NPY plays a role in the integration of sleep and behavioral stages via the BF as NPY injections caused changes in the sleep-wake cycle (Toth et al., 2007).

1.1.2.6 Glutamate

Vesicular glutamate transporters (VGluts) accumulate glutamate into the synaptic vesicles of excitatory neurons. Three isoforms of VGluts were cloned and identified. VGluts are definitive markers for neurons that use glutamate as neurotransmitter (Bai et al., 2001;Bellocchio et al., 2000;Fremeau, Jr. et al., 2001;Fujiyama et al., 2001;Gras et al., 2002;Takamori et al., 2000;Takamori and Moriyama, 2003). Vglut1 and Vglut2 share a complementary distribution, such that Vglut1 is predominantly expressed in the neocortex, whereas Vglut2 mRNA is abundant in subcortical forebrain regions, including thalamic nuclei, hypothalamic areas, basal forebrain, and some amygdaloid nuclei (Fremeau, Jr. et al., 2001;Herzog et al., 2001). Vglut2 mRNA was described to show the distribution of Vglut2 cells in the forebrain. It was found in the septum and VDB/HDB nuclei, the pallidal structures and the internal capsule. Vglut2 cells are scarcely distributed in the VP, in the SI and bed nucleus of the stria terminalis. Vglut2 cells in the SI appear rostrally, rather inconspicuously between the lateral part of the VDB/HDB and the medial part of the ventral pallidum. They were found in the medial preoptic / medial hypothalamic areas. Loosely arranged cells in the entire rostrocaudal extent of the lateral preoptic/hypothalamic areas show moderate Vglut2 staining A direct glutamate effect on cholinergic neurons is suggested by the presence of Vglut1- and Vglut2-type synapses on BF cholinergic neurons (Hur and Zaborszky, 2005).

1.2 Afferent projections to the BF

Tracing studies combined with electron microscopy have identified synapses on BF neurons originating from the brainstem, hypothalamus, amygdala, substantia nigra-ventral tegmental area, striatum, hippocampus and the prefrontal cortex (Cullinan and Zaborszky, 1991;Gaykema et al., 1991;Gaykema and Zaborszky, 1997;Zaborszky, 1989;Zaborszky and Cullinan, 1992;Zaborszky and Cullinan, 1996;Zaborszky et al., 1997).

1.2.1 Cortical afferents

Studies in monkeys, cats and anterograde tracing with PHA-L from different cortical areas in rats (Irle and Markowitsch, 1986); (Cullinan and Zaborszky, 1991) (Mesulam et al., 1984;Mesulam and Mufson, 1984) revealed that the cholinergic neuron population in the basal forebrain only receive a restricted cortical projection, originating from the prefrontal cortical areas (Mesulam, 1986), including the orbitofrontal cortex, the anterior insular cortex, temporal polar, medial inferotemporal region, entorhinal, piriform, and perirhinal cortices. In the rat, the pattern of input to the basal forebrain from the various prefrontal cortical regions seems to be restricted and it follows a specific pattern (Vertes 2004; Zaborszky et al. 1991). The BF cholinergic (BFC) neurons do not appear to receive direct input from primary sensory and motor cortex or from higher order association areas (Zaborszky et al. 1997).

However, it is very likely that cholinergic neurons respond to a range of visual and auditory stimuli (Richardson and DeLong 1990; Rolls et al. 1989; Wilson and Rolls 1990a; Wilson and Rolls 1990b; Wilson and Rolls 1990c), which might reach the BF through the orbitofrontal cortex (Rolls et al., 1989). One of the aims of our experiments was to investigate whether the cholinergic neurons in the BF receive cortical information through a specific interneuron population located in close proximity to the cholinergic neuron population in the BF.

1.2.2 Brainstem afferents

One of the main functions of the brainstem is to regulate vital functions of the organism, such as breathing, heart rate, blood pressure, as well as it serves as a major connection between the motor and sensory systems of the brain and the rest of the body (Detari et al., 1997b;Kihara et al., 2001;Steriade, 1999;Dunbar et al., 1992). The brainstem is also responsible to maintain consciousness and to regulate the sleep-wake cycle. The proposed role of the BF in arousal, attention and dreaming is highly determined by its afferent projections from the brainstem (Sarter and Bruno 2000). Removing the input to the BF from the brainstem resulted in decreased attention performances in rats and degenerating axon terminals in the area of the cholinergic neuron population in the BF (Sarter and Bruno 2000; Zaborszky et al. 1986). Further investigations revealed that a subpopulation of cholinergic neurons, mainly in the magnocellular preoptic nucleus (MCP), may receive cholinergic, presumably inhibitory, input from the LDT/PPT area (Jones and Cuello 1989; Satoh and Fibiger 1986; Semba et al. 1988; Woolf et al. 1986).

Extensive retrograde tracing studies were carried out to identify the areas that send direct projections to the BF. The pattern of dense brainstem labeling obtained with magnocellular preoptic/SI injections was originating from the upper brainstem (rostral pons and midbrain). The brainstem areas that were most prominently labeled included the medial parabrachial nucleus, the pedunculopontine nucleus, the dorsal raphe nucleus, the lateral and ventral tegmental area (VTA) and the supramammillary nucleus. Most of these cell groups were more heavily labeled with magnocellular preoptic/SI injections than with any others (Hallanger and Wainer 1988; Haring and Wang 1986; Jones and Cuello 1989; Martinez-Murillo et al. 1988; Semba et al. 1988; Vertes 1988). The neurotransmitter content of the described projections was also investigated and Semba et al (2000) found that in the mesopontine tegmentum, many retrogradely labeled neurons were immunoreactive for choline acetyltransferase (Semba, 2000). In the dorsal raphe nucleus, some retrogradely labeled neurons were positive for serotonin (5-HT) and some for tyrosine hydroxylase (TH); however, the majority of retrogradely labeled neurons in this region were not immunoreactive for either marker. In vitro measurements resulting in hyperpolarization of the cholinergic neurons by 5-HT suggested an inhibitory modulation

of this system (Khateb et al. 1993). The VTA also contained TH positive retrogradely labeled neurons (Semba, 2000;Horvath et al., 2004;Lightman, 2008;Nogueiras et al., 2008;Valassi et al., 2008;Adamantidis and de Lecea, 2008;Benedict et al., 2009;Silver and Lesauter, 2008) and sent most of its dopaminergic projections to non-cholinergic, mostly parvalbumin and somatostatin containing neurons (Gaykema and Zaborszky 1996; Gaykema and Zaborszky 1997; Zaborszky and Duque 2003). The BF also receives adrenalin-containing projections from the brainstem that form asymmetric synapses on cholinergic neurons, which are most likely excitatory (Hajszan and Zaborszky 2002).

1.2.3 Hypothalamic afferents

The hypothalamus plays an important role in the regulation in many physiological phenomena including energy homeostasis, food intake, circadian rhythm, sleep, body temperature, blood pressure and sexual dimorphism (Adamantidis and de Lecea 2008; Benedict et al. 2009; Ellacott and Cone 2004; Horvath et al. 2004; Lightman 2008; Nogueiras et al. 2008; Silver and Lesauter 2008; Valassi et al. 2008). Afferents to the BF from hypothalamic, together with the already mentioned brainstem regions, are functionally important in the regulation of sleep-wake cycles in the BF. For example, thermosensitive inputs from the anterior hypothalamus modulate the activity of BF sleep- and arousal-related cell types (Szymusiak 1995).

Light and electron microscopy studies revealed that the BFC receives direct input from hypothalamic nucleus in a well organized, topographic manner. Lateral hypothalamic neurons send their axons to more lateral BF areas, such as dorsal part of the SI, lateral part of the bed nucleus of the stria terminalis, the ventral part of the GP. These projections contain hypocretin (orexin) as a neurotransmitter, suggesting that the input serves as an excitatory modulation of the cholinergic cell population in the BF (Eggermann et al., 2001;Nambu et al., 1999;Wu et al., 2004). On the other hand, the medially located hypothalamic nucleus project to the medial parts of the BF, including the HDB and in the MS/VDB complex (Cullinan and Zaborszky 1991; Zaborszky et al. 1991).

1.2.4 Striatal afferents

The striatum is well known for its role in the planning and modulation of movements, but it is also involved in a variety of cognitive processes and it is part of the reward system. One of the main target areas of both the ventral (nucleus accumbens, ventral part of the caudate putamen, olfactory tubercle) and dorsal striatum are the cholinergic neurons in the GP, VP, peripallidal areas and internal capsule (Cullinan and Zaborszky, 1991;Haber et al., 1990;Sesack et al., 1989).

Since the striatum also receives a significant cortical input from various cortical areas, such as prefrontal, auditory, visual cortices, hippocampus and the amygdala (Beckstead 1979; McGeorge and Faull 1989), striatal neurons may provide an indirect connection between descending cortical information and the BF.

1.2.5 Afferents from the amygdala

The main function of the amygdala was described to be in memory consolidation and emotional processes (Pitts et al. 2009; Zheng et al. 2008; Roozendaal et al. 2008). Ventral parts of the amygdala send projections to the hypothalamus, thalamus, striatum, and prefrontal cortical areas (Barbas and De Olmos 1990; Krettek and Price 1978;Price and Amaral 1981; Russchen et al. 1985a; Russchen et al. 1985b), however they also provide axon terminals of passage to the VHD and SI in the BF of monkeys (Russchen et al. 1985a; Russchen et al. 1985b). Several groups reported that fibers from the basolateral amygdaloid nucleus provide synapses on dendrites of both cholinergic and non-cholinergic cells in the VP, ventrolateral and dorsomedial aspects of the SI and the striatum in rats (Jolkkonen et al. 2002; Zaborszky et al. 1984). Further electron microscopic analysis revealed, that the postsynaptic targets of the central nucleus of the amygdala efferents are non-cholinergic, probably GABAergic, neurons via mostly symmetrical synaptic connections (Jolkkonen et al. 2002). The purpose of this connection might be very similar to the function of cortex-amygdala interconnection, suggesting the anticipation of BFC in stimulus-reward-associative learning as well as in the modulation of behavioral responses in life-threatening situations (Groenewegen et al., 1990). In turn, the cholinergic

innervation of the amygdala may also play an important role in memory consolidation processes, more specifically in memory storage (Nagai et al. 1982; Power 2004).

1.3 Efferents from the BF

Various retrograde labeling studies combined with AChE immunohistochemistry provided evidence that the basal forebrain sends projections in an approximately medio-lateral and antero-posterior topography topographical fashion to different regions of the brain, including the entire neocortex, the hippocampus, the amygdala, the thalamus, the hypothalamus and the olfactory bulb (Grove 1988; Jones and Cuello 1989; Mesulam et al. 1983). According to immunohistochemical and biochemical studies, the cholinergic innervation is heterogeneous across various cortical areas and different species. Together with the brainstem cholinergic system, the main function of the BFC cortical projection is to activate the electro-encephalogram, increase cerebral blood flow, regulate sleep-wake cycling, and modulate cognitive function (Armstrong et al. 1983; Bina et al. 1993). Besides the cholinergic efferents, other, non-cholinergic projections also reach various structures in the brain. For understanding the key points of this thesis, I would like to discuss the cortical connection in more details.

1.3.1 Efferents to the cortex

There is a variation, not only in the localization, but also in the nomenclature, of the cholinergic neurons located in the basal forebrain between different species that makes it slightly difficult to follow possible evolutionary changes in the organization and function of this area. In general, in all species, cholinergic efferents from the nucleus basalis magnocellularis (NBM) of the basal forebrain provide the majority of the cholinergic input to the neocortex (Mesulam et al. 1983; Mesulam et al. 1984b; Saper 1984). This area overlaps with the Ch4 in monkeys and humans. The cholinergic cell groups in the area of NMB project mainly to the frontal, parietal, temporal, occipital, cingulated, enthorinal and the motor cortices (Dringenberg et al. 2004; Mesulam et al. 1983; Mesulam et al. 1984b; Saper 1984; Woolf et al. 1986). Cholinergic varicosities are present in all cortical layers

but with higher occurrence in layer V-VI of the motor cortex, layer III-IV in primary sensory cortices, and in layer II-III of the association areas (Mesulam et al. 1992; Mrzljak et al. 1995). A varying proportion of them were reported to form clearly identifiable symmetric synapses on the apical and basal dendrite of innervating pyramidal, spiny stellate and GABAergic interneurons (Houser et al., 1985).

In addition to the cholinergic efferents, a significant portion of non-cholinergic projecting neurons are also located in the BF areas (Rye et al. 1984). The projection pattern of the non-cholinergic neurons is very similar to the cholinergic ones (Woolf et al. 1986) GABAergic projections were found on cortical GABAergic interneurons, providing excitation of cortical activation through disinhibition (Freund and Meskenaite 1992).

1.3.2 Efferents to the thalamus

Thalamic areas receive considerable cholinergic input from brainstem areas (Parent and Descarries, 2008); Steriade et al. 1990; Steriade 1990), however the nucleus reticularis has been shown to receive cholinergic input from the basal forebrain as well (Woolf and Butcher, 1986;Hallanger and Wainer, 1988;Levey et al., 1987;Jourdain et al., 1989). Besides the cholinergic projection to the thalamus, Asanuma et al. also described that GABAergic neurons located in the BF are sending projections to the nucleus reticularis (Asanuma 1989). Other have showed, that the nucleus reuniens (ER), that projects heavily to the medial prefrontal cortex, also receives afferents from various subcortical areas, among others: the SI, the claustrum, tania tecta, lateral septum, and medial and lateral preoptic nuclei of the basal forebrain. This connection may give rise to an additional, indirect pathway between the BF and the neocortex (McKenna and Vertes, 2004).

1.3.3 Efferents to the hippocampus

Combined retrograde and immunohistochemical studies showed that the BF innervation of the hippocampus originated mostly from MS, VDB/HDB, magnocellular preoptic area, and rostral SI (Amaral and Cowan, 1980;Amaral and Kurz, 1985;Rye et al., 1984;Woolf et al., 1984;Zaborszky et al., 1975). It has been shown, that 35-45% of innervation reaching the hippocampus from these areas is cholinergic. These anatomical

findings were later supported by experiments using microdialysis that showed increased level of acetylcholine release in the hippocampus after BF stimulation in awake rats (Nilsson et al. 1992). The functional relationship between the BF and the hippocampus seems to be significant in memory consolidation and attention (Frick et al., 2004).

1.3.4 Efferents to the amygdala

The amygdala is one of the major nearby structures that share a common boarder with the BF, which is also called as the extended amygdala (Alheid, 2003). Grove et al described that the dorsal part of the SI is strongly connected with the lateral, basolateral, and central nuclei of the amygdala, while the ventral part of the SI projects to more anterior parts of the amygdala (Gaykema et al. 1991b; Grove 1988; (Carlsen et al., 1985). This anatomical and functional relationship provides basic information that helps to understand many roles of the brain, including reward and punishment, learning and cognition, and feeding and reproduction.

1.4 The structure and function of the prefrontal cortex

The prefrontal cortex is the most rostral region of the neocortex. In primates it extends from the frontal pole of the brain to the premotor cortex. The existence of the prefrontal cortex in non-primates was not even established until Rose and Wolsey (1948) confirmed that all mammals have a brain area that is homologous to the primate prefrontal cortex (ROSE and WOOLSEY, 1948a;ROSE and WOOLSEY, 1948b)and is defined by the projections received from the mediodorsal thalamic nucleus (MD) (Gabbott et al., 2005), as well as having dense dopaminergic input (Franke et al., 2003). In non-primates, it is dedicated mostly to voluntary motor control, but in primates, it has developed further to serve higher cognitive functions.

The prefrontal cortex evolved probably the most extensively in size and volume during the evolution of mammals, from the insignificant size in rodents to the coverage of one-third of the prefrontal lobe in humans (Fig. 4). For many years, scientists believed that abilities of humans, for example for planning and abstract reasoning, were a result of their highly developed, larger prefrontal cortex compared to other primates. Later, it has been shown that the ’superior’ abilities of the human brain was not correlated to the relative size of the prefrontal cortex, but most likely to the denser interconnections with other areas of the brain. Not only did the size of the mammalian prefrontal cortex increased compared to other vertebrates, still, it disproportionally outgrew other parts of the neocortex as well (Fuster, 1997).

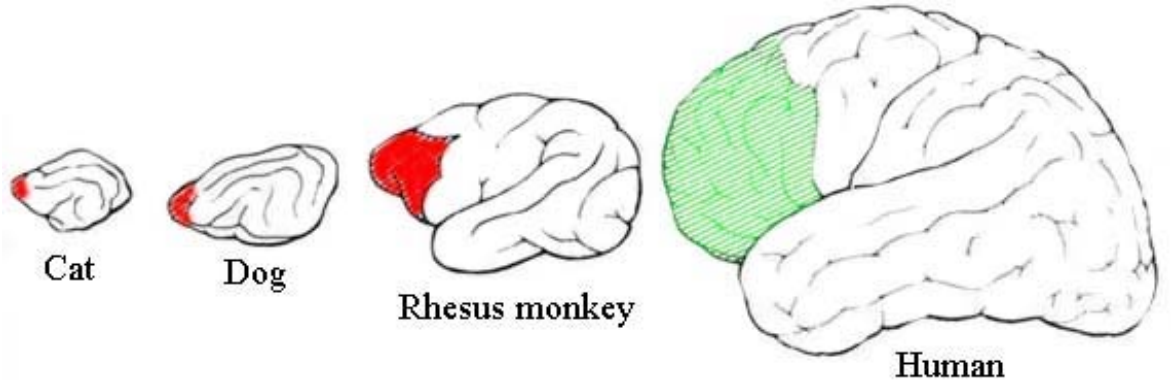

Figure 4. Development of the prefrontal cortex in various mammalian species. It is noteable that prefrontal cortex is the part of the brain that grew the most during evolution.

1.4.1 Anatomy of the prefrontal cortex in rats

In mammalian species the prefrontal cortex encompasses a large and heterogeneous area that has well characterized cytoarchitecture of the consisting layers. First, I would like to review the anatomy and cytoarchitecture of the cortical layers and the neuronal types that are located in the area, focusing on their afferent and efferent connections and neurotransmitter type, then discuss its role in physiological and pathological cognitive processes.

1.4.1.1 Cytoarchitecture of the prefrontal cortex

Throughout the neocortex, different neurons with similar connection properties form a functional subunit called the column. The columns are perpendicular to the surface of the cortex and traverse six (I-VI) cortical layers that determine the cytoarchitecture of the entire neocortex. The columnar organization is currently the most widely held hypothesis to explain the cortical information processing. The columnar layers can be differentiated by the cell types they contain as well as their projection patterns. Based on Brodmann`s classification of the characteristic neuronal cell types and connections with

other cortical and subcortical regions, the following cortical layers has been described (Brodmann, 1909).

However, the prefrontal cortex is an agranular cortex, meaning it lacks a definitive layer IV (Gabbott et al., 2005). Therefore, the prefrontal cortex is often called a proisocortex, since it represents a transition between the neocortex and the allocortex, in terms of their cytoarchitecture. The following VI layers describe the neocortex and are also represented in the prefrontal cortex, except for layer IV.

Supragranular layers:

- Layer I: contains few scattered neurons and consists mainly of the apical dendrites of the pyramidal cells, as well as glia cells (Shipp, 2007). Some Cajal-Retzius and spiny stellate neurons can be found here. It is the projection target of local intracortical afferents from nonspecific thalamic nuclei (molecular layer).
- Layer II: contains small pyramidal neurons and numerous stellate cells. It receives afferents from nonspecific thalamic nuclei (external granular layer).
- Layer III: contains mostly small and medium-size pyramidal neurons, as well as non-pyramidal cells with vertically-oriented intracortical axons; layers I through III are the main target of interhemispheric corticocortical afferents, and layer III is the principal source of corticocortical efferents (external pyramidal layer).

Granular layer:

- Layer IV: contains different types of stellate and pyramidal neurons, and is the main target of specific thalamocortical afferents as well as intra-hemispheric corticocortical afferents (internal granular layer)
-

Infragranular layers:

- Layer V: contains large pyramidal neurons; it is the principal source of information to the subthalamic parts of the brain (internal pyramidal layer)
- Layer VI: contains few large pyramidal neurons and many small spindle-like pyramidal and multiform neurons (multiform layer); it sends efferent fibers to the thalamus, establishing a very precise reciprocal interconnection between those areas (Dick et al. 1991).

The main characteristic cell type of the cortex is the pyramidal cell. Most of the pyramidal cell bodies are located in layer II/III and V/VI. Those located in layer II/III project to other cortical areas (including layer I), while those located in layer V/VI send their projections to the thalamus and other subcortical areas. The neurotransmitter type of these neurons is excitatory.

Basket cells have inhibitory projection output and their axons run horizontally through the grey matter to other cortical columns. Chandelier cells also have inhibitory neurotransmitters in their axon terminal but their axons run vertically and terminate on axons of pyramidal cells of the same cortical column.

The output connections of the smooth stellate cells are also inhibitory and their main function is to turn off the activity of the neighboring cortical column once they are activated (Kisvarday et al., 1990;Budd, 2000).

In primates, the prefrontal cortex has three major, well differentiated regions: medial, lateral and ventral or orbital areas (Fuster, 2002). The medial frontal division, which can be sub-divided into a dorsal region that includes precentral (PrC) and anterior cingulate (ACg) cortices and a ventral component that includes the prelimbic (PrL), infralimbic (IL) and medial orbital (MO) cortices. The lateral region the dorsal and ventral agranular insular (AID, AIV) and lateral orbital (LO) cortices (Mesulam et al., 1977). Finally, a ventral or orbital region can be divided into the ventral orbital (VO) and ventral lateral orbital (VLO) cortices.

The homology between the human and the rat prefrontal cortex has been studied by Preuss et al (1995). He found that the region of rat frontal cortex is homologous to the dorsal lateral PFC of primates and is located along the dorsomedial edge of the hemisphere

and the medial wall, anterior to the corpus callosum. Just as in primates, this region receives dense inputs from MD and from the dopamine-containing nuclei of the brainstem. The dorsomedial cortex is considered to be the rat's frontal eyefield, because stimulation of this zone yields head and eye movements (Preuss and Goldman-Rakic, 1991). My experiments were focused on the medial prefrontal cortex of the rat, so the IL and PrL and their interconnected areas will be discussed in more details.

The IL has been shown to strongly influence visceral/autonomic activity. The stimulation of the IL produces changes in respiration, gastrointestinal motility, heart rate, and blood pressure (Burns and Wyss 1985; Fuster 2002; Hardy and Holmes 1988; Hurley-Gius and Neafsey 1986; Terreberry and Neafsey 1983; Verberne et al. 1987). Because of these effects of the IL, it is viewed as a visceromotor center (Hurley-Gius and Neafsey 1986; Neafsey et al. 1986). The prelimbic cortex, on the other hand, has been implicated mostly in cognitive processes.

Lesions of the PrL have been shown to produce pronounced deficits in delayed response tasks (Brito and Brito 1990; Delatour and Gisquet-Verrier 1996; Delatour and Gisquet-Verrier 1999; Delatour and Gisquet-Verrier 2000; Floresco et al. 1997; Seamans et al. 1995), similar to those seen with lesions of the dorsal part of the lateral PFC of primates (Goldman-Rakic, 1994;Kolb, 1984).

1.4.1.2 Efferent and afferent projections of the medial prefrontal cortex

The afferent and efferent connections of the prefrontal cortex are exceptionally dense towards both cortical and subcortical areas in the mammalian brain (Beckstead 1979; Gabbott et al. 2005; Gaykema et al. 1991c; McGeorge and Faull 1989). The excitatory connections are both local and long-distance, however inhibitory connections project only locally. It has been confirmed that the projecting, long distance connections are almost entirely from pyramidal cells which form excitatory synapses with other neurons. As for inhibitory connections, we find basket cells that send connections horizontally to other columns up to one millimeter away (Conde et al., 1994).

The prefrontal cortex receives highly organized inputs from the basal ganglia via striatopallidal and striatonigral projections, as well as pallidothalamic and nigrothalamic

projections that further reach different areas of prefrontal cortex (Groenewegen et al., 1997). In addition to thalamocortical connections, which are one of the most significant afferents of the prefrontal cortex defining this brain region, it also receives extensive cortico-cortical inputs, for example, from posterior parietal cortex and sensory cortical areas (Grossberg et al., 2008;Tinsley, 2009). The PFC also receives projections form other subcortical structures such as the substantia nigra, ventral tegmental area, amygdala, lateral hypothalamus and hippocampus (Groenewegen et al. 1997; Kolb and Gibb 1990). There are also reciprocal connections from the prefrontal cortex to these structures, as well as direct projections to the lateral septum, mesencephalon and autonomic regions of the brainstem. The prefrontal cortex also targets, in a reciprocal and topographical manner, the main nuclei of the major cholinergic and monoaminergic neurotransmitter systems including noradrenaline (NA)-containing neurons in the pontine central grey, dopamine (DA) neurons in the ventral tegmental area, serotonin (5-HT) neurons in the raphe nuclei and acetylcholine (ACh) neurons in the basal forebrain (McGaughy et al. 2002; Robbins 2005; Gorelova and Yang 1997; Groenewegen et al. 1997; Gaykema et al. 1991a). However, direct anatomical connection between the ACh neurons of the BF and the PFC has not been proved yet (Zaborszky et al. 1997). It is more likely that the descending information from the PFC reaches the ACh neurons in the BF through an indirect pathway, most probably, with interaction of local inhibitory interneurons. The regions innervated by the PFC act in turn to modulate cortical networks by influencing cortical processes through inhibitory and excitatory synaptic transmission (Hasselmo and Barkai 1995; Robbins and Everitt 2002). In addition, a cholinergic projection to the medial prefrontal cortex from the LDT has been described (Satoh and Fibiger 1986).

1.4.2 Role of the prefrontal cortex in various cognitive functions

There is a wide range of overlapping cognitive functions that are regulated by both the BF and the PFC. It is crucial to identify the exact anatomical and functional relationship between these two, relatively distal, areas of the brain to understand the neuronal organization and activity behind higher cognitive function. The medial prefrontal cortex in humans is responsible for many cognitive processes including problem solving,

attention, decision making, planning, goal directed behavior, consciousness, emotions, planning, language evolution and working memory as well as fear, anxiety. (Dalley et al. 2004; Fuster 2002; Goldman-Rakic 1994; Kolb 1984; Ongur and Price 2000; Repovs and Baddeley 2006; Vertes 2006). Dorsal regions of mPFC have been implicated in various motor behaviors, while ventral regions of mPFC (IL and PrL) have been associated with diverse emotional, cognitive, and memory and learning related processes (Heidbreder and Groenewegen, 2003).

1.4.2.1 Working memory

Working memory serves for the function of temporary storing and manipulating information that uses specific structures and processes of the brain. It can be also defined as memory that is required for one trial of an experiment, but not for subsequent trials. Several studies provided results that linked the prefrontal, the parietal and the cingulate cortex and the basal ganglia with working memory processes in rodents that usually involved tasks with a delayed response contingency (Kesner et al. 2000; Larsen et al. 1978; Zahrt et al. 1997).

Rats with lesions of the PrL and IL, but not the anterior cingulate (ACg) or orbitofrontal cortex, are strongly impaired on delayed memory tasks (Delatour and Gisquet-Verrier 1999; Kesner et al. 2000). In a recent study, DeCoteau et al. (2009) described that animals with PrL/IL cortex lesions displayed a profound and sustained deficit on object based, visual-scene memory, whereas, animals with anterior cingulate cortex lesions showed a slight initial impairment but eventually recovered (Decoteau et al., 2009). In this process, the putative involvement of the cholinergic innervations of the prefrontal cortex in working memory has also been investigated (Broersen et al. 1995a; Broersen et al. 1995b; Ragozzino and Kesner 1998; Ragozzino 2007). However, the involvement of the cholinergic system in primarily mnemonic processes is still under debate. For example, infusions of the muscarinic ACh receptor antagonist scopolamine in the hippocampus produce dose- and delay-dependent impairments on delayed non-matching to position tasks, but the same compound infused into the medial prefrontal cortex produces dose-, but not delay-dependent deficits (Dunnett et al., 1999). The data

accumulated about this subject suggest that PrL/IL cortex is not involved in the temporary on-line storage but rather in the control of information required to prospectively organize the ongoing action. This is also supported by the general function of any neocortical areas. The mammalian neocortex is responsible for information processing above all other function.

1.4.2.2 Attention

Besides the basal forebrain cholinergic system, other brain structures are also involved in several aspects of attention function such as the prefrontal cortex (Miller and Cohen, 2001). Lesions of the dorsolateral prefrontal cortex, but not orbitofrontal cortex, produce deficits in shifting from one perceptual dimension to another, whereas lesions of the orbitofrontal cortex, but not dorsolateral cortex, impair reversal learning (Dias et al. 1996; Dias et al. 1997). Thus, in rats with lesions of the PrL, IL cortices produced a selective deficit in extradimensional set-shifting (Birrell and Brown, 2000). Conversely, lesions of the orbitofrontal cortex impair reversal learning, but not the acquisition of intradimensional and extradimensional set-shifting (Brown and Bowman, 2002). The outcome of this and other experiments examining visual discrimination implies that behavior is less flexible in prefrontal cortex-lesioned animals. Interestingly, however close the PrL and IL cortices are located to each other; they show clear differentiation regarding not only their projection patter, but their role in cognitive function.

Although the crucial role of cholinergic inputs in cue detection has been demonstrated by lesion studies, the role of PPC neurons in the cholinergic modulation of cue detection is unclear. Collectively, these findings indicate that cholinergic inputs to PPC neurons amplify cue detection, and may also act to suppress irrelevant distractors (Broussard et al. 2009). Impairments in the function and capacity of attention represent the main aspects of the cognitive symptoms of schizophrenia (Berberian et al., 2009).

1.4.2.3 Pathology of the prefrontal cortex

Besides the previously discussed role of the prefrontal cortex together with the basal forebrain in physiological cognitive functions, it also plays an important part in the

processes of mental dysfunction. Since the prefrontal cortex extensively interacts with other cortical and subcortical areas via various neurotransmitters, the dysfunction of any of these subsystems could result in various manifestation of mental disorders, all correlated with the prefrontal cortex. Pathological processes of psychiatric disorders in association with the malfunction of the prefrontal cortical areas and other connected areas, such as the amygdala, hippocampus, and ventromedial parts of the basal ganglia, have become the center of attention of the research of mental illnesses, such as anxiety, stress and depression (Goldwater et al., 2009). The involvement of the prefrontal cortex in depression has been investigated by many research groups (Koenigs and Grafman, 2009); (Robinson et al., 2009). Depression is one of the most widespread and incapacitating mental illness of our society, affecting about 8-12% of adult population world wide (Andrade et al. 2003; Kessler et al. 2003). There is a growing evidence of changes in the neuronal morphology of the PFC in neuropsychiatric diseases most likely due to stress induction (Cerqueira et al. 2005; Holmes and Wellman 2009; Liston et al. 2006).

The circuits connecting orbitofrontal cortex (OFC), medial prefrontal cortex (mPFC), basal ganglia, and thalamus are central to the pathophysiology and treatment of obsessive-compulsive disorders (Greenberg et al., 2009). In addition, the PFC seems to have a significant role in mediating the aspects of attention, in close correlation with the parietal and temporal cortices. Since the PFC is crucial for regulating attention based on relevance, as well as for screening distractions, sustaining attention and shifting/dividing attention in a task-appropriate manner, it plays an enormous role in attention-deficit hyperactivity disorder (ADHD) (Arnsten 2009b; Arnsten 2009a; Emond et al. 2009).

The different stages of addiction involve various brain areas, including the orbitofrontal cortex and dorsal striatum, prefrontal cortex, basolateral amygdala, hippocampus, and insula that are highly activated in the stage of craving. The inhibitory control of areas in the brain, such as the cingulate gyrus, dorsolateral prefrontal and inferior frontal cortices, are highly disrupted in further recurring addiction processes (Koob and Volkow 2009; Koob 2009; Volkow et al. 2002).

1.5 Properties of the electrocorticogram under urethane anesthesia

Since we examined the electrophysiological properties of the BF neurons in rats in correlation with the cortical electrocorticogram (ECoG) in urethane narcosis, I would like to overview the properties of the ECoG under urethane anesthesia.

The signal of the ECoG is based on the membrane potential changes of the cortical neurons and can be recorded by electrodes placed on the cortex (ECoG) or the skull (EEG). Different EEG waves are separated by their frequencies (0.1-80Hz) and amplitude. The anatomy of the cortical neurons and their synaptic activity play an enormous role in the generation of EEG waves. During synaptic activity, in the dendritic zone of the cortical neurons inward current is generated that runs into the cell (active sink). At the same time, a different, negative current is generated in the soma that results in the dipole nature of the cortical neurons. The main sources of the EEG are the excitatory and inhibitory postsynaptic potential changes (EPSP and IPSP). When membrane potential changes in neurons close to each other are synchronized it results in high amplitude, low frequency EEG waves, the so called slow wave activity (SWA). However, when the activity of the neighboring neurons is not temporarily synchronized, the EEG pattern is characterized by desynchronized, high frequency, lower amplitude waves, the so called low-voltage fast activity (LVFA) (Elul, 1971;Traub et al., 1996).

Detari et al. (1997) described five (1-5) well differentiated EEG patterns in urethane anesthesia that reflected the depth of the narcosis using bipolar transcortical electrodes placed into the frontal cortex (Detari et al. 1997) (Fig. 5). During urethane narcosis, these stages formed a continuous transition from the lighter level of anesthesia (LVFA) to the highly synchronized, low frequency, higher amplitude SWA that describes the deeper level of anesthesia. During our experiments, we aimed to keep the level of anesthesia as deep as possible, to investigate the relationship between cortical slow waves (pattern 1 and 2) and the BF unit activity. Pattern 1 and 2 do not appear during natural sleep, but are very important and prominent property of the deeper level of urethane anesthesia. At the deepest level of anesthesia, there is an almost isoelectric line recorded by the EEG that alternates with large slow wave complexes, or just a single slow wave (Detari et al. 1997).When membrane is depolarized, extracellular space gets more negative, in

contrast negative changes in membrane potential (hyperpolarization) is accompanied by a positive shift in the extracellular space.

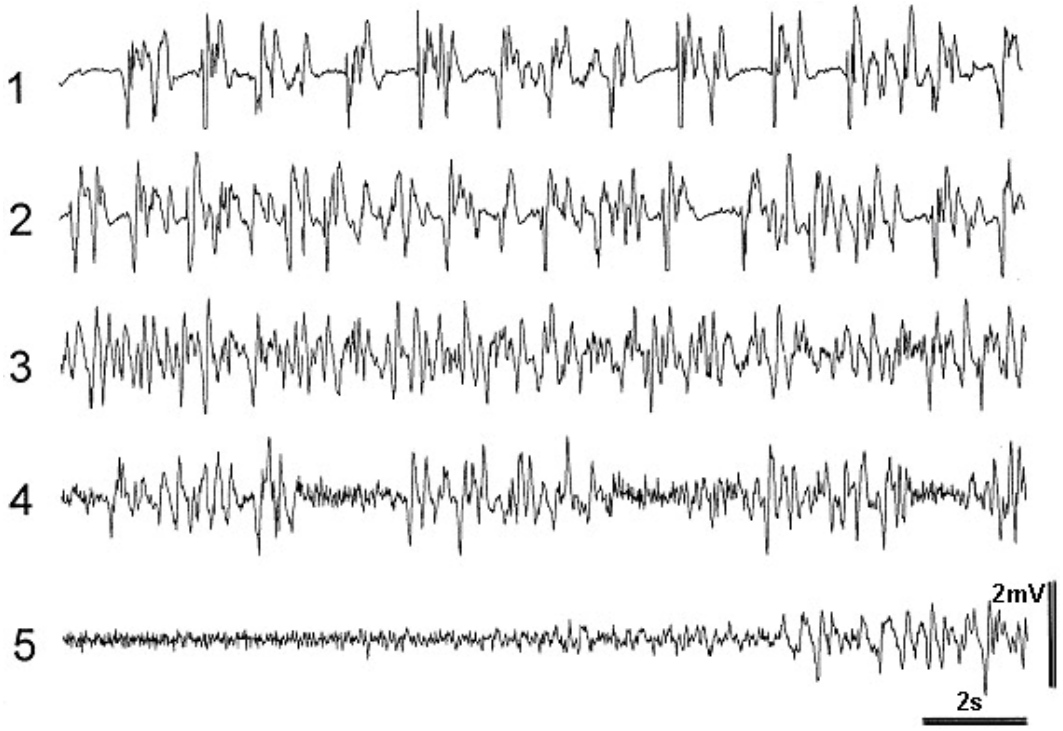

Figure 5. Different EEG patterns in urethane anesthesia registered from the frontal cortex. The depth of the anesthesia is decreasing from pattern 1 to 5, 1 representing the deepest level of anesthesia. Modified from Detari et al., 1997.

1.6 Cortical Up and Down states

The basal forebrain cholinergic system is not the only part of the brain that plays a role in cortical activation. There are several brain areas, including the brainstem, the thalamocortical system and various other pathways defined by a specific neurotransmitter (histamine, noradrenalin, adrenalin, dopamine, serotonin and neuropeptides), that affect the sleep-wake cycle of an organism (MORUZZI and Magoun, 1949).

During natural sleep in humans and under urethane anesthesia in rats, electroencephalogram (EEG) recorded from the neocortex revealed a characteristic slow

(<1 Hz) rhythm, so called cortical Up and Down states (Steriade, 1993). It is important to note here, that the term Up and Down states were first described in relation to a two-state spontaneous membrane potential changes using in vivo intracellular recording from the neostriatum (Wilson and Kawaguchi, 1996).

Cortical Up and Down states are often studied in urethane anesthetized animal models, where slow oscillations in the cortex are similar to those seen during natural slow wave sleep (Destexhe et al. 1996; Destexhe et al. 2007; Mahon et al. 2006; Steriade 1993; Steriade 2001). Contreras and Steriade (1997) performed simultaneous intracellular recordings in thalamic and cortical neurons in anatomically-related areas, and first showed the oscillation of Up and Down states in the neocortex. The Up and Down transitions are synchronous in the thalamus and cortex, and it also shows strong synchronism between distant cortical areas (Contreras et al., 1997). In the generation of cortical Up and Down state, the oscillations of depolarized (active) and hyperpolarized (silent) states of the neurons in the pyramidal layer (V) play an important role. Because of their characteristic features, Up and Down states are sometimes used as a synonym for slow oscillations. To avoid the confusion, I will refer to Up and Down states as a phenomena that describes cortical cellular and network events that occur during two-state (de- and hyperpolarized) neuronal behavior. During the generation of Up and Down states, the membrane potential of both inhibitory and excitatory neurons fluctuates spontaneously between hyperpolarized and depolarized phases. The length of Down states are in strong correlation with the depth of the anesthesia (Kasanetz et al., 2002).

1.6.1 Down states of the neocortex

The Down state in the cortex can be described as an isoelectric state that occurs during periods of decreased synaptic input. The hyperpolarized Down states reflects K+ channel activation and withdrawal of synaptic barrages. There is evidence that inwardly rectifying K^+ currents other than KIR2 may be critical, at least in some kinds of pyramidal cells (Cunningham et al., 2006). Intracellular infusion of an unspecific K^+ channel blocker, Cs^+, abolishes hyperpolarization associated with down states during sleep (Timofeev et al., 2001). It has been shown that hyperpolarization can be produced by two different pathways: activation of inhibitory neurons such as GABA or the reduction of synaptic

excitation, called disfacilitation. The latter phenomena is more likely to be responsible for the spontaneous Down states during slow oscillations of the cortex and in the Down state triggered by cortical or thalamic stimulation (Shu et al. 2003; Sanchez-Vives and McCormick 2000; Waters and Helmchen 2006; Timofeev et al. 2000;Contreras et al. 1996).

1.6.2 Up states of the neocortex

Up states are believed to be initiated in small recurrent cortical networks and are spread through interconnected neurons via synaptic connections (Massimini et al., 2004). During Down states, the cortical network is electrophysiologically 'quiet'. Any input to any subset of cells during Down state will trigger shared excitation and associated inhibition. Inhibition is obvious everywhere in the cortex. Any strong stimulus applied to the cortex evokes a clear inhibitory post-synaptic potential (IPSP) as a part of the response. If enough excitation is present, the network will re-excite itself explosively, and the cells will depolarize toward the Up states. It has been shown that slow oscillations can be seen in the absence of thalamic input to the cortex. Although the thalamus may regulate timing of slow oscillations in vivo, the cortex can create Up states without that input (Destexhe and Sejnowski, 2003).

Interestingly, in both Up and Down states, sensory stimuli can reach the cortex, although sensory-evoked potentials tend to be larger in Up state than in Down state (Toth et al., 2008). The Up-Down state transitions can be initiated in cortical slices of ferrets, rats and mice and cortico-thalamic slices of mice, although, in this case, the Down states are usually longer and the Up states are shorter than *in vivo* (Cunningham et al., 2006;McCormick et al., 2003;Rigas and Castro-Alamancos, 2007;Rigas and Castro-Alamancos, 2009). Anesthetics that increase K+ conductance or potentiate the action of GABA can prolong Down states. In contrast, cortical neurons in the waking state are consistently in Up state by virtue of the ascending cholinergic and monoaminergic systems that decrease K+ conductance (Luczak et al., 2007).

The firing pattern and rate of neurons in subcortical structures, including the striatum, globus pallidus, thalamus, subthalamic nucleus, substantia nigra and zona incerta is strongly correlated with the cortical slow oscillation (Balatoni and Detari, 2003; Bartho

et al., 2007; Bellocchio et al., 2000; Kasanetz et al., 2002; Magill et al., 2000; Tseng et al., 2001). It has been shown that the rhythm of the cortical Up and Down states is transmitted to subcortical structures via direct or indirect pathways and the coupling depends on the strength of cortical synaptic input to these subcortical structures (Bartho et al., 2007).

As previously described, various basal forebrain neurons populations, including cholinergic and non-cholinergic corticopetal cells, play a crucial role in the regulation of cortical activation by innervating most parts of the neocortex (Detari and Vanderwolf, 1987; Detari et al., 1997a; Detari et al., 1997b; Detari et al., 1999; Duque et al., 2000; Lee et al., 2005; Manns et al., 2000). However, in an electron microscopy study, the prefrontal cortex (PFC) was shown to be the only cortical area that sends projections to the BF (Zaborszky et al., 1997). Because of the exclusive nature of this connection that provides the only returning descending link from the cortex to the BF, it would be crucial to understand its anatomical and physiological characteristics.

1.7 Electrophysiological properties of neurons in the BF

In previous studies it has been revealed that the majority of BF neurons (so called F cells) have a strong positive correlation with EEG activity, meaning that cells showed increased firing rate during low-voltage fast activity (LVFA, $f > 16$ Hz) in urethane anaesthetized rats. A smaller group of cells (S cells) also showed correlation with the changes in EEG, but in this case there was an increase in the firing rate during slow wave activity (SWA, $f < 4$ Hz) and they stopped or reduced their firing rate during LVFA (Detari et al., 1997a; Detari et al., 1997b; Detari et al., 1999; Detari, 2000). In vivo extracellular recording with subsequent juxtacellular labeling and immunohistochemistry permitted further characterization of BF neurons (Duque et al., 2000; Manns et al., 2000; Manns et al., 2003). Cholinergic neurons correspond to one of the F cell populations, however, PV-containing, putative GABAergic neurons also belonged to the F category (Duque et al., 2000). Among the S cells, several neurons containing NPY were found. In an effort to characterize the functional relationship between the PFC and BF areas we were interested to distinguish what is the functional effect of prefrontal stimulation on BF unit firing.

Except for one study, that investigated with electrophysiological methods the connection between the dorsomedial part of the PFC and BF, no data are available how more ventral parts of the PFC afferents reach the BF (Golmayo et al., 2003;Sesack et al., 1989). We investigated the connection between BF and prefrontal areas by stimulating PrL/IL areas and recording single unit activity in the BF during EEG monitoring. Recording was followed by juxtacellular labeling of the recorded neurons, and an attempt to immunohistochemically identify the juxtacellularly labeled cells.

2 Proposal

The basal forebrain plays an important role in the activation of the entire neocortex via direct and indirect connections. In turn, however, the only cortical area that sends projections back to the BF is the prefrontal cortex, that plays an enormous role in many cognitive functions. The interconnection between the PFC and the BF has not been extensively studied so far, even though it represents a significant anatomical bond between these two areas. This thesis aimed to investigate the connection between the BF and the neocortex using different technical approaches such as electrophysiological recording, anatomical tracing and immunohistochemistry in rats.

Electrophysiological experiments

We addressed the following problems in acute, in vivo experiments on urethane anesthetized rats:

1. How do the spontaneous changes of cortical activity affect the activity level of BF neurons? What are the temporal associations between spontaneous cortical Up and Down states and single units in the BF?
2. How does the stimulation of the mPFC affect the firing properties of single BF neurons? What is the temporal the relationship between the effect of the mPFC electrical stimulation and basal forebrain unit activity?
3. Do the neuron populations that respond to either PCF stimulation or to spontaneous changes of cortical Up and Down states represent well segregated, anatomically differentiated cell groups in the BF?

Anatomical experiments

Using anatomical tracing methods, electrical lesions and immunohistochemistry, we were looking for the answers of the following questions:

1. What is the projection pattern of the descending axons from the mPFC to the BF?

2. Is there another neuron population, besides the PV containing neurons, in the BF that receives direct input from the mPFC?

3 Materials and Methods

3.1 Electrophysiological experiments

Our first set of experiments were carried out to investigate the electrophysiological properties of individual BF neurons recorded in urethane anesthetized rats and to examine their relationship with cortical Up and Down states. In short, first we recorded the normal firing patter of the BF neurons in relation to the changes of cortical activity. In the next step, we applied electrical stimulation in the mPFC while still recording the electrical activity of the same BF neuron, and finally an attempt was made to juxtacellularly label the BF neuron in question. During the whole procedure, ECoG was recorded from the M1/M2 area of the cortex.

3.1.1 Animal preparation

Experiments were performed on Wistar male rats (n=31) weighing 250-350 g. Animals were housed in temperature controlled environment and had free access to food and water. Animals were anesthetized with urethane (1.0-1.2 g/kg, i.p.), plus 4% lidocaine was injected on the site of the the cranial incision and into the ear canals. Supplementary doses of urethane were also given when slow wave cortical activity decreased. Animals showed no behavioral response to tail pinch during the experiment. Animals were fixed in a stereotaxic instrument (TSE Systems, Bad Hamburg, Germany). Square shaped holes were drilled according to the stereotaxic coordinates measured from the Bregma above BF areas. Body temperature was kept at 37˚C by a heating pad (SuperTech, Pecs, Hungary). All surgical and animal care procedures adhered to the guidelines for the use and care of experimental animals of the European Communities Council Directive and the local Animal Care and Use Committee. All efforts were made to minimalize the discomfort of the animals.

3.1.2 Electrode placement, electrophysiological recording and stimulation

Electrocortical activity (ECoG) was recorded by a transcortical bipolar electrode made of Teflon insulated stainless steel wire (diameter 125 um) at A: +2.0mm, L: 2.0 mm through a small drilled hole on the right hemisphere. The superficial electrode touched the pial surface, while the deep one reached 1.5 mm below the cortical surface. ECoG was filtered between 0.1-100 Hz amplified and sampled at 200Hz. The deep electrode was positive compared to the superficial.

Following craniotomy single unit activity from BF neurons was recorded with glass capillary microelectrodes (OD=2mm x ID=1.12, World Precision Instruments, Sarasota, FL, USA) pulled by a vertical puller (Narishige PE-2, Tokyo, Japan) to a tip size of 0.5-2μm. The electrode was filled up with 1.5-3% Biocytin (Sigma-Aldrich, Schelldorf, Germany) dissolved in 0.5 M NaCl solution resulting in a tip resistance between 10-25MΩ. The electrode was positioned 1.4 mm posterior, and 2.5-3 mm lateral from the Bregma and lowered 6 mm from the surface of the cortex after dura had been removed. The electrode was advanced slowly (approximately 20-30 μm/min) using a piezo-electronic positioner (Burleigh 6000 ULN, Quebec, Canada).

Prefrontal cortex (A: + 3.2mm, L: ± 0.5mm, D: 4mm) was stimulated with constant-voltage square-wave train pulses (I=0.5-1.5mA; delay=50ms; duration=0.3 msec; f=300Hz; n=3) delivered by a Master8 (AMPI, Jerusalem, Israel) stimulator through a bipolar stimulating electrode (d=0.5 mm, stainless steel) (Fig 6).

Following a 5-10-minute baseline recording three series of 35 stimulus trains each was given at different intensities. After the stimulation was completed, an attempt was made to label the recorded neurons using the juxtacellular filling method described by Pinault (1996). The glass micropipette was carefully advanced closer to the neuron, and Biocytin was ejected by applying positive current pulses for 5-15 min (0.1-10 nA, 300 ms duration, 50% duty cycle) through the bridge circuit of the amplifier (Axoclamp – A2, Axon Instruments, Molecular Devices, Sunnyvale, CA, USA).

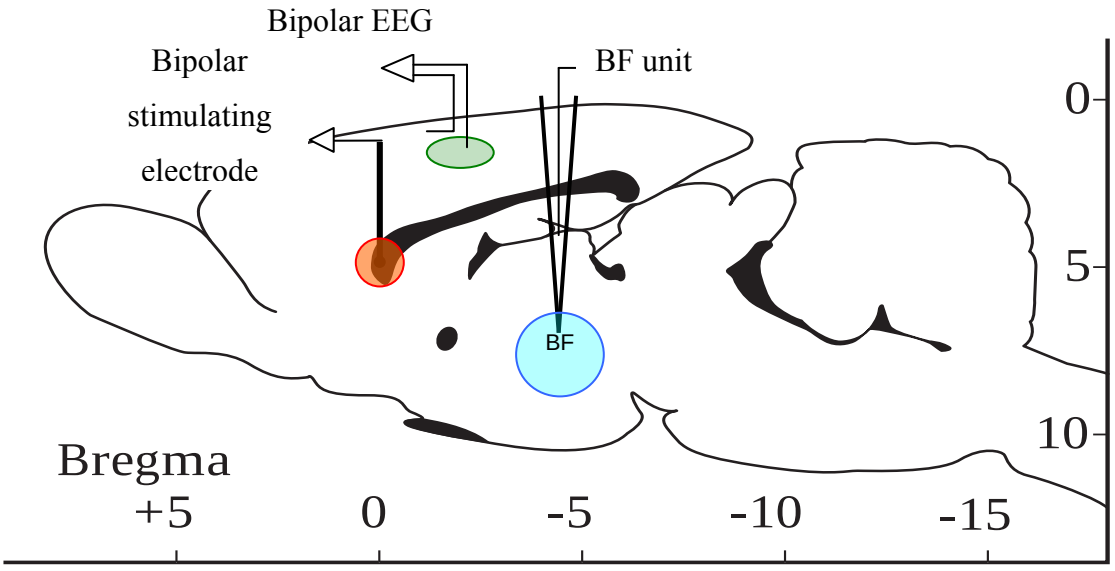

Figure 6. Experimental setup. Extracellular unit recording glass micropipette, filled with Biocytin was placed in the BF area, while cortical EEG was recorded with a bipolar electrode from the M1/M2 area of the neocortex. In addition, a third, bipolar stimulating electrode was aimed to reach the IL/PrL areas of the medial PFC.

3.1.3 Perfusion, tissue processing and immunohistochemical staining

Following the experiment, rats were perfused transcardially with 50 ml PBS at room temperature followed by 400 ml cold 4% paraformaldehyde diluted by 0.1 M PBS (pH 7.4). The brain was removed from the skull and post fixed overnight in the same fixative at 4˚C. The forebrain was cut by a Vibratome at 60µm thickness. Sections were collected from A: 0.5 to A: -2.5 mm from the Bregma. All histochemical procedures were performed using free-floating sections rinsed in 0.1 M PBS. After cutting and rinsing, sections were incubated in Cy3 conjugated Streptavidin–(1:500, Jackson Immuno Research, Suffolk, UK). The recorded and juxtacellularly filled neuron was found under an epiflourescence microscope (Olympus, BX51) and photographs were taken with a digital camera (FlouViewII Software) connected to the microscope. The labeled soma was processed for immunostaining for choline acetyltransferase (ChAT) and PV in the case of F cells, and neuropeptide-Y (NPY) and somatostatin (SS) in the case of S cells. To detect immunoreactivity the following antibodies were used: mouse anti-choline acetyltransferase

monoclonal antibody (1:250, 1% Triton-X, Chemicon Int., Temecula, CA, USA) to visualize cholinergic cells followed by FITC- conjugated donkey anti - mouse IgG (1:300, Jackson Immuno Research); goat anti-PV (1:1000, 1% Triton-X, Swant, Bellinzona, Switzerland) followed by FITC- conjugated donkey anti - goat IgG (1:300, Jackson ImmunoResearch). Following incubation in the primary and secondary antibodies, sections were washed two times in PBS at room temperature then incubated in ABC (1:500, VectorLab, Burlingame, CA, USA) overnight at 4˚C. They were rinsed two times in PBS and once in Tris-buffer (TBS, pH 7.4) and placed in TBS containing DAB (0.025%, Sigma-Aldrich), nickel sulfate (1%,) and ammonium chloride (1%) for 10-15 minutes. Reaction was stopped by extensive rinsing in PBS. Sections were than mounted onto gelatine-coated slides, dehydrated and cover slipped with DepEx (Serva, Heidelberg, Germany). If no cell bodies were found after Cy3 conjugated Streptavidine incubation, sections were mounted and Nissl-stained to visualize all the cell bodies and the electrode tracks.

3.1.4 Data analysis

Data processing was generally performed using MatLab 7.1 (MathWorks, Natick, MA, USA) and Spike software (Cambridge). Cortical Up states were detected by finding negative deflections below two standard deviations on the EEG. Perievent-Time-Histograms (PETHs) were calculated around the local minimum of the Up states. A peak in a PETH was defined significant when at least one of the bins exceeded 95th percentile of the baseline mean (assuming a Poisson distribution, MATLAB ‘poissinv’ function). Similarly, inhibitory troughs were considered significant at least one bins were below 5th percentile of the baseline mean. Peaks and troughs of the spike triggered average (STA) of the EEG were calculated from between -5 to 5 sec relative to the spikes in the BF. The baseline (control number of spikes) was calculated between -2 to 4 secs on the PETH.

Baseline spike trains (5-10 min) were analyzed (Spike and Origin 6.0 software) to obtain mean firing rate and coefficient of variation values, to construct interspike interval histograms, and to test correlation between EEG waveforms and unit firing pattern. To determine characteristics of spike shapes, several spontaneous discharges were averaged using the same filtering conditions (300 Hz-10 kHz). Three variables of spike shape have

been calculated as described below. The width of the spikes was measured between the beginning of the first peak and the end of the first trough or the top of the second peak if there was any. The amplitude of the whole spike was calculated between the largest positive and negative values.

3.2 Anatomical experiments

In order to find anatomical evidence whether or not SS and NPY containing neurons in the BF receive direct input from the medial PFC, an anterograde tracer, biotinylated dextran-amine (BDA), was injected into the IL and in some cases into the PrL regions of the mPFC and BF sections were processed for double immunolabeling for BDA (NiDAB) and SS or NPY (DAB).

3.2.1 Animal preparation and anterograde tracer injection

Experiments were conducted on Sprague-Dawley rats (n=20) weighing between 260 and 290 grams housed on a normal 12:12 h light-dark cycle with food and water ad libitum. The animals were initially anaesthetized with ketamine – xylazine (100 mg/25 mg/kg ip). After anesthesia rats were placed on a stereotaxic frame. Sagittal incision was made along the midline of the head and the skull was exposed. A 2x2 mm craniotomy was performed on the prefrontal skull at 3.2 mm anterior to bregma and 0.5 mm lateral to the midline. Coordinates were based on the Watson-Paxinos Rat Brain atlas (Paxinos et al., 1980). The iontophoretic injections of the anterograde tracer were carried out by using a glass micropipette with a tip diameter of 20-40 μm filled with 10% BDA dissolved in saline. After lowering the pipette to the IL/PrL area (4.5-5 mm from the surface) we applied 5-7 μA positive current pulses (100 msec of duration at 2 Hz) for 15-20 minutes. The opening of the craniotomy was then covered with a piece of a sterile gelfoam and the surgical incision was closed.

For light microscopy (LM) procedures after 7 days survival time, the animals were overdosed with urethane and were perfused transcardially first with 200 ml of 0.9% saline

in 0.1 M PBS followed by 500 ml fixative containing: 4% paraformaldehyde (PF), 0.1% glutaraldehyde and 15% picric acid. Brains were removed and stored overnight in the same fixative as described above but without glutaraldehyde. Brains used for light microscopy were immersed into 30% sucrose in PBS overnight, frozen on powdered dry ice, and sectioned at 50 μm with a cryostat. Sections were collected from A: 0.5mm to P: -2.5 mm from the Bregma.

For electron microscopy (EM), animals were sacrificed after 3 days of survival time and were transcardially fixed with 50 ml 0.1M PBS (pH 7.4) followed by the fixative of: 100ml 2% PF and 4% acrolein in the first step and finally 200 ml 2% PF. Brains were removed and post fixed in 4% PF at 4C overnight. For embedding for electron microscopy, serial sections (50 μm) were prepared on a Vibratome and the same procedures were carried out.

3.2.2 Electrical lesion of the medial prefrontal cortex

Experiments were conducted on Sprague-Dawley rats (n=20) weighing between 260 and 290 grams housed on a normal 12:12 h light-dark cycle with food and water ad libitum. The animals were initially anaesthetized with ketamine – xylazine (100 mg/25 mg/kg ip). Animals were placed in a stereotaxic frame. A 2x2 mm craniotomy was performed on the prefrontal skull at 3.2 mm anterior to bregma and 0.5 mm lateral to the midline and was followed by electrical lesion of the medial prefrontal cortex was carried out by a bipolar electrode. After lowering the electrode to the IL/PrL area (4.5-5 mm from the surface) we applied 5-10 mA positive current pulses for 1-3 minutes. The opening of the craniotomy was then covered with a piece of a sterile gelfoam and the surgical incision was closed. After 24-48 hours of survival time the animals were perfused with 300 ml of 4-5 % paraformaldehyde buffered with 0.1 M cacodylate. For light microscopy, the degeneration was visualized by using silver staining for terminal degeneration and lysosomes (Gallyas et al., 1980c). For electron microscopy studies, a different set of animals after the electrical lesion procedure were sacrificed and perfused with 50 ml 0.1M PBS (pH 7.4) followed by the fixative of: 100ml 2% PF and 4% acrolein in the first step

and finally 200 ml 2% PF. Immunohistochemistry was followed as described below for various markers of neurotransmitters.

3.2.3 Immunohistochemistry for light microscopy

All the treatments described below were carried out at room temperature unless otherwise specified. After rinses in PBS (2 x15 minutes), groups of sections were treated with sodium borohydride [1% sodium borohydride (Sigma) in PBS, 20 minutes] to remove aldehyde groups which were followed by a thorough rinse in PBS again (3 x 15 minutes). To reduce background and prevent any possible cross reaction during the subsequent immunocytochemical procedures, the sections were treated in hydrogen peroxide (1% hydrogen peroxide in PBS, 10 minutes) to reduce intrinsic hydrogen-peroxide activity. Before incubation in antibody solutions, the sections were treated with normal serum [2% normal goat serum (Jackson Immunoresearch Laboratories, West Grove, PA) in PBS, 30 minutes] to prevent nonspecific antibody binding. This was followed first by the mixture of the A and the B component of the avidin/biotin standard kit (Vector Laboratories; 1:500 each in PBS, 30 minutes each). The NiDAB precipitate was silver-gold intensified as described earlier (Gallyas et al., 1980a;Liposits et al., 1984). For the visualization of BDA series of sections were developed with Ni-DAB. Between each incubation step, the sections were rinsed in PBS for 2 x 15 minutes. Prior to development, 2 x 15 minute rinses in Tris-buffered saline [TBS: 38.5 mM Trizma hydrochloride (Sigma), 11.5 mM Trizma base (Sigma), 154 mM sodium chloride, 0.01% thimerosal, pH 7.60) were utilized to increase pH stability. The peroxidase reaction was carried out using the nickel-enhanced diaminobenzidine (NiDAB) chromogen [20–30 minutes incubation in a developer solution containing 0.4 mg/ml 3,3-diaminobenzidine tetrahydrochloride (DAB; Sigma), 0.4 mg/ml nickel ammonium sulfate (Fisher Scientific, Pittsburgh, PA), 0.4 mg/ml ammonium chloride (Fisher Scientific), and 0.006% hydrogen peroxide dissolved in TBS] that revealed adrenergic fibers in black.

To visualize SS -positive structures, the sections already labeled for BDA underwent further immunohistochemical processing. The sections were first incubated rat-anti-somatostatin antibody (1:50 48 hours at 4C) with 0.1% Triton-X as the primary antibody followed by a biotinylated goat-anti rat IgG (Jackson Immunoresearch

Laboratories; 1:300 in the antibody diluent, overnight) followed by the Vectastain peroxidase ABC (1:500 in PBS, 2 hours). The peroxidase reaction was carried out using a developer solution containing 0.4 mg/ml DAB and 0.0006% hydrogen peroxide dissolved in TBS that resulted in the development of brown deposits in somatostatin containing profiles. The sections were mounted onto glass microscope slides from elvanol [0.3% polyvinyl alcohol 70,000 (Sigma), 30 mM ammonium acetate (Sigma), and 0.1% sodium azide], air dried overnight, cleared in xylenes (Fisher Scientific; 2 x 10 minutes), and coverslipped with DPX (Electron Microscopy Sciences).

For NPY staining we used rabbit-anti-NPY antibody (kindly provided by Dr. Istvan Merchenthaler, University of Maryland, Baltimore) followed by a biotinylated goat-anti-rabbit IgG secondary antibody. The same DAB procedure was carried out to visualize NPY as in the case of the SS-containing neurons.

To visualize CB (rabbit-anti-CB, 1:1000) and CR (rabbit-anti-CR, 1:1000) positive profiles we used primary antibodies (48 hrs at 4C with 0.1% Triton-X) followed by a biotinylated goat-anti-rabbit IgG secondary antibody. The same DAB procedure was carried out to visualize CB and CR positive neurons as in the case of the SS-containing neurons.

3.2.4 Immunohistochemistry for electron microscopy

The sections for electron microscopy were also double stained for BDA and SS, NPY, CB and CR in generally the same way as the same way as for light microscopic immunoperoxidase labeling, although the preservation of ultrastructural details required some modifications. For this purpose, the Triton X-100 was completely omitted from all solutions. Instead, before treatment in normal serum, the tissue was cryoprotected in 30% sucrose overnight at 4°C then the sections were freeze-thawed sequentially three times in liquid nitrogen fumes. Also the thioglycolic acid pretreatment was omitted from the protocol for electron microscopy. The double-immunostained sections were osmicated [1% osmium tetroxide (Electron Microscopy Sciences) in PBS, 40 minutes] and then dehydrated in an ascending series of ethanol (30–50–70–90–100%). For contrasting, the tissue was treated with uranyl acetate [1% uranyl acetate (Electron Microscopy Sciences)

added to the 70% ethanol, 30 minutes]. After treatment with propylene oxide (Electron Microscopy Sciences; 2 x 5 minutes), the sections were soaked in durcupan (Fluka Chemie AG, Buchs, Switzerland; overnight) then flat embedded between liquid release agent-pretreated (Electron Microscopy Sciences) microscope glass slides and cover slips. Side-to-side contacts between BDA boutons and somatostatin or NPY containing profiles, suggestive of synaptic input, were selected under the light microscope. The selected structures were documented using a Zeiss Axiocam digital camera. Small tissue pieces containing the selected appositions were cut out and mounted onto blank durcupan blocks. Ribbons of ultrathin sections were cut on a Reichert Ultracut E ultramicrotome and picked up onto formvar-coated (Electron Microscopy Sciences) single-slot grids. The ultrathin sections were analyzed on a Philips Tecnai 12 transmission electron microscope, and pictures were captured using a Gatan BioScan digital camera.

3.2.5 Digital image processing

When it was necessary, contrast and lightness were adjusted on digitally produced pictures. All groups of pictures were assembled and lettering was added using Adobe PhotoShop 7.0.

4 Results

4.1 Electrophysiology and PFC stimulation

As a result of the electrophysiological measurements, a total of 57 neurons in the BF were studied. First we categorized these neurons based on their relationship to the cortical activity and on their response to tail pinch (TP) stimulation. Units were characterized as F cells if their activity increased due to TP stimulation or spontaneous desynchronization. In contrast, the activity of S cells decreased following TP stimulation and/or was only active during spontaneous cortical slow waves. Out of all the recorded neurons, 41 (72%) increased their discharge rate when LVFA was present in the cortical EEG (F cells) and 9 (15%) showed increased firing rate during SWA (S cells). In addition, 7 neurons (13%) showed no correlation with any EEG pattern (Fig. 7).

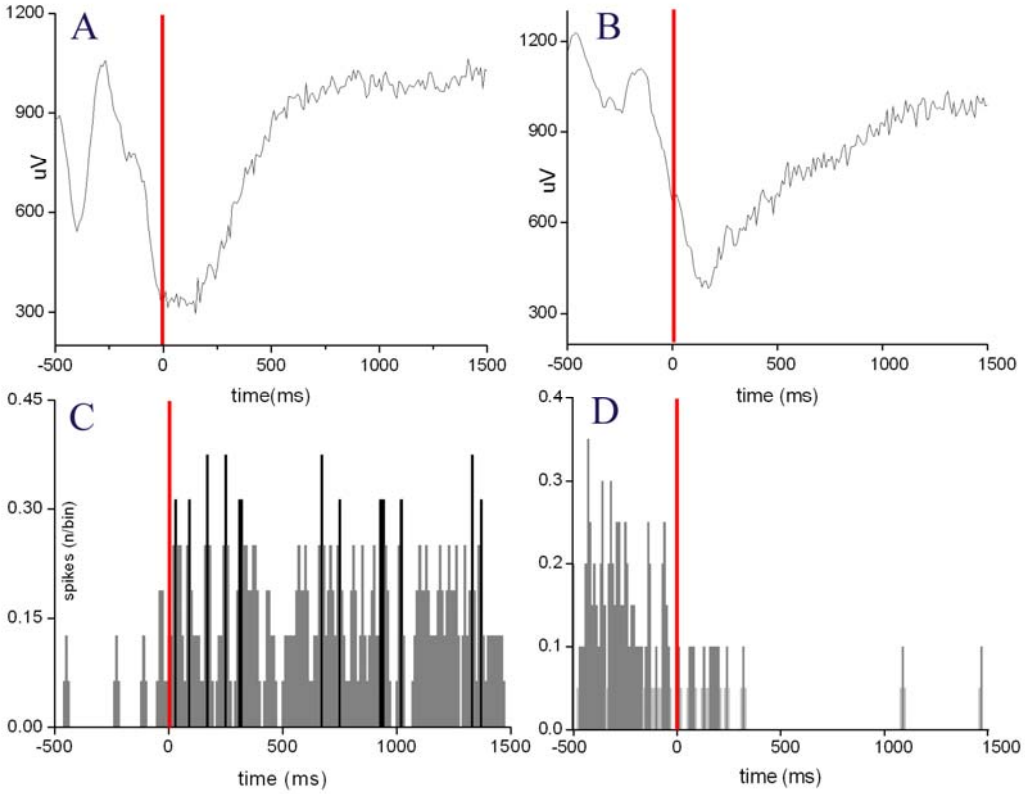

Figure 7. Representative samples of changes in the EEG (A, B) and F and S cell activity (C, D) evoked by 2-5 tail pinch stimuli. A, C) A typical response of F cells was an increase

in firing rate after tail pinch. Note that the number of spikes increased almost four times and remained at that level while desynchronization was present in EEG. B, D.) Due to tail pinch, S cells suspended their firing for a shorter or longer period of time in close correlation with cortical desynchronization (bin width=10 ms). Red line marks beginning of TP.

After the inspection of the stimulation sites in the prefrontal cortex we found that 47 out of 57 stimulation sites were in the infralimbic (IL) area of the medial PFC and in 10 cases the electrode track was found in the prelimbic (PrL) area (Fig. 8).

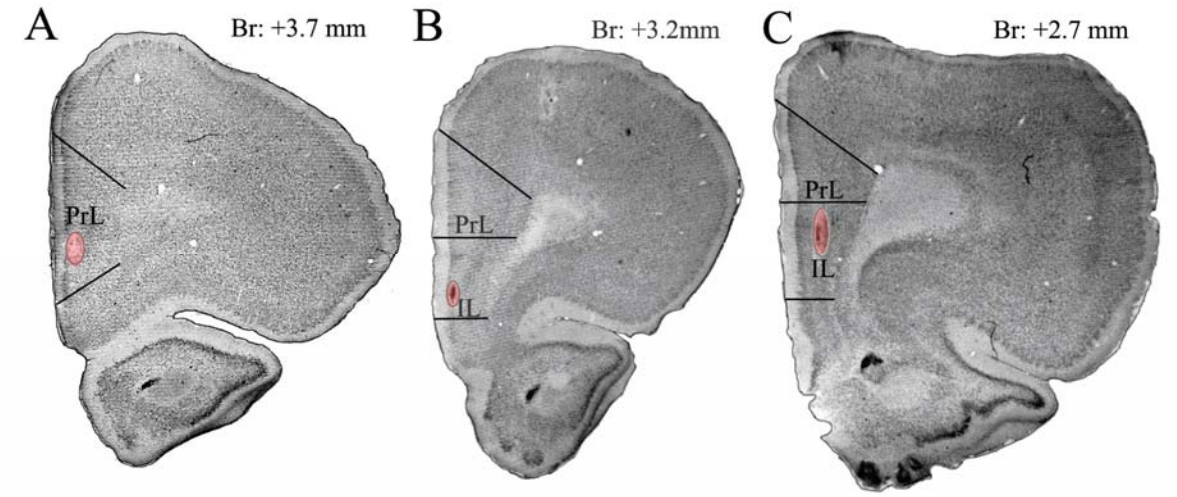

Figure 8. Location of PFC stimulating electrodes. After the immunohistochemical procedures were carried out, stimulating electrode tracks were located in the PFC. Stimulation sites are labeled with red and were detected between +3.7 mm to +2.7 mm anterior to Bregma.

Stimulation effects showed no correlation with the exact position of the stimulating electrode, suggesting that both PrL and IL regions of the mPFC are indeed connected to the BF. F and S cells could be further sorted based on their responses to PFC stimuli. We found that 28/41 F and 8/9 S cells responded to PFC stimulation (Fig 9). The majority of the F cells showed excitation (F/+; n=8) then their activity returned to the background level. Another group of F cells (F+/-) showed massive positive response followed by a long depressed period (n=8). In contrast, a smaller group of F cells (n=6) expressed a short

negative, inhibitory response (F/-) while another 6 cells showed a long inhibition (F/--). In the case of S cells we found a group that showed inhibition (n=6) and a smaller, but clearly defined group (n=2) showing excitation in response to PFC stimuli. Pre-stimulus firing rates in the four groups of F cells during the 5 min period prior to stimulation showed significant (One-Way ANOVA; $p \leq 0.05$) differences: F/+ (0.85±0.31 Hz); F +/- (5.13±1.62 Hz); F/- (12.5±2.5 Hz); and F/-- (7.91±24 Hz) (Fig. 9). Due to the low number of S cells no similar analysis could be performed for these population, however we found the firing rate of the S cells to be 8.44±4.38 Hz (n=7). Latencies of both excitatory and inhibitory responses varied between 10 and 150 msec.

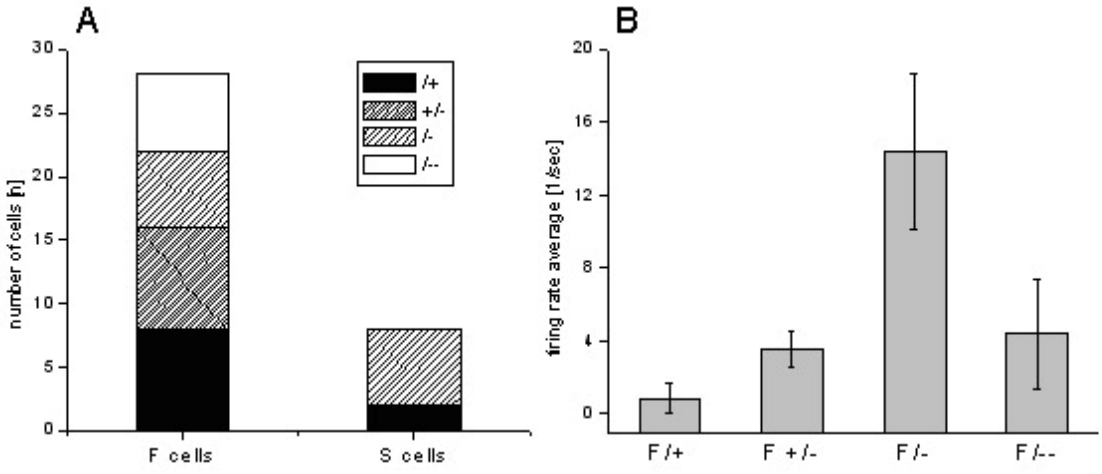

Figure 9. (A) Distribution of F and S cells between the different response categories. (B) Background firing rates of F cells before PFC stimulation in the different response categories. F cells that showed an immediate and short inhibitory response to PFC stimulation had significantly higher firing rates (12.5±2.5 Hz; n=6), than F cells showing excitation (0.85±0.31 Hz; n=6).

4.1.1 EEG field potentials

Following stimulation of the PFC, averaged evoked potentials in the M1/M2 area of the neocortex showed mostly similar features in terms of the shape of the response, however, the amplitude of the large positive waves were different (Fig 10). The field potential waves consisted of an early negative component, lasting up to 50 ms and a late, positive component, with duration of about 500ms. In most cases, firing of BF neurons increased and decreased closely following the positive and negative components of these

evoked field potentials. When the negative component was correlated with increased unit activity in the BF, the positive component of the evoked potentials was expected to correlate with decreased BF neuronal activity. This alternation was a general pattern that has been observed regardless of cell types or responses given to prefrontal stimulus. Facilitation was always followed by inhibition in the activity of the BF units in correlation to the field potential activity. During our recording, the deep electrode represented positivity against the superficial electrode on the surface of the cortex.

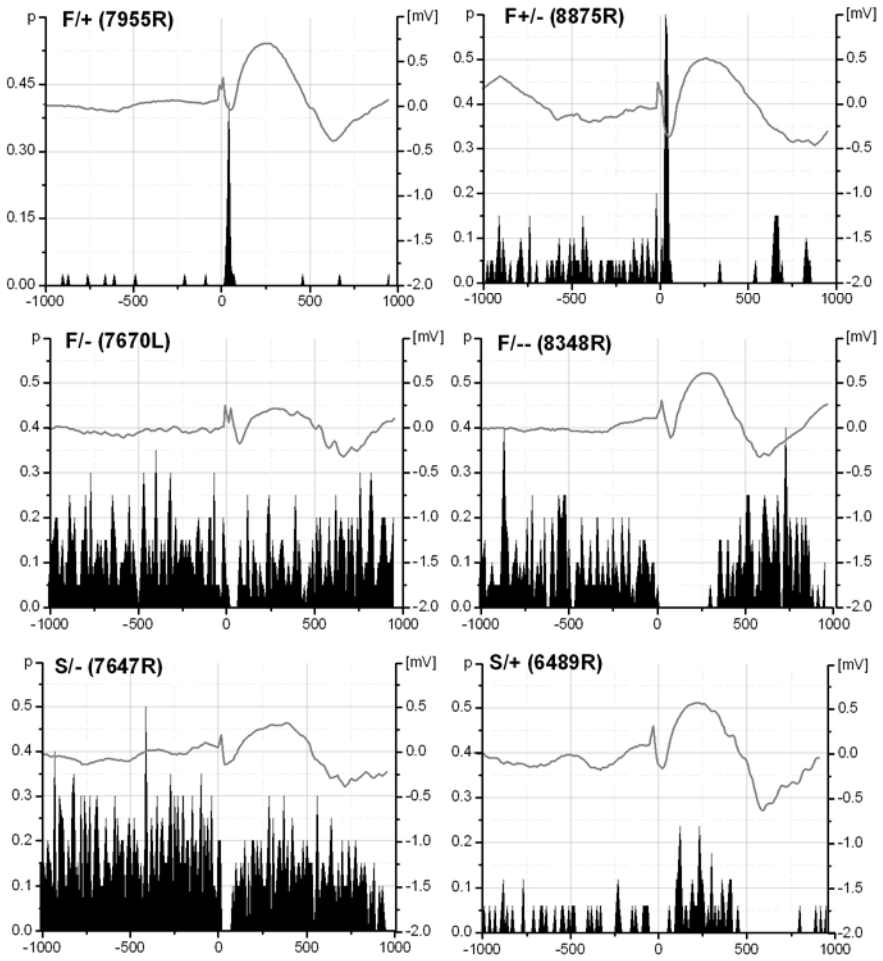

Figure 10. Diversity of changes in neuronal activity in F-, and S-cells following PFC stimulation. Most of the F and S cells responded to PFC stimuli showing inhibition or facilitation, though among F cells, a higher degree of diversity was found. Inhibitory responses were more frequent in neurons with higher background activity while facilitation

occurred in those cases when the neurons showed relatively low discharge rate. Curves show averaged cortical evoked potentials recorded from the M1/M2 cortical areas.

4.1.2 Juxtacellular labeling, localization and identification of the neurons

After PFC stimulation was completed, a total of 22 cells were successfully labeled with Biocytin. Biocytin positive neurons were distributed through the substantia innominata (SI) (n=12), globus pallidus (GP) (n=9) or located at the border of the striatum (n=1). The distribution of the F and S cells overlapped and no separation was found in respect to the different PFC stimulus responses either (Fig. 11).

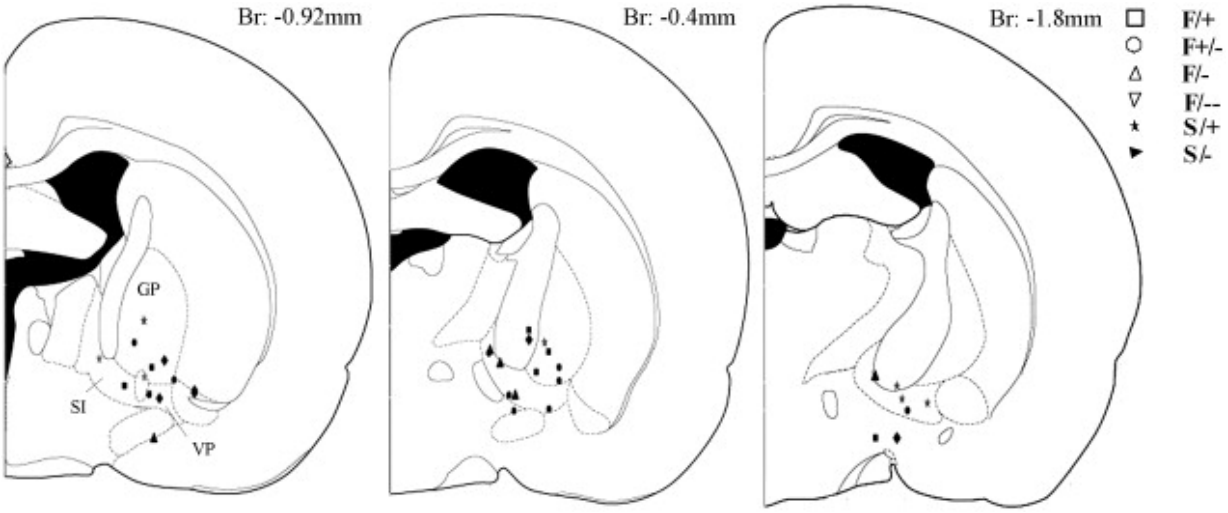

Figure 11. Distribution of biocytin labeled neurons after PFC stimulation in the BF areas. Most of the neurons were located in the SI, GP or at the border of the striatum.

Out of the 22 Biocytin-labeled cells, 21 neurons matched the criteria of F cells and one neuron was classified as S cell based on the criteria described above. Two neurons were successfully identified by immunohistochemical methods: one contained ChAT, while the other PV (Fig. 12). The PV cell was excited with short latency (10 ms) by the PFC stimulation. In contrast, inhibition with long latency (100-300 ms) was seen in the

case of the cholinergic neuron. In both identified cells, neuronal firing showed strong correlation with the changes of the field potential in the cortex and followed closely the PFC stimulus (Fig. 13).

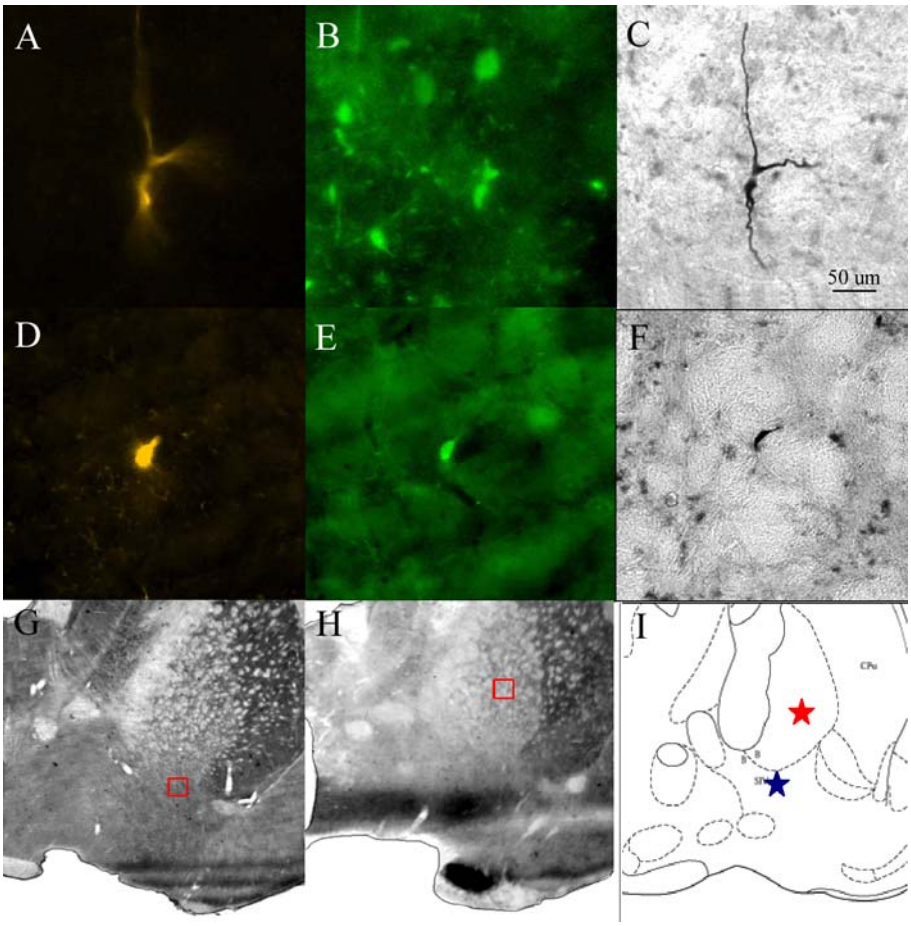

Figure 12. Identified cholinergic and PV containing neurons in the BF. Digital photographs of juxtacellularly labeled and identified PV-containing (first row A, B, C) and cholinergic (D, E, F) neurons. A, D) Cy3-conjugated Streptavidine staining. B) FITC-conjugated donkey anti - mouse IgG to visualize Ms-anti-ChAT staining. E) FITC-conjugated donkey anti - goat IgG to visualize Gt-anti-PV staining. C, F) neurons developed with Ni-DAB. G, H) Location of the PV-containing and ACherg neurons, respectively, marked by a small red square. I) Location of the two identified neurons on a schematic figure from rat brain atlas. ★ represents the cholinergic neuron, while ★ stands for the PV containing cell. Scale bar on picture C is 30μm.

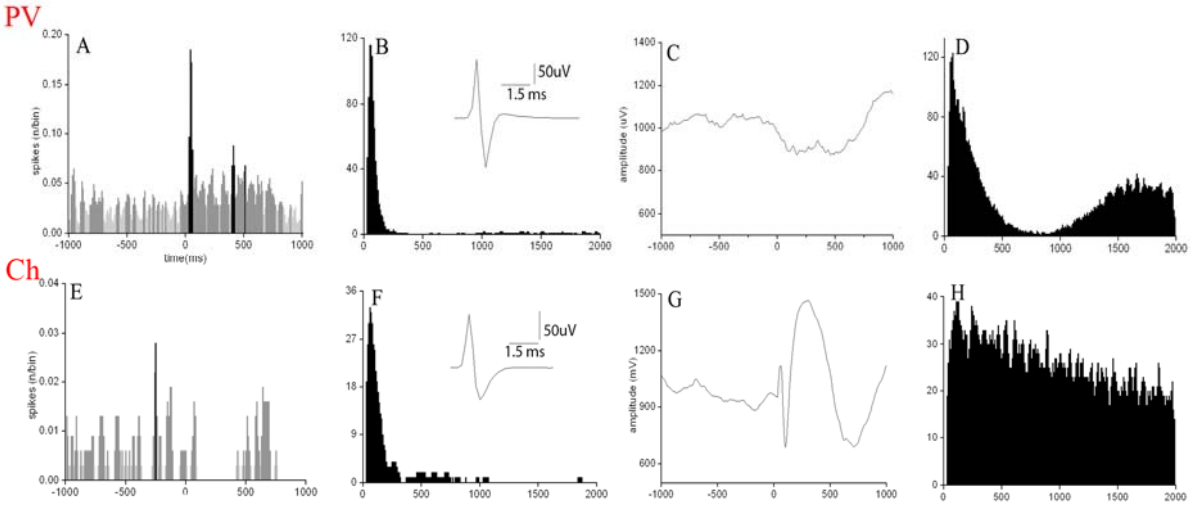

Figure 13. Electrophysiological properties of the identified PV containing and cholinergic neurons in the BF. Analysis of the identified parvalbumin (first row) containing and cholinergic (second row) neurons. A, C) shows the averaged post-stimulus-time-histogram (PSTH) of the PV cell and the simultaneous EP (evoked potential), respectively, following PFC stimulation. Please, note the considerable positive peak in the unit activity E) PSTH for the identified cholinergic neuron, in which case only a minor change in the discharge activity compared to the baseline activity was observed. G) Averaged EP in this case. B, D) and F, H) show the intervallum histogram and autocorrelogram of the unit activity of the PV and the cholinergic neuron, respectively. Insets in panels B and F illustrate the spike shapes of the neurons. While the spike width of the two neurons were approximately the same (0.8-2ms) the difference in the spike amplitude was remarkable

4.1.3 Morphometry

After immunohistochemical analysis, sections were processed for NiDAB, to study juxtacellularly filled neurons under the light microscope. Altogether 19 cells were recovered out of 22. The loss of numbers of the labeled neurons was due to severe damage on the sections that undergone several immunohistochemical procedures. The average diameter of the juxtacellularly filled neurons was 18.36±8.1 µm and 17±4.7 µm of their longer and shorter axis. The vast majority of the cells were small to medium sized (10-25 µm in horizontal and vertical expansion) but 23% of the neurons were in the range of 25-35 µm. After measuring the horizontal and vertical diameters of each neuron we expressed the quotient of the values by dividing the larger value by the smaller one. Those cells in which the quotient was between 1.00 and 1.2, i.e. less than 20% difference were

considered to be round, while a quotient larger than 1.2 indicated an ovoid neuron shape. Using Statistica 7 (StatSoft, Tulsa, OK, USA) software, we found 13 neurons to have ovoid cell body shape while 6 were categorized as having round shaped cell bodies. We applied a 2x2 contingency table to examine the relationship between positive or negative responses to PFC stimulation and the shape of the soma. We found that ovoid shaped neurons gave significantly more positive responses, while round shaped neurons were more frequently inhibited following PFC stimulus than expected (degree of freedom = 1; chi-square = 4.38; p = 0.0363).

We also tested if there is any correlation between spike shape and neuronal geometry. Spike width in ovoid shaped neurons (1.69±0.42 ms, mean±SD) was smaller than in round shaped ones (1.9±0.44 msec – ($p \leq 0.05$)). Peak-to-peak amplitude of spikes generated by ovoid shaped cells were significantly bigger (219±80 μV) compared to the round shaped cells (142±33 μV, $p \leq 0.05$).

4.1.4 Relationship between cortical up and down states and BF unit activity

By inspecting the firing pattern of the recorded neurons in correlation with cortical Up and Down phases, we found three distinct activity patterns. Many cells (22/51, 43.1%) fired phase-locked to the cortical Up states (Fig. 14 A, Up state-on cells) with a significant excitatory peak on the Up-state triggered PETH (Fig. 14F), and a negative peak on the spike-triggered average (STA, Fig 14G). Up states are represented as negative deflection, showing downward signals on our recordings. A minority of cells (6/51, 11.7%), while tonically active during Down states, decreased or ceased firing during Up states (Fig. 15A, Up state-off cells), thus displayed a significant inhibitory trough on the PETH (Fig. 15F), and a positive peak on the STA (Fig. 15G). The rest of the cells (23/51) either did not show any significant changes, or their firing was completely independent of Up and Down states. Based on their inhibition and excitation indexes, these groups of neurons reveal well segregated neuron populations (Fig. 16). The Up state-on cells form a distinct group, while the Up state-off cells are contiguous with the non-significant cell group.

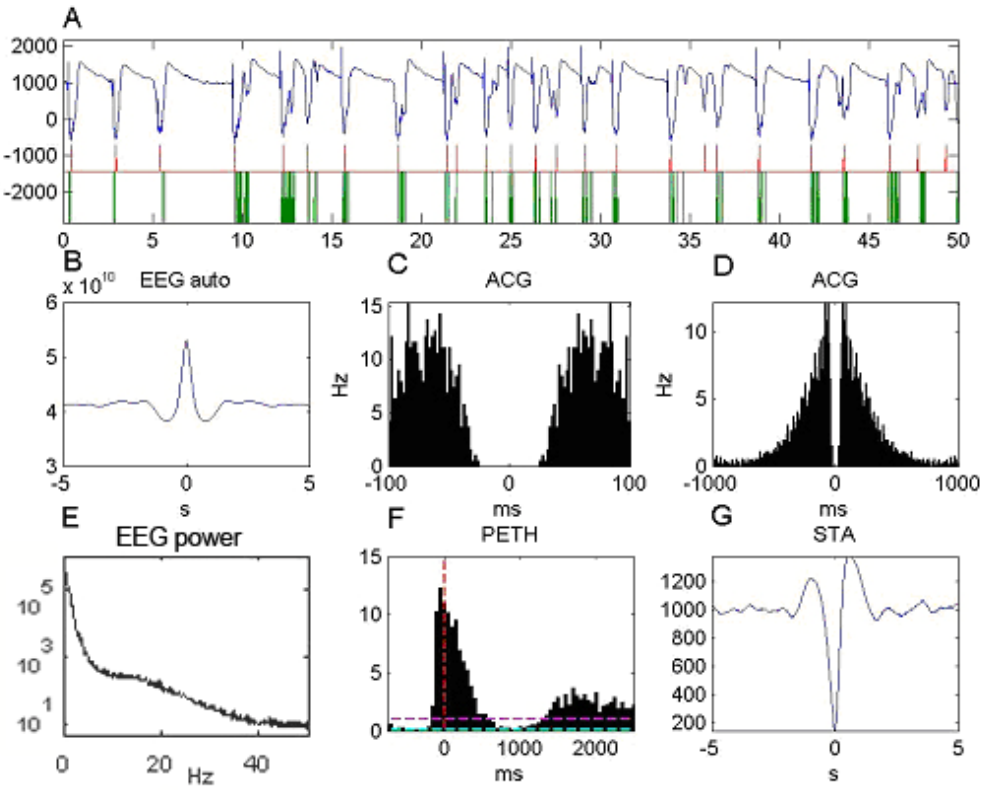

Figure 14. Representative example for an Up state-on neuron. A) Raw EEG and unit activity showing significant correlation between up states and unit activity. Red tracks represent the peaks of Up states, while the green tracks correspond with the BF unit activity. Because of the negativity in the field potential, Up states are negative deflections that are presented as a downward line in our recordings. B) EEG autocorrelogram figures demonstrate the rhythmical activity of the EEG during our recording. E) We found a peak in the EEG power at less than 1Hz. The last two figures show the Up state triggered peri-event time histograms (PETHs). The horizontal dotted lines represent the lower and the upper limits of the confidence interval (F) and spike triggered average (STA) of the EEG waves that show a strong BF unit-Up state locked relationship (G).

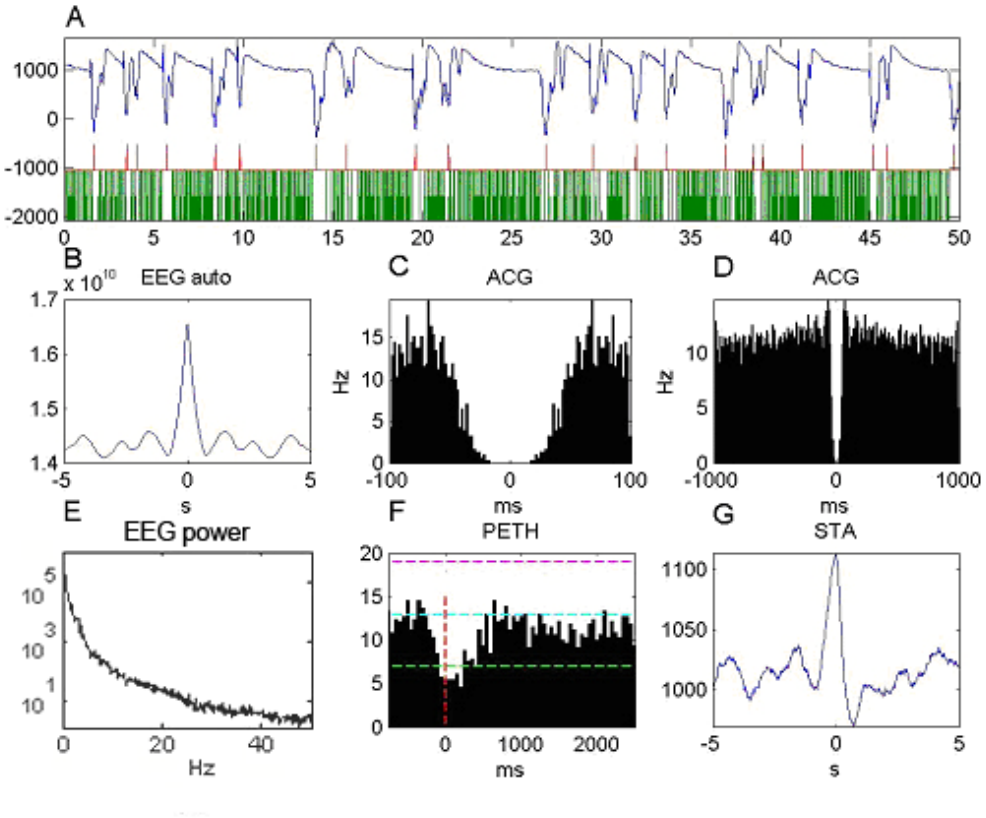

Figure 15. Representative example for Up state-off neurons. A) Raw EEG and unit activity showing significant correlation between up states and unit activity. B) EEG autocorrelogram figures demonstrate different groups of neurons found in the BF based on their correlation to cortical slow oscillation. Figures show the Up state triggered peri-event time histograms (PETHs) (F) and spike triggered average (STA) EEG waves (G).

The three groups, separated according to their correlation with cortical UP states, were different in other respects as well. We found that the mean firing frequency of up state-on cells was significantly (One-way ANOVA; $p<0.05$) lower (3.17±0.8 Hz) compared to up state-off cells (14.88±3.08 Hz) or non-correlated neurons (9.73±1.02 Hz).

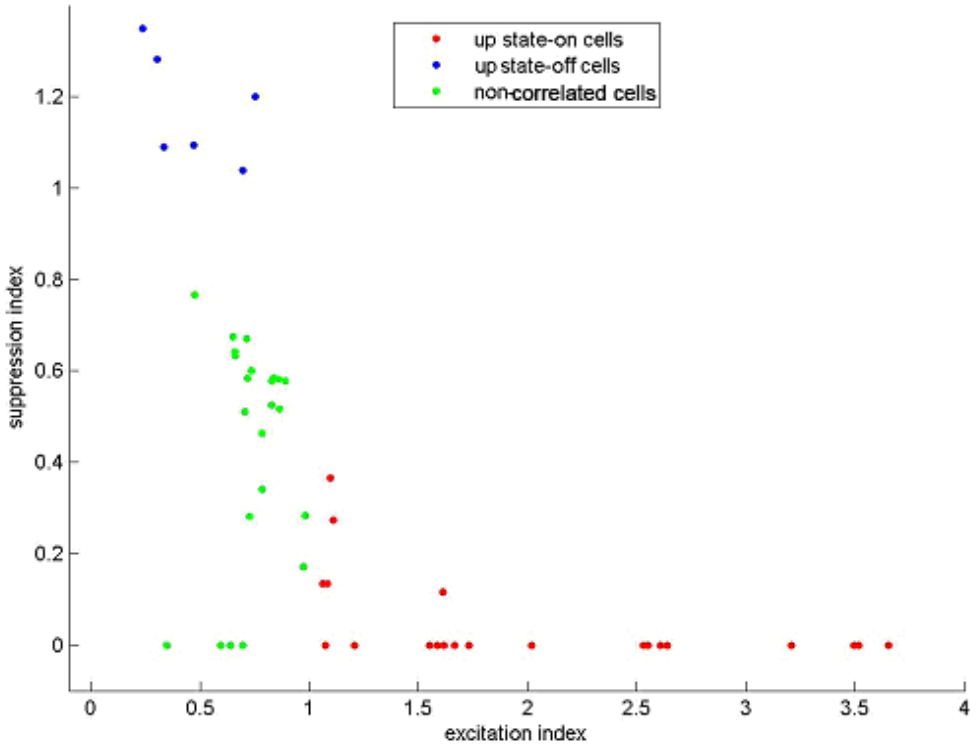

Figure 16. Diagram showing the correlation between the three different groups and their suppression (inhibition) and excitation index. Inhibition and excitation indexes are representing the percentage of how much the activity of the given neuron crossed the line of the 95% confidence interval of the PETH. Up state-off cells are clearly separated having a relatively high inhibition index, while up state on cells are mostly have high excitation index, however it is expanded on a wider range.

We found that changes in the BF neuronal firing occur with a delay in every case that we recorded (0.28±0.036 sec, in case of facilitation and 0.14±0.006 sec in case of inhibition) in relation to the onset of the Up state. The heterogeneity of BF neurons in terms of electrophysiology is further supported by the observation that out of 22 Up state-on cells, using the criteria of Detari et al (1997), we identified 14 F cells and 1 S cell, while from the 6 up state-off cells there were 4 F cells and 2 S cells. These findings show that F and S cells do not completely correspond to Up state-on or Up state-off cells.

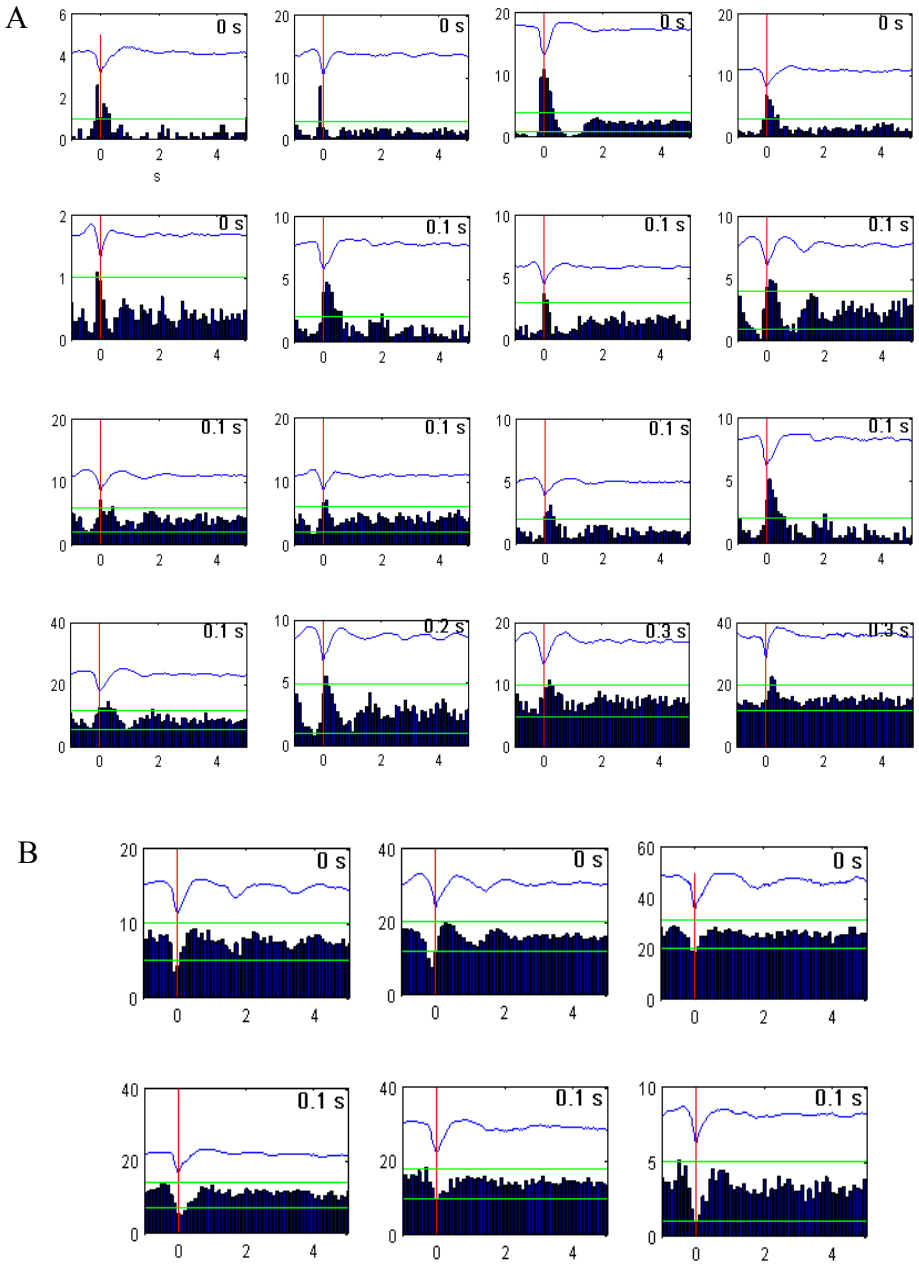

Figure 17. Up state triggered peri-event time histograms (PETH) in neurons that were excited (A, n=16) or inhibited (B, n=6) during Up states. Green lines indicate confidence intervals assuming Poisson distribution, while the red line shows the peak of upstate. The blue line is the averaged EEG at point 0 (the peak of the Up state) showing the averaged shape of the Up states. The right corner insets indicate the latencies from the peak of Up state in every recorded neuron, that showed a significant correlation with the cortical Up state. Axis x represents time (s), axis y shows number of spikes (counts).

The spike width was also different in these three groups. In the Up state-off cells, it was significantly longer (2.15±0.25ms) compared to the Up state-on cells (1.6±0.09 ms), while in the case of the none-correlated neurons, the width was between these two values (1.7±0.12 ms). Spike amplitudes turned out to be significantly different in the three groups, by using a one-way ANOVA test ($p<0.005$). We found that the amplitude of Up state-on cells was the highest (181.0±18.66μV), while the amplitude of both the Up state-off (135.9±9.68μV) and non-correlated (130.0±6.24 μV) neurons were lower and differed significantly.

We identified the localization of 13 Up state-on and 6 Up state-off neurons, as well as 19 non-correlated neurons in the BF by either localizing the biocytin labeled cell bodies or locating the electrode track on Nissl stained sections (Fig 18A-B). However, our spatial analysis revealed no correlation between the localization of these cells and their association with cortical state changes. With few exceptions, the recorded neurons were located in the cholinergic areas of the BF. From this pool of neurons, 16 cell bodies that were successfully labeled with biocytin and recovered. We measured the longest extension of the cells, and the diameter perpendicular to it. Both measures were significantly larger in Up state-on cells than in non-correlated neurons. Since no Up state-off cell was successfully labeled, this comparison cannot be done on that group.

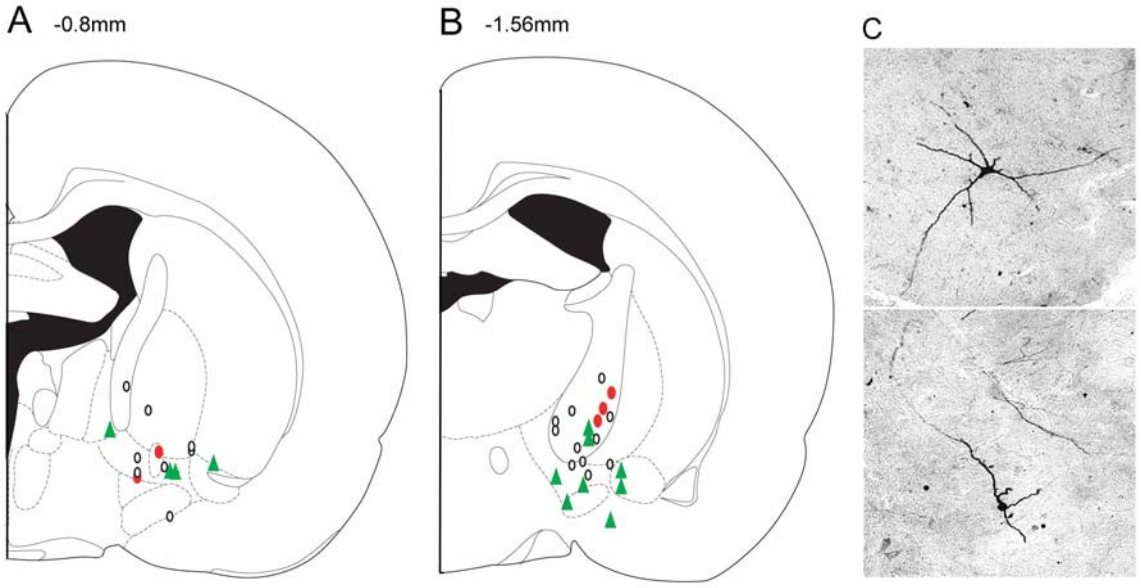

Figure 18. A, B) Diagram showing the location of Up state-on and -off cells, as well as non-correlated neurons. C) Example light microscopy photographs of biocytin labeled, non-identified neurons in the BF. Green triangles represent Up state-on cells, red circles Up state-off and empty circles non-correlated neurons on figure A and B.

4.2 Anterograde tracer injection results – light and electron microscopy

Zaborszky et al (1997) has previous described mPFC terminating on PV containing neurons in the BF. However, besides the labeled PV containing small dendrites, dendritic shafts and spines, various unlabeled structures have also received axons from the medial prefrontal areas. It has also been shown, that acetylcholine containing neurons in the BF do not receive direct input from the PFC (Zaborszky et al., 1997). Thus, either NPY or SS containing, local interneurons would be good candidates to receive direct cortical input and forward that information to the cholinergic cell population. In order to investigate the immunohistochemical nature of the unknown neuron populations we used the method of anterograde tracing from the mPFC, as well as electrolytic lesion of the same prefrontal areas in separate experiments, combined with immunohistochemical identification of specific BF neurons. Our results revealed that BDA containing terminals are in close proximity with SS containing neurons in the BF areas, more precisely in the SI. Our analysis contains mostly qualitative data that I would like to present in the following paragraphs.

4.2.1 Distribution of BDA labeled axon terminals

Based on what is already known from the literature, the PrL and IL as well as the OF cortices project heavily to BF structures, however the neurotransmitter content of all the targeted cells remained unknown. In our experiment we injected these prefrontal areas with anterograde trace BDA in order to possibly identify the postsynaptic target of the descending axons (Fig. 18). Even though the PrL and IL areas are located relatively close to each another, their projection patterns are significantly different.

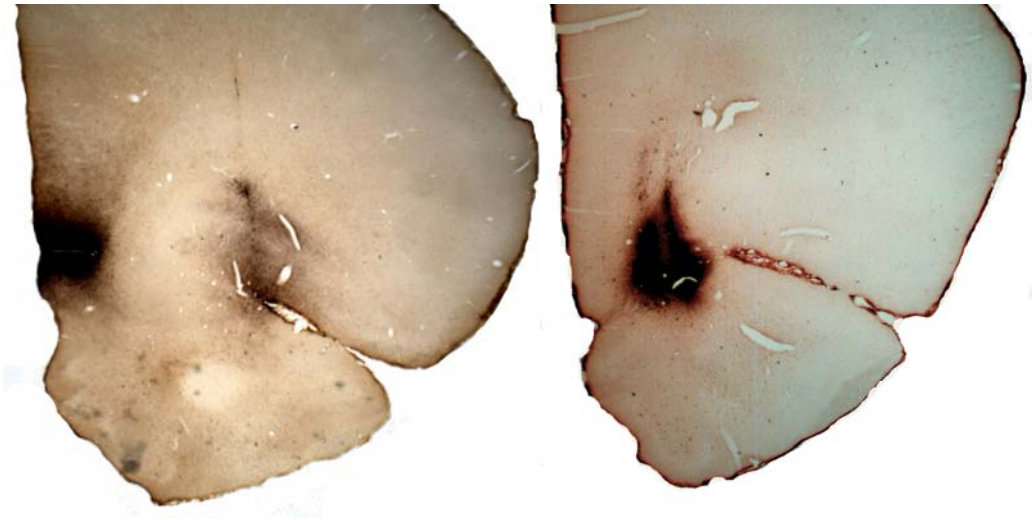

Figure 19. Examples of the location of BDA injection sites in the IL of the medial PFC (A) and orbitofrontal (B) cortices. Pictures were taken under 4 x magnifications.

4.2.1.1 Projections from the prelimbic cortex

After the anterograde traced BDA was applied to the prelimbic area of the mPFC, we could follow the descending projections terminating onto various parts of the brain, including BF areas. Labeled fibers coursed forward from the site of injection to distribute to the medial orbitofrontal cortex and olfactory structures of the anterior forebrain. Main cortical terminal sites were in the anterior PrL and MO of the medial prefrontal cortex, in the dorsal and ventral tenia tecta, in the anterior piriform cortex, and anterior olfactory nucleus of the olfactory forebrain.

Further caudally, labeling remained pronounced in PrL and IL. A prominent bundle of labeled axons densely innervated the dorsal and ventral agranular insular cortices. Labeled fibers descended from the site of injection mainly through dorsomedial aspects of the cortex and through the medial striatum, distributing en route to anterior cingulate cortex and to dorsomedial parts of caudate-putamen/striatum, respectively, and beyond the striatum to the nucleus accumbens, olfactory tubercule, the claustrum and the dorsal agranular insular cortex. Unlike pronounced labeling rostrally in the nucleus accumbens, there was a virtual absence of labeled fibers in the caudal pole (medial shell). Labeled axons swept dorsomedially from the internal capsule into the thalamus to distribute heavily

to the thalamic nucleus. A second group took a more ventral course terminating lightly to moderately in the lateral hypothalamic area, the claustrum and the basolateral nucleus of the amygdala. The SI and the zona incerta were sparsely labeled.

4.2.1.2 Projections from the infralimbic and orbitofrontal cortex

BDA labeled fibers coursed forward from the site of injection to distribute to frontal regions of cortex and olfactory structures (Fig. 19/2A-C). Labeled fibers spread dorsoventrally throughout the medial wall of medial PFC terminating in the medial frontal polar cortex, the rostral prelimbic cortex, and the medial orbital cortex. Significant numbers also extended laterally from the medial orbitofrontal cortex to distribute to the ventrolateral and lateral orbital cortices. The primary olfactory targets were the anterior olfactory nucleus and the dorsally adjacent dorsal tenia tecta, with some extension to the ventral tenia tecta. The anterior olfactory nucleus was moderately labeled. Rostrally the principal destination of labeled fibers at the site of injection was regions of the cortex and olfactory structures.

Labeled fibers descended from the site of injection primarily through dorsomedial aspects of cortex and through the medial putamen/striatum to distribute strongly to anterolateral regions of the septum, and less heavily to the olfactory tubercle, ventral agranular insular cortex and the endopiriform nucleus. The nucleus accumbens was lightly labeled ipsilaterally. Further caudally, labeled fibers, grouped in small bundles, descended through the medial striatum, distributing en route to dorsal and ventral parts of medial caudate putamen, and beyond the striatum to the lateral septum, the olfactory tubercule, the endopiriform nucleus, the posterior agranular insular cortex and the HDB. Labeled axons appeared to mainly traverse the medial anterior cingulate cortex bound for caudal regions of the basal forebrain.

At the mid-septum, labeled fibers spread widely over the basal forebrain, strongly targeting anterior regions of the bed nucleus of stria terminalis, the SI, HDB and the endopiriform nucleus. At the caudal septum, labeling was mainly confined to structures of the medial basal forebrain and anterior hypothalamus. Labeled fibers surrounded but did

not appear to terminate in the magnocellular preoptic nucleus, while some distributed to the medial preoptic nucleus.

4.2.2 Distribution and quantitative analysis of BDA/SS appositions

The infralimbic (IL) together with the orbital (OF) cortex is primarily involved in affective/visceromotor functions like the orbitofrontal PFC in primates, while PrL and adjacent ventral cingulate cortex participates in cognitive/limbic functions, homologues to the lateral prefrontal areas of primates (Hoover and Vertes, 2007). The pattern of distribution of labeled fibers in the basal forebrain areas with injections in the infralimbic (IL) and prelimbic (PrL) cortices were described above. In two cases, one with an injection in IL/PrL (Fig 19A) and the other with an injection in OF (Fig 19B), we mapped the BDA labeled axons together with the immunohistochemically labeled SS containing neurons in the BF areas. We followed the ipsilateral extension of the BDA containing fibers in the brain. We found many putative contact sites at the light microscopy level (100x) that were further processed for electron microscopic examination (Fig. 20).

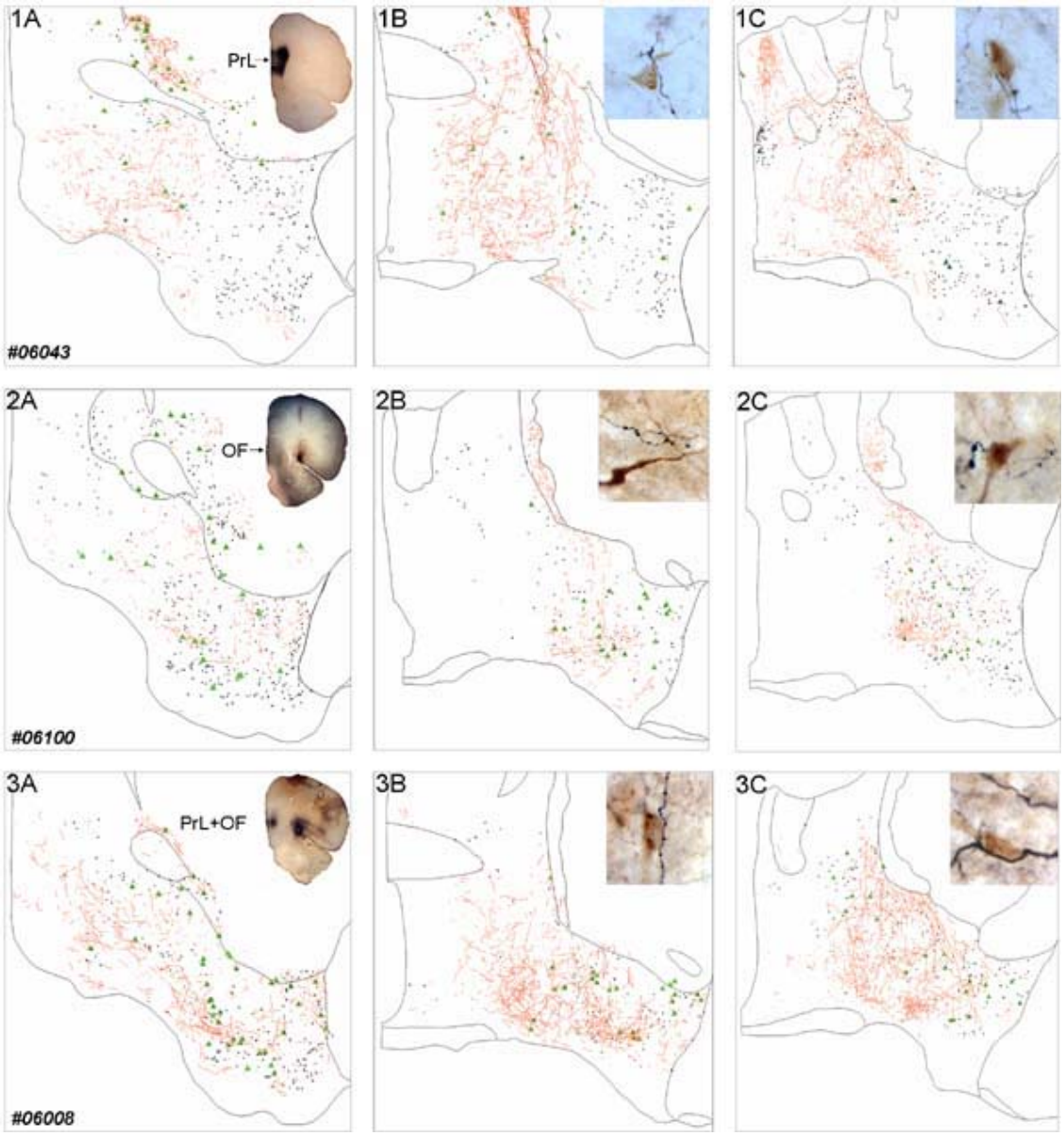

Figure 20. Distribution of BDA axons and SS-containing neurons in series of coronal sections though BF areas. Injection sites are shown in the inset photomicrographs. 1A: PL; 2A: lateral orbital; 3A: double injections in the same areas as (1) and (2). BDA axons in red, SS cell bodies in black; putative contact sites: green triangles. Insets in Figs. 1B-1C, 2B-2C, 3B-3C shows images from the corresponding sections. Note that BDA axons with their varicosities approach SS cell bodies (3B) and dendrites (2B) that are suggestive of synaptic contacts.

In our correlated light and electron microscopic studies, DAB was used to label somatostatin containing neurons and the silver gold-intensified NiDAB to stain BDA-

positive structures. At the light microscopic level, BDA fibers and terminals appeared in black and were easily differentiated from SS-positive elements that were revealed by brown deposits of DAB (Fig. 20). This color difference persisted after osmication and plastic embedding of the sections for light microscopy selection for further electron microscopy procedures. Furthermore, the presence of the highly electron-dense silver-gold grains in the BDA-positive structures made the electron microscopic identification of BDA profiles straightforward.

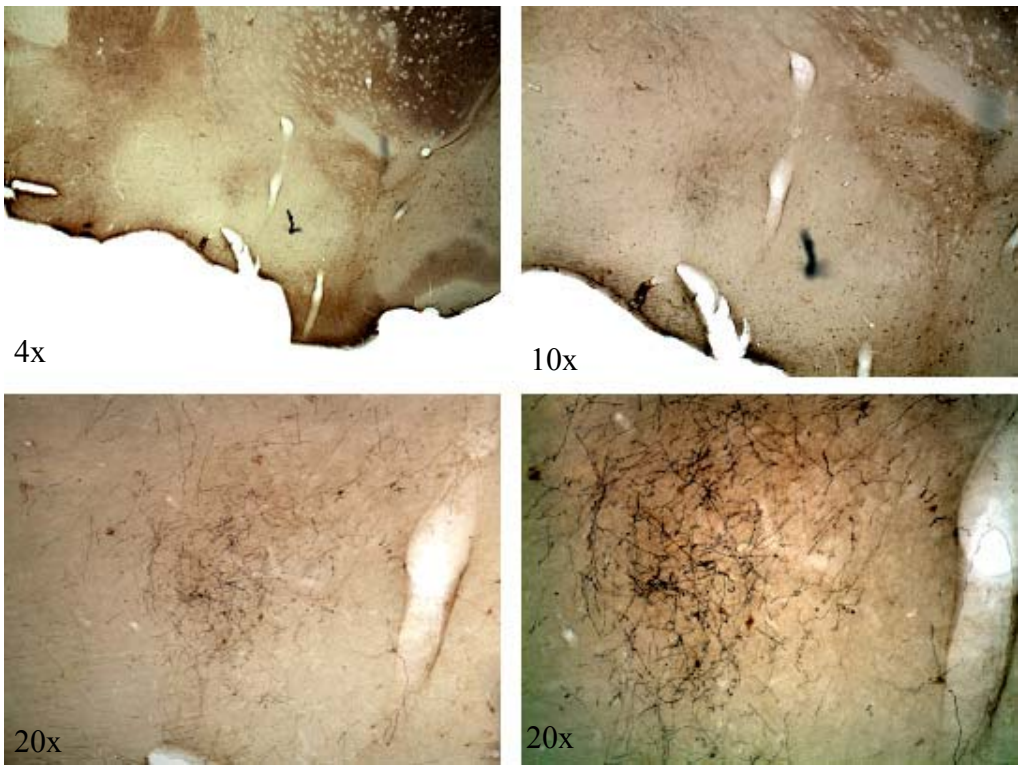

Figure 21. Representative example for BDA injection and SS double immunostaining, showing significant overlapping in the areas of the descending axon collaterals and SS containing neurons located in the BF.

4.2.3 Ultrastructural characteristics of BDA/SS relations

Prefrontal fibers distribute according to medio-lateral topography in BF areas and found frequently in close proximity to SS-containing dendrites and cell bodies. In total 18

individual BDA varicosities closely associated with SS profiles were selected for ultrastructural analysis. The selection was based on the examination of the putative contact sites under 100x with light microscope and the selected assumed synaptic contacts were further processed for EM. BDA-labeled terminals were often found in synaptic contact with unlabeled dendritic shafts (Fig 22/6B), and entered into synaptic contacts with unlabeled spines that were in perisomatic position to SS cell bodies (inset to Fig 22/6C) or adjacent to SS dendrites. In the few cases where BDA terminals were adjacent to SS dendrites (Fig 22/4B) or SS soma (Fig 22/5B), the identification of synapses was precluded by either the presence of dense immunoprecipitate at the contact site (Fig 22/5C) or the ultrastructural investigation did not reveal unequivocal signs of synapses.

After investigating 18 putative contact sites between BDA labeled axon terminals and SS containing profiles (cell bodies, small dendrites and spines) no preferential relationship was found between the localization of BDA fibers and individual SS neurons. Since the distribution of orbitofrontal axons show larger overlap with the bulk of SS cells, slightly more contacts were detected in cases #06008 and #06100 than with BDA deposits in medial PFC areas.

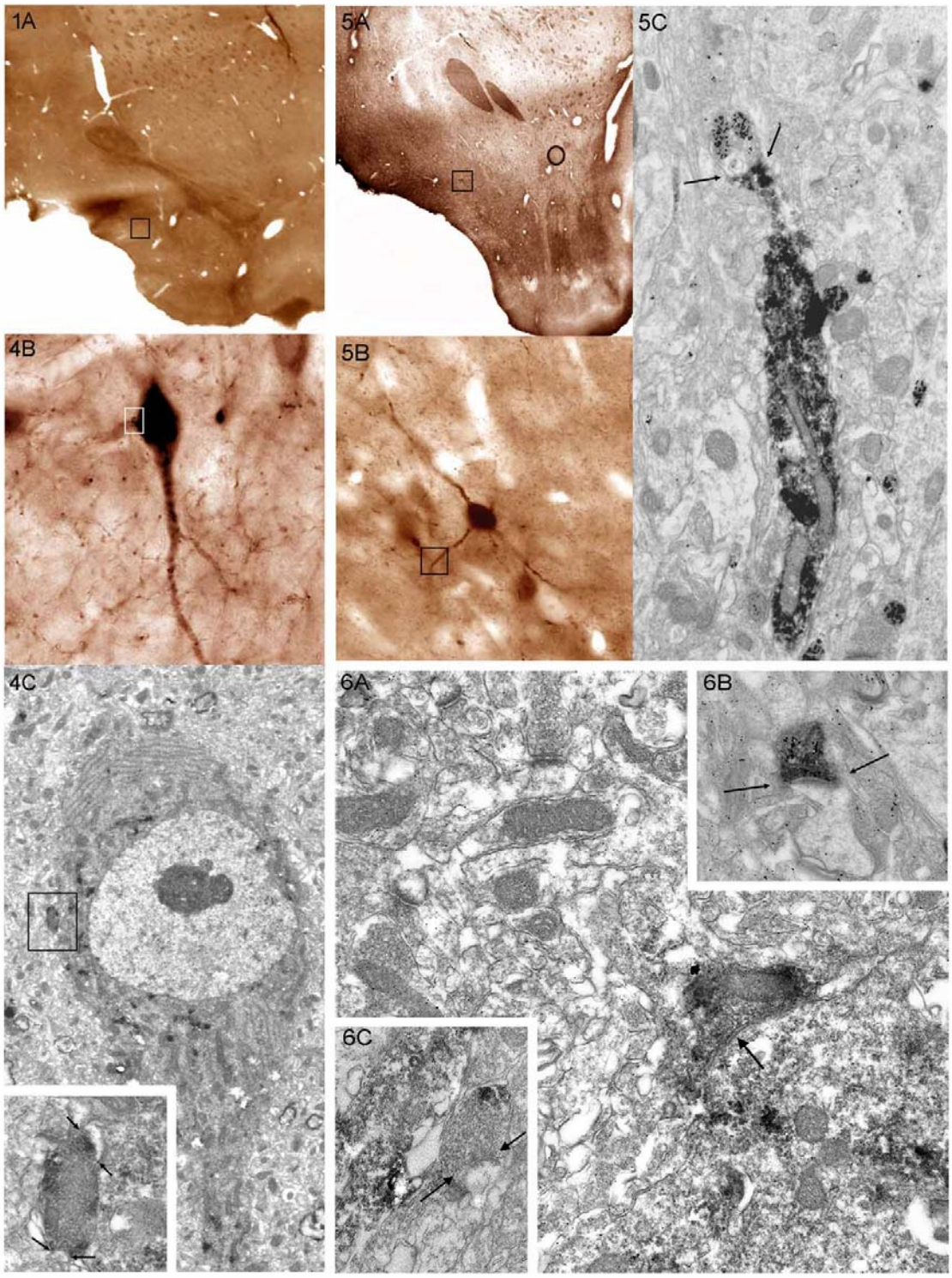

Figure 22. Electron micrograph displays an SS cell body located in the ventral part of the ventral pallidum. Inset from the boxed area of panel 4C shows a BDA-labeled bouton in close apposition of this SS cell body. However, it seems that this bouton synapses with unlabeled spines (black arrows). Electron micrograph of panel 5C displays an SS dendrite (heavy DAB reaction) with close apposition of a BDA-axon terminal (silver-gold deposit) without clear synaptic specialization. This SS dendrite belongs to a neuron located in the ventrolateral border of the ventral pallidum 1A-5A. 4C/5C shows a

SS-labeled cell body that is approached by a BDA-labeled terminal. The presence of short parallel arrangement of pre-post-junctional membranes may be part of a symmetric synapse. Inset of 6A shows a BDA-labeled terminal with asymmetric synapse with an unlabeled dendritic shaft. 6C) shows a BDA-labeled terminal adjacent to a SS dendrite. The BDA-bouton is in asymmetric synapse with an unlabeled spine.

4.3 Distribution of degenerating prefrontal axon terminals and their apposition with labeled neurons in the BF

The axons originating from the PrL/IL tend to project to more medial areas, while orbitofrontal axons distribute more caudal and lateral areas in the BF. It has been shown that cortical axon terminals synapse with dendritic shafts of PV containing neurons as well as with spines of unidentified neurons in the BF (Zaborszky et al., 1997). We reinvestigated the prefrontal-BF connection, not only by combining anterograde tracing with immunohistochemistry, but by combining lesions in various prefrontal areas and immunostaining BF sections for somatostatin (n=18), NPY (n=8), CB (n=3) and CR (n=3).

4.3.1 Electrolytic lesion of the medial prefrontal cortex

Out of 20 attempt of lesioning the medial prefrontal cortex, we selected 5 cases and processed them further for immunohistochemical identification of specific BF neuron populations. The low success ratio of the experiments resulted from either the insufficient lesions in the mPFC or from the extensive lesion to more anterior areas, especially to the anterior olfactory nucleus. A sufficient lesion covered the medial prefrontal cortex, including the PrL and IL areas, preferably in layer V (Fig. 23).

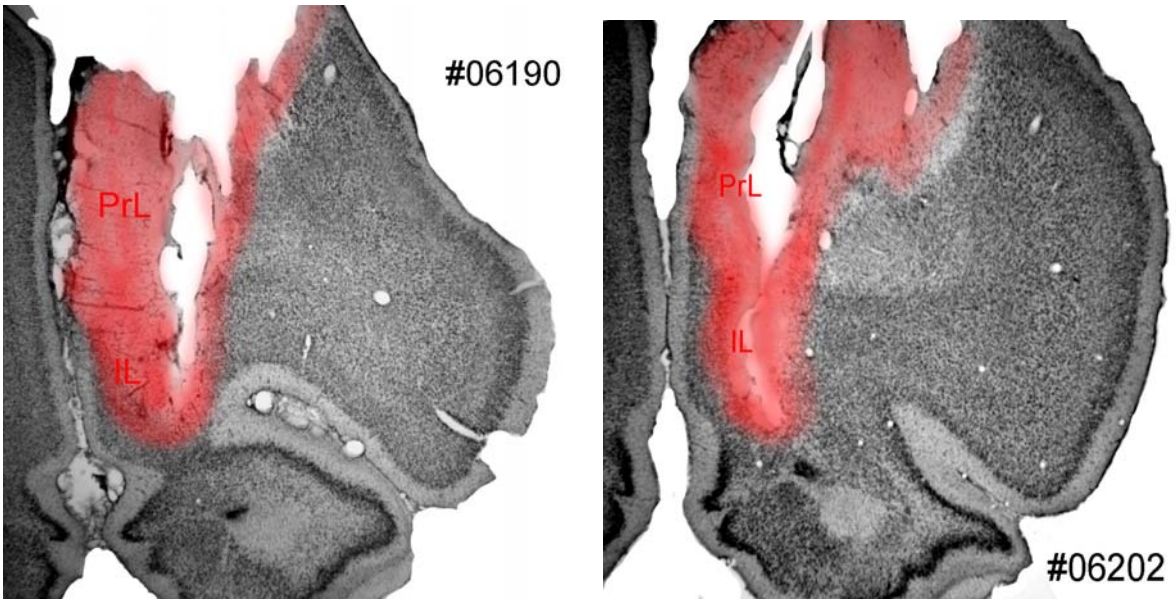

Figure 23. Two example of successful electrical lesion of the mPFC, in which the PrL and IL areas are damaged. Red color indicates the place of the electrode as well as the extension of the electrolytic lesion.

4.3.2 Somatostatin

After the electrolytic lesion, we processed the tissue for immunohistochemical staining for SS. Since we have previously determined the area of the descending axon arborization from the prefrontal cortex based on the BDA fibers visualized for light microscopy (Fig. 20), we selected 14 SS immunopositive neurons from 3 different animals to examine under electron microscope. In the case of the electrolytic lesion, the degenerating axon terminals remain unseen under the light microscope and can be only visualized under the electron microscope. In the examined blocks selected for further processing we always found the immunopositive cell structures for SS as well as degenerating axon terminals in the scanned area (Fig. 24).

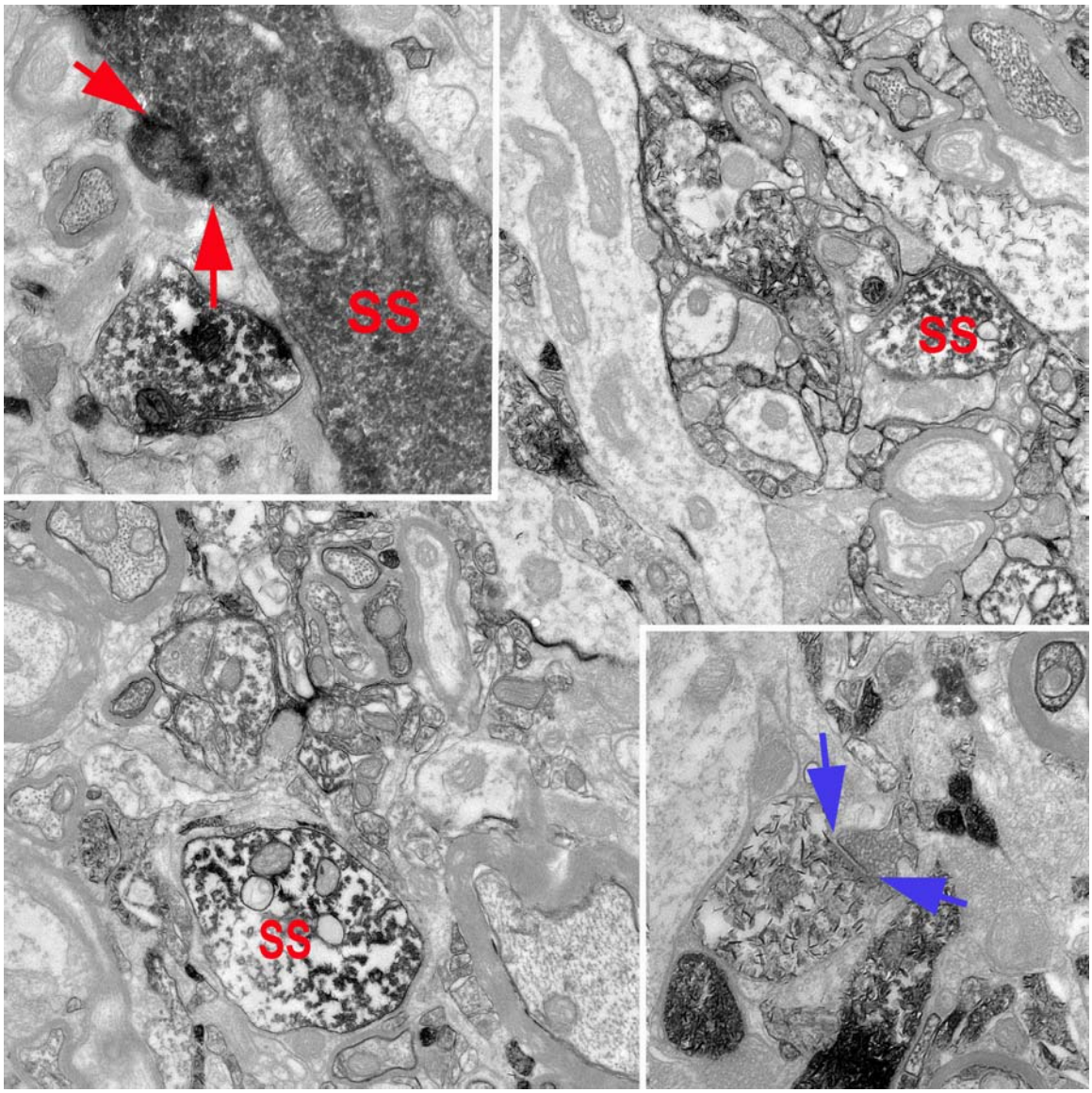

Figure 24. Somatostatin immunopositive profiles in the SI area of the BF. On the upper left inset, SS positive neuron is close to another SS axon terminal, while a degenerating axon terminates on it, forming a putative synapse. On the lower right inset, degenerating axon with round shaped vesicles (putative glutamatergic, excitatory terminal) terminates of SS positive dendrite.

4.3.3 Neuropeptide-Y (NPY)

After the electrical lesion, we processed the tissue for immunohistochemical staining for NPY. Having determined the area of the descending axon arborization from the prefrontal cortex, we selected 5 blocks for further processing for electron microscopy. Our results have not revealed apparent connection between labeled NPY structures and

degenerated axon terminals (Fig. 25), however further investigation on this question might be necessary due to the drawbacks of the technique that we used. The immunohistochemical labeling of NPY neurons with specific primary antibodies visualizes a smaller fraction of NPY neurons, compared to either colchicine treated animals or GFP tagged NPY neurons in transgenic animals.

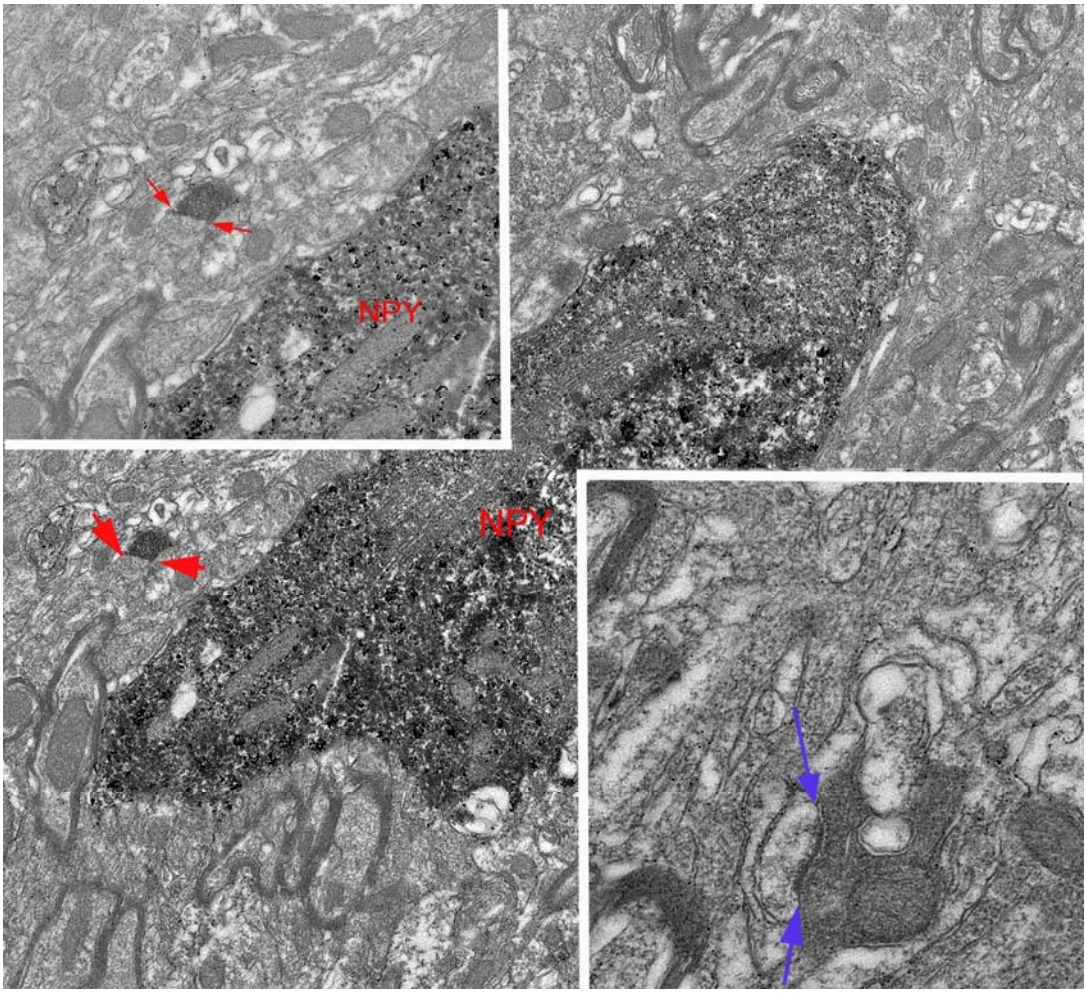

Figure 25. Degenerating axon terminals were found in close proximity with NPY immunopositive profiles however they only formed synapses with unlabeled structures. Upper left inset shows the degenerating axon terminal in close proximity with the NPY immunopositive cell body. Red arrows point to the synaptic connection with unlabeled profile. Lower right inset shows a different degenerating axon terminal also in synaptic contact (blue arrows) with an unknown profile.

4.3.4 Calcium binding proteins - calbindin, calretinin

Calbindin (n=3) and calretinin (n=3) immunohistochemical staining was also carried out on some of the brain sections that undergone electrolytic lesion and were further processed for electron microscopy examination and evaluation. After scanning through the chosen areas that were known to receive prefrontal input and also contained several CB or CR cell bodies, we found no clear interaction between degenerating axons and CB or CR containing profiles. However we did found degenerating axon terminals on unlabeled structures (Fig. 26). Further analysis of the data might be necessary to completely exclude the possibility of the existence of the direct connection.

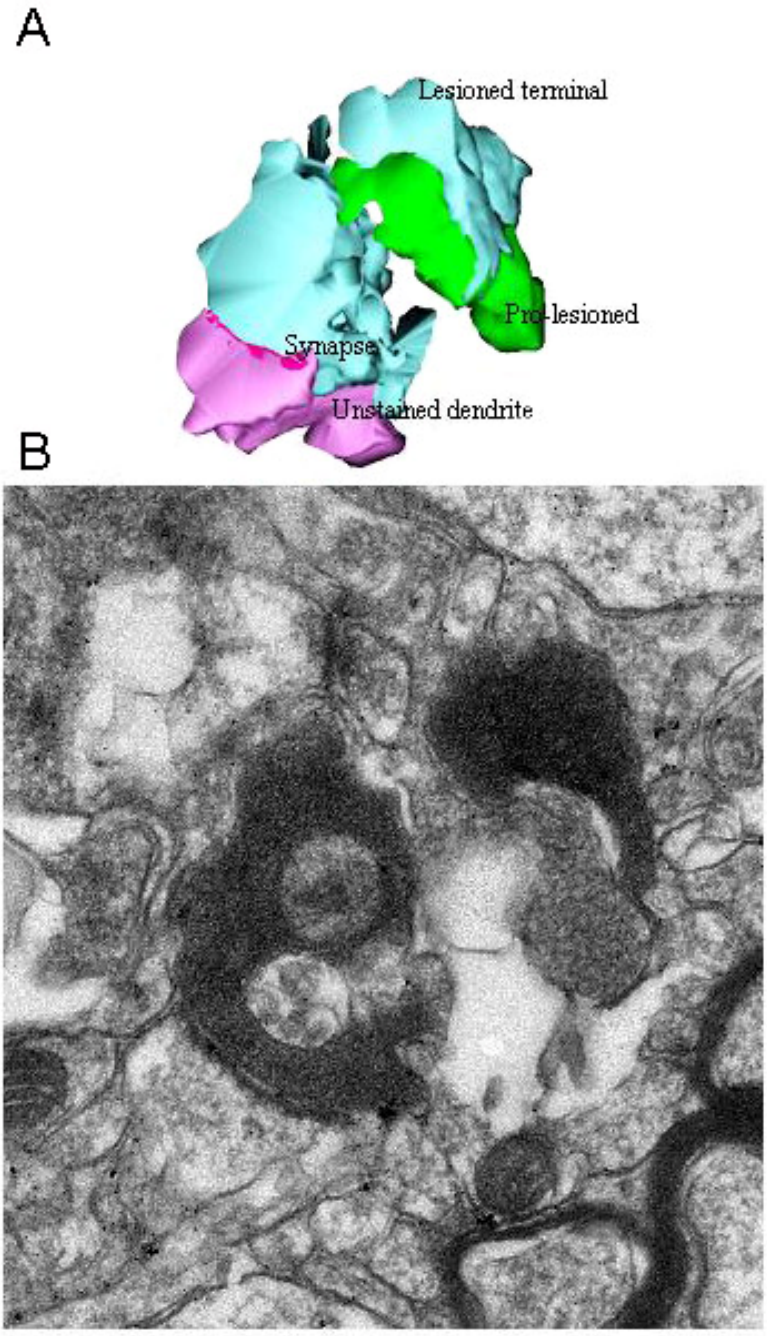

Figure 26. Completely and partially degenerated axons from the prefrontal cortex make synapses with unlabeled profile in the BF, in close proximity with CB and CR immunopositive profiles (not shown on picture). A) 3D reconstruction of the synaptic terminals based on serial sections. B) Electron photomicrograph of the same area showing degenerating axon terminals on unlabeled profiles.

5 Discussion

In this thesis, we examined the medial prefrontal cortical input onto basal forebrain areas in the rat brain. In our experiments we used a variety of approaches to investigate the link between these connected areas. By using various electrophysiological and anatomical methods, including electrical stimulation of the mPFC and studying the effect of the spontaneous changes of the cortical activity on single BF neurons, as well as anatomical track tracing and ultra structural EM studies combined with electrolytic lesion of the mPFC, we gained significant fundamental information about the function and structure about the relationship between the mPFC and the BF. These findings might serve as an important starting point for further, more focused exploration of this connection.

5.1 Electrophysiology

We analyzed the spontaneous activity of the BF neurons, examined their responses to PFC stimulation and during the spontaneously occurring Up and Down states and related the electrophysiological characteristics of the examined neurons to the morphological features of the labeled cell bodies.

5.1.1 Correlation between BF unit and cortical activation

Our results confirmed previous findings regarding the firing pattern and correlation of BF unit activity to cortical EEG (Detari et al., 1997a;Detari et al., 1997b;Detari et al., 1999;Detari, 2000;Zaborszky et al., 1997). Activity in the majority of the recorded neurons (50/57) changed its firing in close correlation with cortical EEG. The unit activity of F cells (41/50) was strongly correlated to LVFA while S cells (9/50) remained silent or decreased their firing rate during fast EEG epochs.

The existence of such a strong correlation can be explained by either direct or indirect anatomical connections between the two areas. Either cortical activation is elicited by BF activity, or cortical activation descends from the cortex to apply an affect the function of the BF neurons. While it is well known, that ascending projections from the brainstem, for example from the stimulation of PPT or tail pinch causes EEG activation

through the BF, our experiments were focused on the second pathway. In the case of PFC stimulation or the supposedly cortically generated Up states, this pathway can only play role, and your experiments were aimed to examine this.

5.1.2 Responses to prefrontal stimulation

The medial PFC in both rats and primates gives rise to an important excitatory input to extensive BF regions in which cholinergic neurons are located (Sesack et al., 1989; Zaborszky et al., 1997), though prefrontal axons exclusively synapse on non-cholinergic neurons, at least in rats (Zaborszky et al., 1997). Stimulation of the medial prefrontal cortex affected 28 F and 8 S cells evoking diverse responses. In slightly less than half of the responding F cells (12/28) inhibition was the primary response, while the rest of the neurons were excited. In half of these cases, excitation was followed by inhibition. Those neurons that showed inhibition as a primary response differed further by the duration of their responses, which was either short (around 50 ms) or long (up to 300 ms). Most of the S cells (6/8) were inhibited by the PFC stimulation, but we also found two neurons that showed excitatory responses. It has already been proposed that the group of F cells show a higher degree of diversity than the S cells (citation), which is in agreement with our results from PFC stimulation as well.

Despite of the glutamatergic, excitatory nature of the projection, a large proportion of primary inhibitory responses were observed following PFC stimulation. This fact suggests that part of the cortical input could be relayed by inhibitory interneurons. The participation of interneurons is further supported by the long latencies observed in most of the responses (30-150 ms).

The BF contains numerous GABAergic neurons (Gritti et al., 1994) that co-localize different neuropeptides including NPY and SS (Zaborszky et al., 1997). NPY and SS containing axon terminals were found to reach or even surround cholinergic cells (Duque et al., 2000;Zaborszky and Duque, 2000). A subgroup of the inhibitory cells most likely consisted of smaller interneurons and was probably hidden from the recording electrode due to the sampling bias of the method toward larger projection neurons. We are

suggesting that glutamatergic input from the PFC reached local inhibitory interneurons (such as NPY and SS), that would be good candidates to induce the observed inhibitions in the recorded neurons following PFC stimulation. It is also known that PV containing, probably GABAergic neurons receive PFC input (Zaborszky et al., 1997), and hence they also may contribute to inhibitory responses evoked by PFC stimulation in BF neurons. However, whether or not PFC axons would reach local excitatory or inhibitory interneurons (PV and VGlut2) as well raises an additional question to investigate. It has been reported that VGlut2 is present in the BF area (Hur and Zaborszky, 2005), also a large population of VGlut2-immunoreactive neurons are located primarily in the posterior division of the septum (Hajszan et al., 2004). A similar mechanism might explain the dependency of results of PFC stimuli on the background activity, observed in the present experiments. At last, cortical input could be relayed by inhibitory neurons located outside the BF. For example, the nucleus accumbens is an important target of descending prefrontal fibers (Gorelova and Yang, 1997). GABAergic cells of this striatal structure in turn, innervate cholinergic BF neurons (Zaborszky and Cullinan, 1992).

Excitatory responses were also recorded following PFC stimulation. As cortical input is excitatory, activation could be evoked through direct connections in non-cholinergic BF neurons or through antidromic invasion in corticopetal neurons. However, indirect pathways through excitatory interneurons or by disinhibition could be also responsible for the excitatory responses. The possibility of the antidromic activation was excluded because the neuronal responses did not meet even the two basic criteria of antidromic invasion: constant latency and high frequency following. Latencies of the excitatory responses were also relatively long, thus in most cases the indirect connection seems to be more probable.

In a previous paper, Golmayo et al. (Golmayo et al., 2003) found mostly short-latency (15-20 ms) excitatory responses in BF neurons following stimulation of the prefrontal cortex. These findings seem to contradict our results. However, we observed in the present experiments that stimulation effects depended on the baseline activity in BF neurons. Those neurons that displayed a primary inhibitory response had a significantly higher firing rate than those cells, in which the response started with excitation. Baseline activities of BF cells were very low in the experiments reported by Golmayo et al. judged

by their figures. The depression of firing might have been caused by a deeper level of anesthesia that was presented in our experiments, since firing rate has been shown to continuously decrease with the deepening of anesthesia (Detari et al., 1997a). The exact explanation of the dependency of responses on baseline activity levels is not known, but similar observations were made earlier by Detari et al. (Detari et al., 1997a). Higher baseline firing rate predestined BF neurons to give smaller excitatory, or even inhibitory responses to short train stimulation of brainstem cholinergic (PPT) and serotoninergic (dorsal raphe) nuclei that was strongly excitatory at a low background firing rate. PPT effect on cholinergic BF neurons has been shown to be relayed by glutamatergic mechanisms, as cortical ACh release after PPT stimulation was blocked by BF injection of the nonspecific glutamatergic antagonist kynurenate acid, but not by scopolamine (Rasmusson et al., 1994).

Cholinergic neurons correspond to some of the F-type neurons shown earlier in that they show increased action potential firing during EEG cortical activation (Duque et al., 2000;Manns et al., 2000). PV-containing, putative GABAergic neurons, similar to cholinergic neurons, had a strong positive correlation with EEG activation, indicating that there are also PV cells among the F-cells (Duque et al., 2000). Since GABAergic basalo-cortical axons were found to terminate exclusively on cortical GABAergic interneurons (Freund and Meskenaite, 1992), this finding is compatible with the notion that at least a subpopulation of PV-containing basalo-cortical neurons promotes functional activation in the cerebral cortex by disinhibition (Jimenez-Capdeville et al., 1997).

Using juxtacellular filling, we identified one cholinergic and one PV containing F cell. Latency data measured in these cells were in good agreement with the fact that PFC input terminates on non-cholinergic neurons (Zaborszky et al., 1997), as in the PV-containing neuron a short latency (10 ms) excitatory response was seen, while the cholinergic cell was inhibited with a latency of about 100 ms.

Electrical stimulation of the prefrontal cortex or activation of glutamatergic and cholinergic receptors led to increased ACh release in neocortical areas (Dringenberg and Vanderwolf, 1997;Sarter and Parikh, 2005). These findings seem to contradict to the inhibitory response induced by PFC stimulation in the identified cholinergic cell in our experiments. However, our stimulation consisted of a short train of three stimuli inducing

no generalized changes in EEG, while in the above cited papers more sustained stimulation was applied that led to desynchronization of the cortical EEG. The exact mechanism by which sustained stimulation caused activation of BF cholinergic cells is not known, but it should occur through indirect, polysynaptic pathways as cholinergic cells receive no direct innervations from the PFC.

Following PFC stimulation, clear evoked field potentials were recorded in the M1/M2 areas, which were composed of the same waves in all animals. Field potential changes started with a sharp wave (50 ms), negative at the deep layers of the cortex, thus indicating activation. This wave was followed by a longer positive wave (500 ms). This sequence was often followed by a second, slower negative wave. Vanderwolf et al. (Vanderwolf et al., 1987) in freely moving animals found cortical evoked responses following electrical stimulation of the contralateral sensorimotor cortex that were very similar to what we have described in our experiments. However, despite the similar sequence of negative and positive curves, durations were considerably longer and amplitudes smaller in our recordings. These differences might be explained by the presence of the anesthetic in our studies.

Previous studies suggested that the early component represents summed excitatory postsynaptic potentials; while the late component summed inhibitory postsynaptic potentials (Vanderwolf et al., 1987). Unit activity changes in the BF following PFC stimulation displayed strong correlation with the evoked cortical field potentials. Not all components were always present in the neuronal responses; however latency and duration of excitatory and inhibitory periods ran parallel with field potential waves. An explanation for the very similar time course of the responses would be an excitation-inhibition-excitation sequence induced by the stimulus in the PFC itself. This activity pattern would then reach the neocortical areas and the BF separately and would ensure the similar timing of events. However, no important intercortical connection has been described between the mPFC and the M1/M2 areas either anatomically or electrophysiologically (Hurley et al., 1991;Sesack et al., 1989;Vertes, 2004). Therefore, it is highly unlikely that this strong correlation between the BF and M1/M2 areas can be explained by this mechanism. In contrast, it is well known that the BF provides a topographically organized projection to the whole cortical mantle (Zaborszky et al., 1999) thus it is a more reasonable suggestion

that BF neuronal changes were primary, evoked by the top-down projection from the PFC to the BF. Corticopetal projections from the BF would then induce the cortical responses. Similarly strong correlation has been reported between spontaneous neuronal activity in the BF and the cortical EEG and was explained by the bottom-up effects ascending from the BF to the cortex (Detari et al., 1997a). This observation could also give further support for the existence of the prefronto-basalo-cortical circuitry that has been already suggested (Zaborszky et al., 1997).

5.1.3 BF unit activity and cortical Up and Down states

Even in the absence of sensory stimulation, the neocortex shows complex spontaneous activity patterns, often consisting of alternating Up states of massive, persistent network activity and Down states of generalized neural silence (Luczak et al., 2007;Steriade, 1993). The dynamics of spontaneous Up states show striking similarities to those of sensory-evoked activity (Kenet et al., 2003), suggesting that spontaneous patterns may be a useful experimental model for the flow of activity through cortical circuits. The way spontaneous activity propagates through cortical populations is unclear: whereas *in vivo* optical imaging results suggest a random and unstructured process (Kerr, 2005), *in vitro* models suggest a more complex picture involving local sequential organization and/or traveling waves (Cossart et al., 2003;Ikegaya et al., 2004;Mao et al., 2001;Sanchez-Vives and McCormick, 2000;Shu et al., 2003;Yuste et al., 2005).

Cortical Up and Down states appear in sleep and under anesthesia but not during normal wakefulness. It has been proposed that Up and Down states are generated throughout the entire neocortex that receives afferents from various subcortical areas, including the BF. However based on an electron microscopy study, the prefrontal cortex was shown to be the only cortical area that sends projections back to the BF (Zaborszky et al., 1997). Since Up states can be considered as a more natural input that reaches subcortical areas, compared to the artificial electrical stimulation of a restricted area in our experiments, we aimed to test how the activity of the cortex influences the BF.

BF neurons based on their spontaneous activity show heterogeneous responses the PFC stimulation as discussed earlier, perhaps reflecting their diversity of their

neurotransmitters. In the next step of our analysis, we used the same experimental setup described earlier to determine the temporal relationship between cortical Up and Down states and the BF unit activity. Prior to the electrical simulation, spontaneous activity of the EEG and BF unit activity was recorded for 5-10 minutes. Although the spontaneous discharge pattern may change under varying physiological and pathological conditions, during this time, the level of anesthesia was deep enough that cortical Up and Down states were clearly recognizable in the ECoG.

The importance of our results comes from the fact, that while recording the activity of one single neuron in the BF we were able to examine the effect of various stimulations, including noxious stimulation of tail pinching, electrical stimulation of a well localized area in the mPFC as well as the effects of cortical Up and Down states. Our findings imply that even though different input may converge onto the same neurons, their effect results in various responses in the activity of the given cell. In other words, the groups of neurons that might show clear and similar responses to one kind of stimulus would reveal a completely different kind of response to different stimulus.

The most straightforward way to examine the activity of a neuron is to investigate the changes of their firing rates. We found a significant correlation between averaged BF unit firing and spontaneous ECoG Up and Down state transitions. About 43.1% of cells (22 out of 51) significantly increased their firing rate preferentially on the depth-negative phase of the cortical EEG indicating Up states (Up state-on cells). A smaller group of cells (6 out of 51, 11.7%) decreased or ceased firing on the depth-negative phase of EEG, that produced a significant inhibitory response (Up state-off cells). These neurons were active only in Down states and were almost always completely silent during Up states. The rest of the analyzed neurons (23 out of 51; 45.2%) showed no significant temporal correlation with Up or Down states. In comparison, we found that within the group of Up state-on neurons (n=22) 14 was identified as F cells, 1 as an S cell and 7 were not grouped either. The same analysis was carried out for Up state-off cells (n=6) as well, and we found 4 neurons to fall into the category of F cells and 2 to be S cells. It is important to note here that there is a great diversity among F- and S-cells in terms of conduction velocity, spontaneous and evoked neuronal activity, and in terms of correlation between EEG and

unit activity, indicating that F- or S-cells are far from being a homogeneous cell population (Detari, 2000).

We found that the initial firing rates of Up state-on and Up state-off cells in the BF was found to be significantly different. Since these groups of neurons displayed different, often opposite responses to not only ascending (tail pinch) or descending (prefrontal) stimulus, it suggests that the prevalent state of activity of neurons may be important in determining or predict their response.

Several studies revealed correlation between neuronal morphology and electrophysiological properties in different brain areas (Sim and Allen, 1998;Uusisaari et al., 2007;Washburn and Moises, 1992), while others claimed that no reliable anatomical criteria can be defined to distinguish certain neurotransmitter groups (Likhtik et al., 2006;Margolis et al., 2006).

In vivo extracellular recordings combined with juxtacellular labeling permitted further morphological and chemical characterization of neurons in relation to well defined EEG epochs.

We were able to confirm significant anatomical and electrophysiological differences not only between Up state-on and Up state-off neurons but compared to non-correlated cells as well. We found that the spike width of the Up state-on neurons was significantly narrower (1.6±0.09 ms) than the same parameter of the Up state-off neurons (2.15±0.25ms). In addition, the spike amplitude of these groups showed also significant differences (Up state-on neuron had a significantly larger (181.0±18.66μV) amplitudes, compared to Up state-off (135.9±9.68μV) or non-correlated neurons (130.0±6.24 μV)). These results, in accordance with our morphological findings about the labeled neurons (Up state-on cells displayed a larger diameter, resulting in a bigger neuron size), suggest that the neuron population of the Up state-on cells might represented by an anatomically more uniform population, containing larger neurons than the Up state-off or non-correlated cells.

Due to the small number of immunohistochemically identified neurons, we were unable to draw any conclusions concerning the relationship of the electrophysiological properties - such as spike shape or response for a given stimulus – and the neurotransmitter content of the recorded cells. However, our findings revealed a significant correlation

between spike shape, response to PFC stimulus and neuronal soma shape suggesting that, by increasing the number of identified neurons, it might be possible to establish criteria that would allow the reliable classification of neurons after careful electrophysiological analysis.

The electrophysiological diversity of the recorded neurons based on their spontaneous activity and responses to the PFC stimulation reflect the existence of different BF cell types that receive direct or indirect prefrontal input. Unfortunately, we were able to identify only very few neurons immunohistochemically, preventing us to determine whether or not the different electrophysiological categories correspond to different cell types or different functional states.

5.1.4 Various categorization of BF neurons in relation to cortical activity

Previously, several groups have established different categorization of BF neurons, based on their correlation to natural sleep rhythms (Jones, 2004), ascending input from the brain stem (Detari et al., 1997b;Dringenberg and Vanderwolf, 1997), their relationship to medial prefrontal stimulation (Gyengesi et al., 2008;Manns et al., 2000;Nunez, 1996).

Jones at al (2004) described 13 different groups of BF neurons based on their correlation to natural sleep waves. They concluded that there is a relationship of spike rate to gamma, delta, and theta EEG activity and to electromyogram amplitude that was examined across epochs and states for each unit by simple correlations. Functional sets of cell groups were inferred by the correlations between unit discharge rate and various EEG activities.

Based on the changes of BF unit firing rate in correlation with somatosensory stimulation of the cortex in urethane anesthesia Manns et al (2000) established two major categories. These were named “on” and “off” cells. Stimulation resulted in desynchronization of the EEG. They further investigated the electrophysiological and anatomical properties of identified GAD and ChAT positive neurons after somatosensory stimulation. Their results about cell size indicated mostly bigger (> 15um) and are in agreement with our finding, that the largest diameter of the up state-on cells were significantly bigger. Based on their investigations, several subpopulations of GAD+ cells

emerged. One was categorized as “off” and tonically discharging cells, meaning they decreased their firing rate significantly with somatosensory stimulation. The largest subgroup (40%) was “on” and tonic firing, amongst which several could be antidromically driven from the prefrontal cortex. The second largest group was “off”, tonic firing, not driven antidromically from the medial prefrontal cortex. Their findings also suggest that inhibited neurons from the PFC are not directly/monosynaptically connected, however, ”on” cells could be connected directly to the mPFC through monosynaptic anatomical connection.

Golmayo et al (2003) also confirmed that a subpopulation of BF neurons responded to electrical stimulation of either the visual- or the somatosensory-responsive PFC areas. The responsive neurons were located in the VP, in the SI and in dorsal part of the HDB areas. Some of BF neurons were orthodromically driven from PF areas that receive inputs from somatosensory and visual cortex (Golmayo et al., 2003).

Nunez (1996) separated two neuronal populations in the BF that have different discharge patterns during desynchronized and synchronized EEG periods. One of them, called bursting type expressed rhythmic firing, while the other showed tonic firing during synchronized EEG. The correlation of these two different types of neurons has been investigated to cortical slow oscillation, and concluded that bursting neurons may be included in the slow oscillation network that is activated during behavioral states when many parts of the brain are isolated from outside sensory stimuli. In this paper, Nunez suggested that the rhythmic activity of bursting BF neurons may be commanded by the medial prefrontal cortex, although some intrinsic properties of BF neurons could probably also distribute to the generation of the cortical slow oscillation. In addition, there were also neurons observed whose activities remain unchanged despite EEG cortical changes (Nunez, 1996).

In agreement with our results, in addition to neurons that increased their firing during cortical activation, several studies described the presence of a small number of BF cells that reduced their firing during EEG activation (Detari et al., 1997a;Manns et al., 2000). Szymusiak and McGinty (1989) described some projecting BF cells in cat that increased their discharge in anticipation of non-REM sleep onset. These ‘sleep active’ neurons in cats were antidromically driven from the external capsule and cingulate bundle,

and were tentatively identified as either cholinergic (Manns et al., 2000;Szymusiak and McGinty, 1986) or GABAergic neurons (Manns et al., 2000;McGinty and Szymusiak, 1990). Several functionally S-type cells were stained positively for NPY (Duque et al., 2000). Reconstruction of NPY neurons suggests that they represent either local or projection neurons towards the thalamus (Duque et al., 2007). Both local and projection NPY neurons are silent during spontaneous or tail pinch induced desynchronization, but become accelerated during episodes of cortical delta oscillations.

In deeper anesthesia, in which deep-positive inactive periods and short activations riding on deep-negative deflections alternate at a rate < 1 Hz (corresponding to Up and Down states of present study), cholinergic, PV and NPY neurons showed increased firing with 50-200 msec delay, suggesting that under this condition cortical activations may be transmitted via descending corticofugal fibers to the BF. On the other hand, under light anesthesia, in which periods with low-voltage fast activity alternate with epochs of slow waves at a frequency of 0.1-0.3 Hz, change in the firing of cholinergic and PV-containing neurons preceded the change in EEG pattern, suggesting that these BF cells could contribute to this EEG pattern (Duque et al., 2000).

5.2 Anatomical connection of the mPFC and the BF

The medial prefrontal cortex has been associated with diverse functions including attention processes, visceromotor activity, decision making, goal-directed behavior and working memory. With the exception of a few common target areas such as the orbitomedial prefrontal cortex, olfactory forebrain and midline thalamus, the infralimbic and prelimbic areas of the medial prefrontal cortex project to different areas throughout the brain.

In our experiments, we focused on the IL and PrL areas of the mPFC project heavily towards the BF giving rise to axonal varicosities in various areas of BF including the MS, VP, HDB/VDB, SI, and peripallidal regions (Vertes, 2004). Our results revealed that the BF receives dense projection from the prefrontal cortex, especially from the PrL and OF areas that project heavily to the medial BF areas, including the SI and HDB.

These areas contain cell types that differ in transmitter content, morphology, and projection pattern. Cholinergic projection neurons represent only about 20% of the total cell population in these forebrain areas, and anatomical and electrophysiological studies identified a high diversity of BF neurons, including local neurons that express NPY and Somatostatin (SS), in addition to cholinergic, GABAergic and glutamatergic projection neurons (Duque et al., 2000;Gritti et al., 2006;Hur and Zaborszky, 2005;Jones, 2008;Lee et al., 2005;Manns et al., 2000;Szymusiak et al., 2000;Zaborszky et al., 1999;Zaborszky and Duque, 2000). Neurons in these areas also contain various calcium-binding proteins, including CB, PV and CR. Cholinergic, CB, CR and PV cells represent non-overlapping populations of neurons in rat and they show specific spatial and numerical relations in the various BF areas (Zaborszky et al., 2005). A substantial proportion of PV cells contain GABA and project to the cerebral cortex (Gritti et al., 2003). A small percentage of CB and CR cells also project to the cortex (Zaborszky et al., 1999), although their transmitter content remains to be determined.

In previous EM studies Zaborszky et al found extensive axon arborization adjacent to cholinergic neurons. However, synaptic terminals from the PFC were established exclusively with non-cholinergic neurons, including PV containing projection cells (Zaborszky et al., 1997). Further investigation of the same material revealed that besides mPFC axons terminating on labeled PV profiles, including dendrites and dendritic shafts, unlabeled structures in the BF also seemed to receive prefrontal terminals.

Our electrical stimulation results of the prefrontal areas indicated that more than half of the responsive units in the BF expressed inhibitory responses, which suggested that mostly local inhibitory interneurons maybe recipients of prefrontal input. Somatostatin (SS) and neuropeptide Y (NPY) are two peptides that are expressed in BF inhibitory interneurons that innervate cholinergic neurons (Zaborszky and Duque, 2000), emerged to be good candidates for delivering input from the mPFC to the BF cholinergic cell population.

To examine the possible PFC input to these interneurons, we carried out combined LM and EM studies. The paraformaldehyde-glutaraldehyde-picric acid containing fixative should give satisfactory results for both LM and EM procedures. However, while we found the injected BDA in an extended arborization of fibers, the number of labeled SS-

containing neurons, especially in the BF areas, was lower than expected based on earlier studies (Zaborszky and Duque, 2000). Therefore, we decided to use different fixatives for the LM and EM processes. With an acrolein containing fixative, the number of the visible SS-containing neurons increased, but, unfortunately, labeling for the BDA turned out to be very poor and in some cases disappeared completely, which made the combination of these two labeling technique fairly difficult.

Using BDA as an anterograde tracer, we injected three different sites of the mPFC using iontophoresis. While BDA can be used either as an anterograde or as a retrograde tracer, using iontophoresis resulted in satisfactory results of anterograde track tracing, avoiding the labeling of retrograde neurons in various interconnected parts of the brain. Those cases where retrogradely labeled neurons appeared in any parts of the brain were eliminated from further analysis.

After mapping the descending fibers from the IL, PrL or OF areas of the PFC, we found that mPFC innervate mostly the medial parts of the BF, such as MS, VP, HDB/VDB, SI, and peripallidal regions. To decide whether or not mPFC axons converge onto SS containing neurons in the BF, we examined the synaptic input of the SS neurons in the medial BF areas under electron microscope. Within the above mentioned regions, we examined every SS containing profiles in plastic embedded sections and processed further those that revealed putative contact sites under 100x magnification of light microscopy. Out of the 18 examined putative synaptic contacts, we could not identify clear synapses between BDA containing terminals and SS-labeled profiles in the BF. Since the sample size was relatively high in this portion of the experiment, we should conclude that prefrontal fibers probably do not reach to SS containing cell bodies or dendrites directly in the BF areas. However, one of the disadvantages of using immunohistochemical staining methods is the unreliability regarding the depth of the penetration of the antibody used against SS. Since previously unlabeled dendritic shafts and spines were described to receive direct medial prefrontal input, it is not unimaginable that those profiles remained unlabeled and hidden in our experiments as well.

To eliminate the problem of the incompatibility of using BDA as an anterograde tracer and acrolein as a fixative, that in turn increased the labeled SS containing neurons, in the next step, we chose to use electrolytic lesions in the medial PFC and to look for

degenerated axon terminals on SS-, NPY-, CB-, and CR-positive neurons in the basal forebrain under EM. In this way, we could use the acrolein containing fixative, and avoided the tracer injection as well as the double immohistochemistry. In addition, using acrolein revealed significantly higher number of SS stained neurons throughout the brain. Since degenerating axon terminals cannot be seen under LM without further staining procedures, in addition to the EM studies, an attempt was also made to visualize degenerated axons to BF areas under the LM by using the silver impregnation protocol described by Zaborszky and Gallyas (Gallyas et al., 1980a;Gallyas et al., 1980b). After silver impregnations, our results revealed that the distribution of the degenerating axon terminals is in accordance with the distribution of the BDA labeled terminals and are in close proximity with NPY and SS neurons in the BF.

From the plastic embedded sections that were stained for various histological markers, we selected neurons from the areas of the BF that contained possibly the most concentrated innervations of mPFC axons, based on our light microscopy studies. We selected 14 SS, 5 NPY, 3CB and 3 CR neurons and processed further for EM investigation. After evaluating the EM photographs taken with high magnification of the given neurons and dendrites, we found no compelling evidence that degenerating axon from the mPFC would converge on these neurons. Since the sample size in the case of NPY, CB and CR neurons is not high enough to draw a final conclusion. However, together with the BDA tracing data we can conclude that the SS containing cell bodies in the BF probably do not receive direct prefrontal input. Our studies suggest that the prefrontal effect on BF cholinergic function may not be mediated by SS neurons. Further investigation of other neuron population is needed to decide about the case of NPY, CB and CR.

In spite of the various methods that we used and the high number of putative contact sites examined with electron microscope, we were unable to identify the exact postsynaptic target of degenerating terminals or BDA containing axons that had obvious synaptic connection with unlabeled dendritic shafts and spines in the BF. The shaft synapses may correspond to the synaptic terminals on PV dendrites as reported earlier; however, the nature of spine synapses needs further investigations. Due to technical limitations of these methods we could not identify if the same neurons that receive shaft synapse receive also input to their spines or the spiny cells represent a separate cell types.

If the spines belong to non-PV cells then the effect of prefrontal input could be different according to the postsynaptic target: cortical excitatory axons can invade the somatic regions along the thick dendritic segments without attenuation in PV cells, while synapses on spines may have smaller effect.

5.3 Prefrontal-Basal Forebrain-Cortical Loop

Our anatomical and electrophysiological studies raise the possibility that the basal forebrain may actively participate in the prefronto-basalo-cortical circuitry via its input from the prefrontal cortex and its output to distributed, functionally-related cortical areas. This hypothesis is based upon a) the strict topography in cortico-prefrontal (Ongur and Price, 2000;Zaborszky et al., 1999), b) prefrontal-basal forebrain (Sesack et al., 1989;Zaborszky et al., 1997) c) basal forebrain-cortical projections and d) the close spatial relationship among basal forebrain cells that project to the prefrontal cortex.

Our finding confirmed a close correlation between the BF unit activities and desynchronized and synchronized EEG epochs that supports the notion that BF cholinergic neurons play a considerable role in the desynchronization of the cortical activity (Balatoni and Detari, 2003;Detari, 2000;Detari et al., 1999;Detari et al., 1997a;Duque et al., 2000;Szentgyorgyi et al., 2006). On the other hand, the temporal correlation between the BF and cortical Up and Down states supports the idea of the descending information back to the BF through the medial prefrontal cortex. Since it was already known that the generation of cortical Up and Down states is independent from other subcortical areas, it was not unexpected to find that the formation of cortical Up state always precedes the changes of BF activity. However, that both the excitatory and the inhibitory changes of BF single unit activity are modulated by the alteration of cortical Up and Down states proved to be a novelty. In addition, electric stimulation of the medial prefrontal cortex also supported the existence of a functional connection between the BF and the mPFC. Interestingly, despite the excitatory (presumably glutamatergic) nature of the prefrontal input to the BF, we also found significant inhibitory responses in correlation to both the mPFC stimulation and the cortical Up and Down states, which suggests that a significant portion of the medial prefrontal input terminates on inhibitory interneurons in the BF.

Thus, by examining the anatomical target of the prefrontal axons in the BF, tried to identify what type of neurons receive direct input. By using various methods we excluded the SS containing neurons, however, stating the final conclusion about various other neuropeptides and calcium binding protein containing neurons is still left to complete. An interesting addition to our speculation is the involvement of local, glutamatergic neurons in the circuitry.

6 Conclusions

6.1 Electrophysiological properties of the connection between the PFC and the BF

From acute, in vivo experiments on urethane anesthetized rats we found the following results:

1. A certain neuron population of the BF is significantly correlated with low voltage fast activity (LVFA) in urethane narcosis in rats, while a different, smaller group of BF neurons are in strong correlation with cortical slow waves (SWS).
2. The spontaneous as well as the stimulus evoked changes of cortical activity result in changes of the activity levels of BF neurons.
3. The electrical stimulation of the mPFC affects the firing properties of single BF neurons. Based on the response for the stimulation of the medial PFC, BF neurons could be further categorized and differentiated. We found two basic responses for mPFC stimulation: excitatory and inhibitory.
4. A well categorized group of neurons of the BF are significantly associated with spontaneous cortical Up and Down states which does not necessarily overlap with previous categorizations.
5. Based on the three criteria, correlation with LVFA and SWS, effects of electrical stimulation of the mPFC, correlation with spontaneously occurring cortical Up and Down states, we found that it might be possible that the descending information from the cortex and the ascending pathways from the brainstem can converge onto the same neurons in the BF.

6.2 Anatomical properties of the prefrontal-basal forebrain connection

1. It is conformed that the BF areas defined by the localization of corticopetal cholinergic neurons, receive massive, putative excitatory input from the mPFC.

2. Based on our anatomical results we can conclude that the interneuron population that receives direct input from the mPCF is not likely to be SS. The neurochemical nature of the unlabeled spiny neuron population needs to be identified.

7 Acknowledgements

I would like to thank to my advisors **Dr. Laszlo Detari** and **Dr. Laszlo Zaborszky** for all their help and relentless support in the past years, not only about my work in their laboratories but about my future career as a scientist. Having completed this thesis under the guidance of such mentors was an experience that established my vision of how research should be conducted and helped me to set goals that hopefully will contribute to a better understanding of how the brain works.

I would also like to express gratitude for all the help of our technicians, **Primas Jozsefne Marika** and **Erzsebet Rommer**. I would like to specially show my appreciation to Erzseber Rommer for the amazing and exquisite job she did on the electron microscopy material.

I would like to thank my coworkers, **Dr. Attila Toth**, **Dr. Tunde Hajnik** and **Dr. Elizabeth E. Hur** for all their support in daily work, suggestions and assistance in both electrophysiological and anatomical problems, as well as keeping me company through the hours spent in the lab. I would like to thank **Dr. Peter Bartho**, for all his help with data analysis.

In general, I would like to say thank for all the colleagues and personnel of the Department of Physiology and Neurosciences at the Eotvos Lorand University and the personnel of the laboratory of Dr. Laszlo Zaborszky at the State University of Rutgers, Newark.

At least, but not last, I cannot be thankful enough for all the support of my family, who were always behind me, providing strong background both emotionally and financially throughout these years.

8 Abstract in English

Structural and functional relationship between the basal forebrain and the medial prefrontal cortex

The BF has been intensively studied because of its connection with physiological processes such as the sleep-wake cycle regulation, circadian rhythm, learning and memory consolidation. The BF sends abundant innervations to many parts of the brain, including the neocortex and receives numerous inputs from other brain areas; however the prefrontal cortex (PFC) is the only cortical area that sends direct projections back the BF from the higher cortical regions. Consequently, the prefrontal cortical input to the BF represents an extraordinary and influential link has not been extensively studied.

This thesis was aimed to examine the functional and anatomical connection between PFC and the BF by using electrophysiological and anatomical methods. We found that the activity of single neurons in the BF is strongly connected to the spontaneous activity of the neocortex. More over, we identified several subpopulation of BF neurons that were positively or negatively correlated with the electrical stimulation of the mPFC. Using cortical Up and Down states, as a more natural descending stimulus from the cortex, we found a group of neurons that showed significant excitation during Up states, while a smaller, yet well defined group of cells showed inhibition. Given the fact that the descending axons from the PFC are known to be excitatory, we are suggesting that the prefrontal input is terminating on local interneurons that might be connected to the cortically projecting cholinergic BF neurons. This hypothesis would provide an indirect connection between the mPFC and the basal forebrain cholinergic system.

In the second part of our experiments, we focused on the clarification of the anatomical connection between the basal forebrain and the medial prefrontal cortex. By using anterograde tracing or electrical lesion combined with immunohistochemical labeling, an effort was made to visualize and identify the anatomical connection between the medial prefrontal cortex and certain neuron populations in the BF.

9 Abstract in Hungarian

A bazális előagy és a prefrontális kéreg anatómiai és funkcionális kapcsolata

A bazális előagy szerepét számos élettani működéssel, mint például az alvás ébrenlét ciklus szabályozásával, a napi ritmussal, a tanulással, az emlékezéssel kapcsolatban már hosszú idő óta tanulmányozzák. A bazális előagy az agy számos területét ellátja beidegzéssel, kapcsolatot teremtve ezzel az egymástól anatómiailag távol elhelyezkedő részek között. Az egyik legprominensebb kimenete az agykéreg, melynek majdnem az egészét ellátja serkentő bemenettel, azonban a kéregből a bazális előagyra csak egy terület küld axonokat, mégpedig a prefrontális kéreg.

A bazális előagy és a medialis prefrontális kéreg anatómiai és működésbeli kapcsolatának vizsgálatát különböző elektrofiziológiai és anatómiai módszerek segítségével valósítottuk meg. A kísérleteink első részében a bazális előagy és az agykéreg kapcsolatát vizsgáltuk elektrofiziológiai módszerekkel, párhuzamosan regisztrálva a kéreg működését (EEG), valamint egy sejt aktivitását a bazális előagyban in vivo, urethannal altatott patkányon. Az alapjelenségek leírása után megvizsgáltuk a prefrontális kéreg stimulációjának hatását mind a bazális előagyi sejtek, mind pedig a kéreg aktivitásával. Ezek alapján azt találtuk, hogy a bazális előagyi sejtek különböző csoportokra oszthatóak a kérgi leszálló pályán érkező stimulációra adott válaszaik alapján. A következő lépésként megvizsgáltuk a bazális előagyi sejtek kapcsolatát a lassú kérgi ritmussal. Ezen eredmények alapján a sejtek további csoportjait különíthettük el, melyek azonban nem feltétlenül fedtek át egymással.

Az elektrofiziológiai különbségek alapján elkülönített bazális előagyi sejtcsoportok direkt vagy indirekt bemenetet kapnak a prefrontális kéreg felől. Anatómiai pályajelöléses módszerek és immunohisztokémiai festés kombinálásával megpróbáltuk felderíteni a két terület kapcsolatatrendszerét. Mint már ismert, a bazális előagyi kolinerg sejtek nem kapnak direkt bemenetet a prefrontalis kéreg felől, viszont közvetett módon a PV vagy esetleg a SS-t vagy NPY-t tartalmazó sejtpopuláció közvetítheti a kéreg felől érkező információt. Eredményeink alapján nem kizárt hogy akár a SS-, akár a NPY-tartalmú sejtek fontos szerepet játszanak a kéreg felől leszálló információ továbbításában a kolinerg sejtek felé.

10 Publication list

Peer reviewed publications about related to the topic of this thesis:

Gyengési E., Zaborszky L, Détári L. The effect of prefrontal stimulation on the firing of basal forebrain neurons in urethane anesthetized rat. Brain Research Bulletin 75 (2008) 570-580.

Toth A, **Gyengési E**, Zaborszky L, Détári L. Interaction of slow cortical rhythm with somatosensory information processing in urethane-anesthetized rats. Brain Research 1226 (2008) 99-110.

Peer reviewed publications about other unrelated topics:

Nicholas Wallingford, Adam L. Diament, Anna Coppola, **Erika Gyengesi**, Bertrand Perroud, Qian Gao, Kari A. Haus, Xiao-Bing Gao, Zia Shariat-Madar, Fakhri Mahdi, Marvin Nieman, Gretchen LaRusch, Yongming Sun, Julie Blake, Alvin H. Schmaier, Craig H & Sabrina Diano. Warden: Prolylcarboxypeptidase regulates food intake by promoting breakdown of α-MSH. Journal of Clinical Investigation (2009)

Gajda Z, Hermesz E, **Gyengesi E**, Szupera Z, Szente M. The functional significance of gap junction channels in the epileptogenicity and seizure susceptibility of juvenile rats. Epilepsia. 2006 Jun; 47(6):1009-22.

Gajda Z, **Gyengesi E**, Hermesz E, Ali KS, Szente M. Involvement of gap junctions in the manifestation and control of the duration of seizures in rats in vivo. Epilepsia. 2003 Dec; 44(12):1596-600.

Kovacs A, Mihaly A, Komaromi A, **Gyengesi E**, Szente M, Weiczner R, Krisztin-Peva B, Szabo G, Telegdy G. Seizure, neurotransmitter release, and gene expression are closely related in the striatum of 4-aminopyridine-treated rats. Epilepsy Res. 2003 Jun-Jul; 55(1-2):117-29.

Reference List

1. Adamantidis A, de Lecea L (2008) Sleep and metabolism: shared circuits, new connections. Trends Endocrinol Metab 19: 362-370.

2. Alheid GF (2003) Extended amygdala and basal forebrain. Ann N Y Acad Sci 985: 185-205.

3. Amaral DG, Cowan WM (1980) Subcortical afferents to the hippocampal formation in the monkey. J Comp Neurol 189: 573-591.

4. Amaral DG, Kurz J (1985) An analysis of the origins of the cholinergic and noncholinergic septal projections to the hippocampal formation of the rat. J Comp Neurol 240: 37-59.

5. Aoki C, Pickel VM (1990) Neuropeptide Y in cortex and striatum. Ultrastructural distribution and coexistence with classical neurotransmitters and neuropeptides. Ann N Y Acad Sci 611: 186-205.

6. Arendt T, Bigl V, Tennstedt A, Arendt A (1985) Neuronal loss in different parts of the nucleus basalis is related to neuritic plaque formation in cortical target areas in Alzheimer's disease. Neuroscience 14: 1-14.

7. Averback P (1981) Lesions of the nucleus ansae peduncularis in neuropsychiatric disease. Arch Neurol 38: 230-235.

8. Bai L, Xu H, Collins JF, Ghishan FK (2001) Molecular and functional analysis of a novel neuronal vesicular glutamate transporter. J Biol Chem 276: 36764-36769.

9. Balatoni B, Detari L (2003) EEG related neuronal activity in the pedunculopontine tegmental nucleus of urethane anaesthetized rats. Brain Res 959: 304-311.

10. Bartho P, Slezia A, Varga V, Bokor H, Pinault D, Buzsaki G, Acsady L (2007) Cortical control of zona incerta. J Neurosci 27: 1670-1681.

11. Bellocchio EE, Reimer RJ, Fremeau RT, Jr., Edwards RH (2000) Uptake of glutamate into synaptic vesicles by an inorganic phosphate transporter. Science 289: 957-960.

12. Benedict C, Kern W, Schmid SM, Schultes B, Born J, Hallschmid M (2009) Early morning rise in hypothalamic-pituitary-adrenal activity: a role for maintaining the brain's energy balance. Psychoneuroendocrinology 34: 455-462.

13. Berberian AA, Trevisan BT, Moriyama TS, Montiel JM, Oliveira JA, Seabra AG (2009) Working memory assessment in schizophrenia and its correlation with executive functions ability. Rev Bras Psiquiatr 31: 219-226.

14. Birrell JM, Brown VJ (2000) Medial frontal cortex mediates perceptual attentional set shifting in the rat. J Neurosci 20: 4320-4324.

15. Bobkova NV, Nesterova IV, Nesterov VV (2001) The state of cholinergic structures in forebrain of bulbectomized mice. Bull Exp Biol Med 131: 427-431.

16. Bondareff W, Harrington C, Wischik CM, Hauser DL, Roth M (1994) Immunohistochemical staging of neurofibrillary degeneration in Alzheimer's disease. J Neuropathol Exp Neurol 53: 158-164.

17. Braak H, Braak E (1991) Neuropathological stageing of Alzheimer-related changes. Acta Neuropathol 82: 239-259.

18. Brann MR, Ellis J, Jorgensen H, Hill-Eubanks D, Jones SV (1993) Muscarinic acetylcholine receptor subtypes: localization and structure/function. Prog Brain Res 98: 121-127.

19. Brown VJ, Bowman EM (2002) Rodent models of prefrontal cortical function. Trends Neurosci 25: 340-343.

20. Budd JM (2000) Inhibitory basket cell synaptic input to layer IV simple cells in cat striate visual cortex (area 17): a quantitative analysis of connectivity. Vis Neurosci 17: 331-343.

21. Carey RG, Rieck RW (1987) Topographic projections to the visual cortex from the basal forebrain in the rat. Brain Res 424: 205-215.

22. Carlsen J, Zaborszky L, Heimer L (1985) Cholinergic projections from the basal forebrain to the basolateral amygdaloid complex: a combined retrograde fluorescent and immunohistochemical study. J Comp Neurol 234: 155-167.

23. Caulfield MP, Birdsall NJ (1998) International Union of Pharmacology. XVII. Classification of muscarinic acetylcholine receptors. Pharmacol Rev 50: 279-290.

24. Celio MR (1990) Calbindin D-28k and parvalbumin in the rat nervous system. Neuroscience 35: 375-475.

25. Chen-Izu Y, Xiao RP, Izu LT, Cheng H, Kuschel M, Spurgeon H, Lakatta EG (2000) G(i)-dependent localization of beta(2)-adrenergic receptor signaling to L-type Ca(2+) channels. Biophys J 79: 2547-2556.

26. Chesselet MF, Graybiel AM (1986) Striatal neurons expressing somatostatin-like immunoreactivity: evidence for a peptidergic interneuronal system in the cat. Neuroscience 17: 547-571.

27. Conde F, Lund JS, Jacobowitz DM, Baimbridge KG, Lewis DA (1994) Local circuit neurons immunoreactive for calretinin, calbindin D-28k or parvalbumin in monkey prefrontal cortex: distribution and morphology. J Comp Neurol 341: 95-116.

28. Contreras D, Destexhe A, Sejnowski TJ, Steriade M (1997) Spatiotemporal patterns of spindle oscillations in cortex and thalamus. J Neurosci 17: 1179-1196.

29. Cossart R, Aronov D, Yuste R (2003) Attractor dynamics of network UP states in the neocortex. Nature 423: 283-288.

30. Cullinan WE, Zaborszky L (1991) Organization of ascending hypothalamic projections to the rostral forebrain with special reference to the innervation of cholinergic projection neurons. J Comp Neurol 306: 631-667.

31. Cunningham MO, Pervouchine DD, Racca C, Kopell NJ, Davies CH, Jones RS, Traub RD, Whittington MA (2006) Neuronal metabolism governs cortical network response state. Proc Natl Acad Sci U S A 103: 5597-5601.

32. Davies P, Maloney AJ (1976) Selective loss of central cholinergic neurons in Alzheimer's disease. Lancet 2: 1403.

33. Davis J, Cribbs DH, Cotman CW, Van Nostrand WE (1999) Pathogenic amyloid beta-protein induces apoptosis in cultured human cerebrovascular smooth muscle cells. Amyloid 6: 157-164.

34. Decoteau WE, McElvaine D, Smolentzov L, Kesner RP (2009) Effects of rodent prefrontal lesions on object-based, visual scene memory. Neurobiol Learn Mem 92: 552-558.

35. Dell'Acqua ML, Carroll RC, Peralta EG (1993) Transfected m2 muscarinic acetylcholine receptors couple to G alpha i2 and G alpha i3 in Chinese hamster ovary cells. Activation and desensitization of the phospholipase C signaling pathway. J Biol Chem 268: 5676-5685.

36. Destexhe A, Sejnowski TJ (2003) Interactions between membrane conductances underlying thalamocortical slow-wave oscillations. Physiol Rev 83: 1401-1453.

37. Detari L (2000) Tonic and phasic influence of basal forebrain unit activity on the cortical EEG. Behav Brain Res 115: 159-170.

38. Detari L, Rasmusson DD, Semba K (1997a) Phasic relationship between the activity of basal forebrain neurons and cortical EEG in urethane-anesthetized rat. Brain Res 759: 112-121.

39. Detari L, Rasmusson DD, Semba K (1999) The role of basal forebrain neurons in tonic and phasic activation of the cerebral cortex. Prog Neurobiol 58: 249-277.

40. Detari L, Semba K, Rasmusson DD (1997b) Responses of cortical EEG-related basal forebrain neurons to brainstem and sensory stimulation in urethane-anaesthetized rats. Eur J Neurosci 9: 1153-1161.

41. Detari L, Vanderwolf CH (1987) Activity of identified cortically projecting and other basal forebrain neurones during large slow waves and cortical activation in anaesthetized rats. Brain Res 437: 1-8.

42. Drachman DA, Leavitt J (1972) Memory impairment in the aged: storage versus retrieval deficit. J Exp Psychol 93: 302-308.

43. Dringenberg HC, Vanderwolf CH (1997) Neocortical activation: modulation by multiple pathways acting on central cholinergic and serotonergic systems. Exp Brain Res 116: 160-174.

44. Dunbar JC, Ergene E, Anderson GF, Barraco RA (1992) Decreased cardiorespiratory effects of neuropeptide Y in the nucleus tractus solitarius in diabetes. Am J Physiol 262: R865-R871.

45. Dunnett SB, Nathwani F, Brasted PJ (1999) Medial prefrontal and neostriatal lesions disrupt performance in an operant delayed alternation task in rats. Behav Brain Res 106: 13-28.

46. Duque A, Balatoni B, Detari L, Zaborszky L (2000) EEG correlation of the discharge properties of identified neurons in the basal forebrain. J Neurophysiol 84: 1627-1635.

47. Duque A, Tepper JM, Detari L, Ascoli GA, Zaborszky L (2007) Morphological characterization of electrophysiologically and immunohistochemically identified basal forebrain cholinergic and neuropeptide Y-containing neurons. Brain Struct Funct 212: 55-73.

48. Eggermann E, Serafin M, Bayer L, Machard D, Saint-Mleux B, Jones BE, Muhlethaler M (2001) Orexins/hypocretins excite basal forebrain cholinergic neurones. Neuroscience 108: 177-181.

49. Elul R (1971) The genesis of the EEG. Int Rev Neurobiol 15: 227-272.

50. Esclapez M, Houser CR (1995) Somatostatin neurons are a subpopulation of GABA neurons in the rat dentate gyrus: evidence from colocalization of pre-prosomatostatin and glutamate decarboxylase messenger RNAs. Neuroscience 64: 339-355.

51. Farris TW, Butcher LL, Oh JD, Woolf NJ (1995) Trophic-factor modulation of cortical acetylcholinesterase reappearance following transection of the medial cholinergic pathway in the adult rat. Exp Neurol 131: 180-192.

52. Farris TW, Woolf NJ, Oh JD, Butcher LL (1993) Reestablishment of laminar patterns of cortical acetylcholinesterase activity following axotomy of the medial cholinergic pathway in the adult rat. Exp Neurol 121: 77-92.

53. Forloni G, Hohmann C, Coyle JT (1990) Developmental expression of somatostatin in mouse brain. I. Immunocytochemical studies. Brain Res Dev Brain Res 53: 6-25.

54. Francis PT, Palmer AM, Snape M, Wilcock GK (1999) The cholinergic hypothesis of Alzheimer's disease: a review of progress. J Neurol Neurosurg Psychiatry 66: 137-147.

55. Franke H, Schelhorn N, Illes P (2003) Dopaminergic neurons develop axonal projections to their target areas in organotypic co-cultures of the ventral mesencephalon and the striatum/prefrontal cortex. Neurochem Int 42: 431-439.

56. Fremeau RT, Jr., Troyer MD, Pahner I, Nygaard GO, Tran CH, Reimer RJ, Bellocchio EE, Fortin D, Storm-Mathisen J, Edwards RH (2001) The expression of vesicular glutamate transporters defines two classes of excitatory synapse. Neuron 31: 247-260.

57. Freund TF, Antal M (1988) GABA-containing neurons in the septum control inhibitory interneurons in the hippocampus. Nature 336: 170-173.

58. Freund TF, Meskenaite V (1992) gamma-Aminobutyric acid-containing basal forebrain neurons innervate inhibitory interneurons in the neocortex. Proc Natl Acad Sci U S A 89: 738-742.

59. Frick KM, Kim JJ, Baxter MG (2004) Effects of complete immunotoxin lesions of the cholinergic basal forebrain on fear conditioning and spatial learning. Hippocampus 14: 244-254.

60. Fujiyama F, Furuta T, Kaneko T (2001) Immunocytochemical localization of candidates for vesicular glutamate transporters in the rat cerebral cortex. J Comp Neurol 435: 379-387.

61. Fuster JM (1997) Network memory. Trends Neurosci 20: 451-459.

62. Fuster JM (2002) Frontal lobe and cognitive development. J Neurocytol 31: 373-385.

63. Gabbott PL, Warner TA, Jays PR, Salway P, Busby SJ (2005) Prefrontal cortex in the rat: projections to subcortical autonomic, motor, and limbic centers. J Comp Neurol 492: 145-177.

64. Gallyas F, Wolff JR, Bottcher H, Zaborszky L (1980a) A reliable and sensitive method to localize terminal degeneration and lysosomes in the central nervous system. Stain Technol 55: 299-306.

65. Gallyas F, Wolff JR, Bottcher H, Zaborszky L (1980b) A reliable method for demonstrating axonal degeneration shortly after axotomy. Stain Technol 55: 291-297.

66. Gallyas F, Zaborszky L, Wolff JR (1980c) Experimental studies of mechanisms involved in methods demonstrating axonal and terminal degeneration. Stain Technol 55: 281-290.

67. Gaykema RP, van Weeghel R, Hersh LB, Luiten PG (1991) Prefrontal cortical projections to the cholinergic neurons in the basal forebrain. J Comp Neurol 303: 563-583.

68. Gaykema RP, Zaborszky L (1997) Parvalbumin-containing neurons in the basal forebrain receive direct input from the substantia nigra-ventral tegmental area. Brain Res 747: 173-179.

69. Geula C (1998) Abnormalities of neural circuitry in Alzheimer's disease: hippocampus and cortical cholinergic innervation. Neurology 51: S18-S29.

70. Geula C, Mesulam MM (1994) Cholinergic systems and related neuropathological predilection patterns in Alzheimer Disease. pp 263-291. Raven Press, New York.

71. Goedert M, Jakes R (2005) Mutations causing neurodegenerative tauopathies. Biochim Biophys Acta 1739: 240-250.

72. Goldman-Rakic PS (1994) Working memory dysfunction in schizophrenia. J Neuropsychiatry Clin Neurosci 6: 348-357.

73. Goldwater DS, Pavlides C, Hunter RG, Bloss EB, Hof PR, McEwen BS, Morrison JH (2009) Structural and functional alterations to rat medial prefrontal cortex following chronic restraint stress and recovery. Neuroscience.

74. Golmayo L, Nunez A, Zaborszky L (2003) Electrophysiological evidence for the existence of a posterior cortical-prefrontal-basal forebrain circuitry in modulating sensory responses in visual and somatosensory rat cortical areas. Neuroscience 119: 597-609.

75. Gorelova N, Yang CR (1997) The course of neural projection from the prefrontal cortex to the nucleus accumbens in the rat. Neuroscience 76: 689-706.

76. Gras C, Herzog E, Bellenchi GC, Bernard V, Ravassard P, Pohl M, Gasnier B, Giros B, El Mestikawy S (2002) A third vesicular glutamate transporter expressed by cholinergic and serotoninergic neurons. J Neurosci 22: 5442-5451.

77. Greenberg BD, Rauch SL, Haber SN (2009) Invasive Circuitry-Based Neurotherapeutics: Stereotactic Ablation and Deep Brain Stimulation for OCD. Neuropsychopharmacology.

78. Gritti I, Henny P, Galloni F, Mainville L, Mariotti M, Jones BE (2006) Stereological estimates of the basal forebrain cell population in the rat, including neurons containing choline acetyltransferase, glutamic acid decarboxylase or phosphate-activated glutaminase and colocalizing vesicular glutamate transporters. Neuroscience 143: 1051-1064.

79. Gritti I, Mainville L, Jones BE (1993) Codistribution of. J Comp Neurol 329: 438-457.

80. Gritti I, Mainville L, Jones BE (1994) Projections of GABAergic and cholinergic basal forebrain and GABAergic preoptic-anterior hypothalamic neurons to the posterior lateral hypothalamus of the rat. J Comp Neurol 339: 251-268.

81. Gritti I, Manns ID, Mainville L, Jones BE (2003) Parvalbumin, calbindin, or calretinin in cortically projecting and GABAergic, cholinergic, or glutamatergic basal forebrain neurons of the rat. J Comp Neurol 458: 11-31.

82. Groenewegen HJ, Berendse HW, Wolters JG, Lohman AH (1990) The anatomical relationship of the prefrontal cortex with the striatopallidal system, the thalamus and the amygdala: evidence for a parallel organization. Prog Brain Res 85: 95-116.

83. Groenewegen HJ, Wright CI, Uylings HB (1997) The anatomical relationships of the prefrontal cortex with limbic structures and the basal ganglia. J Psychopharmacol 11: 99-106.

84. Grossberg S, Bullock D, Dranias MR (2008) Neural dynamics underlying impaired autonomic and conditioned responses following amygdala and orbitofrontal lesions. Behav Neurosci 122: 1100-1125.

85. Gyengesi E, Zaborszky L, Detari L (2008) The effect of prefrontal stimulation on the firing of basal forebrain neurons in urethane anesthetized rat. Brain Res Bull 75: 570-580.

86. Haber SN, Wolfe DP, Groenewegen HJ (1990) The relationship between ventral striatal efferent fibers and the distribution of peptide-positive woolly fibers in the forebrain of the rhesus monkey. Neuroscience 39: 323-338.

87. Hajszan T, Alreja M, Leranth C (2004) Intrinsic vesicular glutamate transporter 2-immunoreactive input to septohippocampal parvalbumin-containing neurons: novel glutamatergic local circuit cells. Hippocampus 14: 499-509.

88. Hall AM, Moore RY, Lopez OL, Kuller L, Becker JT (2008) Basal forebrain atrophy is a presymptomatic marker for Alzheimer's disease. Alzheimers Dement 4: 271-279.

89. Hallanger AE, Wainer BH (1988) Ascending projections from the pedunculopontine tegmental nucleus and the adjacent mesopontine tegmentum in the rat. J Comp Neurol 274: 483-515.

90. Hassel B, Solyga V, Lossius A (2008) High-affinity choline uptake and acetylcholine-metabolizing enzymes in CNS white matter. A quantitative study. Neurochem Int 53: 193-198.

91. Heidbreder CA, Groenewegen HJ (2003) The medial prefrontal cortex in the rat: evidence for a dorso-ventral distinction based upon functional and anatomical characteristics. Neurosci Biobehav Rev 27: 555-579.

92. Hellstrom-Lindahl E (2000) Modulation of beta-amyloid precursor protein processing and tau phosphorylation by acetylcholine receptors. Eur J Pharmacol 393: 255-263.

93. Hendry SH, Jones EG, DeFelipe J, Schmechel D, Brandon C, Emson PC (1984) Neuropeptide-containing neurons of the cerebral cortex are also GABAergic. Proc Natl Acad Sci U S A 81: 6526-6530.

94. Henny P, Jones BE (2008) Projections from basal forebrain to prefrontal cortex comprise cholinergic, GABAergic and glutamatergic inputs to pyramidal cells or interneurons. Eur J Neurosci 27: 654-670.

95. Herzog E, Bellenchi GC, Gras C, Bernard V, Ravassard P, Bedet C, Gasnier B, Giros B, El Mestikawy S (2001) The existence of a second vesicular glutamate transporter specifies subpopulations of glutamatergic neurons. J Neurosci 21: RC181.

96. Hoover WB, Vertes RP (2007) Anatomical analysis of afferent projections to the medial prefrontal cortex in the rat. Brain Struct Funct 212: 149-179.

97. Horvath TL, Diano S, Tschop M (2004) Brain circuits regulating energy homeostasis. Neuroscientist 10: 235-246.

98. Houser CR, Crawford GD, Salvaterra PM, Vaughn JE (1985) Immunocytochemical localization of choline acetyltransferase in rat cerebral cortex: a study of cholinergic neurons and synapses. J Comp Neurol 234: 17-34.

99. Hur EE, Zaborszky L (2005) Vglut2 afferents to the medial prefrontal and primary somatosensory cortices: a combined retrograde tracing in situ hybridization. J Comp Neurol 483: 351-373.

100. Hurley KM, Herbert H, Moga MM, Saper CB (1991) Efferent projections of the infralimbic cortex of the rat. J Comp Neurol 308: 249-276.

101. Ikegaya Y, Aaron G, Cossart R, Aronov D, Lampl I, Ferster D, Yuste R (2004) Synfire chains and cortical songs: temporal modules of cortical activity. Science 304: 559-564.

102. Iraizoz I, de Lacalle S, Gonzalo LM (1991) Cell loss and nuclear hypertrophy in topographical subdivisions of the nucleus basalis of Meynert in Alzheimer's disease. Neuroscience 41: 33-40.

103. Irle E, Markowitsch HJ (1986) Afferent connections of the substantia innominata/basal nucleus of Meynert in carnivores and primates. J Hirnforsch 27: 343-367.

104. Jellinger K (1996) New developments in the pathology of Parkinson's disease. In Advances in neurology. pp 1-6. Plenum Press, New York.

105. Jimenez-Capdeville ME, Dykes RW, Myasnikov AA (1997) Differential control of cortical activity by the basal forebrain in rats: a role for both cholinergic and inhibitory influences. J Comp Neurol 381: 53-67.

106. Jones BE (2004) Activity, modulation and role of basal forebrain cholinergic neurons innervating the cerebral cortex. Prog Brain Res 145: 157-169.

107. Jones BE (2008) Modulation of cortical activation and behavioral arousal by cholinergic and orexinergic systems. Ann N Y Acad Sci 1129: 26-34.

108. Jourdain A, Semba K, Fibiger HC (1989) Basal forebrain and mesopontine tegmental projections to the reticular thalamic nucleus: an axonal collateralization and immunohistochemical study in the rat. Brain Res 505: 55-65.

109. Kasanetz F, Riquelme LA, Murer MG (2002) Disruption of the two-state membrane potential of striatal neurones during cortical desynchronisation in anaesthetised rats. J Physiol 543: 577-589.

110. Kenet T, Bibitchkov D, Tsodyks M, Grinvald A, Arieli A (2003) Spontaneously emerging cortical representations of visual attributes. Nature 425: 954-956.

111. Kihara M, Nishikawa S, Nakasaka Y, Tanaka H, Takahashi M (2001) Autonomic consequences of brainstem infarction. Auton Neurosci 86: 202-207.

112. Kiss J, Borhegyi Z, Csaky A, Szeiffert G, Leranth C (1997) Parvalbumin-containing cells of the angular portion of the vertical limb terminate on calbindin-immunoreactive neurons located at the border between the lateral and medial septum of the rat. Exp Brain Res 113: 48-56.

113. Kisvarday ZF, Gulyas A, Beroukas D, North JB, Chubb IW, Somogyi P (1990) Synapses, axonal and dendritic patterns of GABA-immunoreactive neurons in human cerebral cortex. Brain 113 (Pt 3): 793-812.

114. Koenigs M, Grafman J (2009) The functional neuroanatomy of depression: distinct roles for ventromedial and dorsolateral prefrontal cortex. Behav Brain Res 201: 239-243.

115. Kohler C, Eriksson LG (1984) An immunohistochemical study of somatostatin and neurotensin positive neurons in the septal nuclei of the rat brain. Anat Embryol (Berl) 170: 1-10.

116. Kolb B (1984) Functions of the frontal cortex of the rat: a comparative review. Brain Res 320: 65-98.

117. Kosaka T, Wu JY, Benoit R (1988) GABAergic neurons containing somatostatin-like immunoreactivity in the rat hippocampus and dentate gyrus. Exp Brain Res 71: 388-398.

118. Kosik KS, Joachim CL, Selkoe DJ (1986) Microtubule-associated protein tau (tau) is a major antigenic component of paired helical filaments in Alzheimer disease. Proc Natl Acad Sci U S A 83: 4044-4048.

119. Launer LJ, Andersen K, Dewey ME, Letenneur L, Ott A, Amaducci LA, Brayne C, Copeland JR, Dartigues JF, Kragh-Sorensen P, Lobo A, Martinez-Lage JM, Stijnen T, Hofman A (1999) Rates and risk factors for dementia and Alzheimer's disease: results from EURODEM pooled analyses. EURODEM Incidence Research Group and Work Groups. European Studies of Dementia. Neurology 52: 78-84.

120. Lee MG, Hassani OK, Alonso A, Jones BE (2005) Cholinergic basal forebrain neurons burst with theta during waking and paradoxical sleep. J Neurosci 25: 4365-4369.

121. Levey AI, Hallanger AE, Wainer BH (1987) Cholinergic nucleus basalis neurons may influence the cortex via the thalamus. Neurosci Lett 74: 7-13.

122. Lightman SL (2008) The neuroendocrinology of stress: a never ending story. J Neuroendocrinol 20: 880-884.

123. Likhtik E, Pelletier JG, Popescu AT, Pare D (2006) Identification of basolateral amygdala projection cells and interneurons using extracellular recordings. J Neurophysiol 96: 3257-3265.

124. Liposits Z, Setalo G, Flerko B (1984) Application of the silver-gold intensified 3,3'-diaminobenzidine chromogen to the light and electron microscopic detection of the luteinizing hormone-releasing hormone system of the rat brain. Neuroscience 13: 513-525.

125. Luczak A, Bartho P, Marguet SL, Buzsaki G, Harris KD (2007) Sequential structure of neocortical spontaneous activity in vivo. Proc Natl Acad Sci U S A 104: 347-352.

126. Magill PJ, Bolam JP, Bevan MD (2000) Relationship of activity in the subthalamic nucleus-globus pallidus network to cortical electroencephalogram. J Neurosci 20: 820-833.

127. Manns ID, Alonso A, Jones BE (2000) Discharge properties of juxtacellularly labeled and immunohistochemically identified cholinergic basal forebrain neurons recorded in association with the electroencephalogram in anesthetized rats. J Neurosci 20: 1505-1518.

128. Manns ID, Alonso A, Jones BE (2003) Rhythmically discharging basal forebrain units comprise cholinergic, GABAergic, and putative glutamatergic cells. J Neurophysiol 89: 1057-1066.

129. Manns ID, Mainville L, Jones BE (2001) Evidence for glutamate, in addition to acetylcholine and GABA, neurotransmitter synthesis in basal forebrain neurons projecting to the entorhinal cortex. Neuroscience 107: 249-263.

130. Mao BQ, Hamzei-Sichani F, Aronov D, Froemke RC, Yuste R (2001) Dynamics of spontaneous activity in neocortical slices. Neuron 32: 883-898.

131. Margolis EB, Lock H, Hjelmstad GO, Fields HL (2006) The ventral tegmental area revisited: is there an electrophysiological marker for dopaminergic neurons? J Physiol 577: 907-924.

132. Mascagni F, McDonald AJ (2003) Immunohistochemical characterization of cholecystokinin containing neurons in the rat basolateral amygdala. Brain Res 976: 171-184.

133. Massimini M, Huber R, Ferrarelli F, Hill S, Tononi G (2004) The sleep slow oscillation as a traveling wave. J Neurosci 24: 6862-6870.

134. McCormick DA, Shu Y, Hasenstaub A, Sanchez-Vives M, Badoual M, Bal T (2003) Persistent cortical activity: mechanisms of generation and effects on neuronal excitability. Cereb Cortex 13: 1219-1231.

135. McGinty D, Szymusiak R (1990) Keeping cool: a hypothesis about the mechanisms and functions of slow-wave sleep. Trends Neurosci 13: 480-487.

136. McKenna JT, Vertes RP (2004) Afferent projections to nucleus reuniens of the thalamus. J Comp Neurol 480: 115-142.

137. Mesulam MM (1986) Frontal cortex and behavior. Ann Neurol 19: 320-325.

138. Mesulam MM (2004) The cholinergic innervation of the human cerebral cortex. Prog Brain Res 145: 67-78.

139. Mesulam MM, Mufson EJ (1984) Neural inputs into the nucleus basalis of the substantia innominata (Ch4) in the rhesus monkey. Brain 107 (Pt 1): 253-274.

140. Mesulam MM, Mufson EJ, Levey AI, Wainer BH (1984) Atlas of cholinergic neurons in the forebrain and upper brainstem of the macaque based on monoclonal

choline acetyltransferase immunohistochemistry and acetylcholinesterase histochemistry. Neuroscience 12: 669-686.

141. Mesulam MM, Mufson EJ, Wainer BH, Levey AI (1983) Central cholinergic pathways in the rat: an overview based on an alternative nomenclature (Ch1-Ch6). Neuroscience 10: 1185-1201.

142. Mesulam MM, Van Hoesen GW, Pandya DN, Geschwind N (1977) Limbic and sensory connections of the inferior parietal lobule (area PG) in the rhesus monkey: a study with a new method for horseradish peroxidase histochemistry. Brain Res 136: 393-414.

143. Miettinen RA, Kalesnykas G, Koivisto EH (2002) Estimation of the total number of cholinergic neurons containing estrogen receptor-alpha in the rat basal forebrain. J Histochem Cytochem 50: 891-902.

144. Miller EK, Cohen JD (2001) An integrative theory of prefrontal cortex function. Annu Rev Neurosci 24: 167-202.

145. Momiyama T, Zaborszky L (2006) Somatostatin presynaptically inhibits both GABA and glutamate release onto rat basal forebrain cholinergic neurons. J Neurophysiol 96: 686-694.

146. MORUZZI G, Magoun HW (1949) Brain stem reticular formation and activation of the EEG. Electroencephalogr Clin Neurophysiol 1: 455-473.

147. Nambu T, Sakurai T, Mizukami K, Hosoya Y, Yanagisawa M, Goto K (1999) Distribution of orexin neurons in the adult rat brain. Brain Res 827: 243-260.

148. Nogueiras R, Tschop MH, Zigman JM (2008) Central nervous system regulation of energy metabolism: ghrelin versus leptin. Ann N Y Acad Sci 1126: 14-19.

149. Nunez A (1996) Unit activity of rat basal forebrain neurons: relationship to cortical activity. Neuroscience 72: 757-766.

150. Ongur D, Price JL (2000) The organization of networks within the orbital and medial prefrontal cortex of rats, monkeys and humans. Cereb Cortex 10: 206-219.

151. Orgogozo JM, Gilman S, Dartigues JF, Laurent B, Puel M, Kirby LC, Jouanny P, Dubois B, Eisner L, Flitman S, Michel BF, Boada M, Frank A, Hock C (2003) Subacute meningoencephalitis in a subset of patients with AD after Abeta42 immunization. Neurology 61: 46-54.

152. Pang K, Tepper JM, Zaborszky L (1998) Morphological and electrophysiological characteristics of noncholinergic basal forebrain neurons. J Comp Neurol 394: 186-204.

153. Parent M, Descarries L (2008) Acetylcholine innervation of the adult rat thalamus: distribution and ultrastructural features in dorsolateral geniculate, parafascicular, and reticular thalamic nuclei. J Comp Neurol 511: 678-691.

154. Paxinos G, Watson CR, Emson PC (1980) AChE-stained horizontal sections of the rat brain in stereotaxic coordinates. J Neurosci Methods 3: 129-149.

155. Peralta EG, Winslow JW, Peterson GL, Smith DH, Ashkenazi A, Ramachandran J, Schimerlik MI, Capon DJ (1987) Primary structure and biochemical properties of an M2 muscarinic receptor. Science 236: 600-605.

156. Perry EK (1993) Cholinergic transmitter and neurotrophic activities in Lewy body dementia: similarity to Parkinson's and distinction from Alzheimer disease. Alzheimer Dis. assoc. Disord.

157. Perry EK, Marshall EF, Blessed G, Tomlinson BE, Perry RH (1983) Decreased imipramine binding in the brains of patients with depressive illness. Br J Psychiatry 142: 188-192.

158. Prensa L, Richard S, Parent A (2003) Chemical anatomy of the human ventral striatum and adjacent basal forebrain structures. J Comp Neurol 460: 345-367.

159. Preuss TM, Goldman-Rakic PS (1991) Myelo- and cytoarchitecture of the granular frontal cortex and surrounding regions in the strepsirhine primate Galago and the anthropoid primate Macaca. J Comp Neurol 310: 429-474.

160. Qiu C, Kivipelto M, von Strauss E (2009) Epidemiology of Alzheimer's disease: occurrence, determinants, and strategies toward intervention. Dialogues Clin Neurosci 11: 111-128.

161. Rasmusson DD, Clow K, Szerb JC (1994) Modification of neocortical acetylcholine release and electroencephalogram desynchronization due to brainstem stimulation by drugs applied to the basal forebrain. Neuroscience 60: 665-677.

162. Ribak CE, Roberts RC (1990) GABAergic synapses in the brain identified with antisera to GABA and its synthesizing enzyme, glutamate decarboxylase. J Electron Microsc Tech 15: 34-48.

163. Rigas P, Castro-Alamancos MA (2007) Thalamocortical Up states: differential effects of intrinsic and extrinsic cortical inputs on persistent activity. J Neurosci 27: 4261-4272.

164. Rigas P, Castro-Alamancos MA (2009) Impact of persistent cortical activity (up States) on intracortical and thalamocortical synaptic inputs. J Neurophysiol 102: 119-131.

165. Robinson MJ, Edwards SE, Iyengar S, Bymaster F, Clark M, Katon W (2009) Depression and pain. Front Biosci 14: 5031-5051.

166. Rolls ET, Baylis GC, Hasselmo ME, Nalwa V (1989) The effect of learning on the face selective responses of neurons in the cortex in the superior temporal sulcus of the monkey. Exp Brain Res 76: 153-164.

167. ROSE JE, WOOLSEY CN (1948a) Structure and relations of limbic cortex and anterior thalamic nuclei in rabbit and cat. J Comp Neurol 89: 279-347.

168. ROSE JE, WOOLSEY CN (1948b) The orbitofrontal cortex and its connections with the mediodorsal nucleus in rabbit, sheep and cat. Res Publ Assoc Res Nerv Ment Dis 27 (1 vol.): 210-232.

169. Rubio A, Perez M, Avila J (2006) Acetylcholine receptors and tau phosphorylation. Curr Mol Med 6: 423-428.

170. Rye DB, Wainer BH, Mesulam MM, Mufson EJ, Saper CB (1984) Cortical projections arising from the basal forebrain: a study of cholinergic and noncholinergic components employing combined retrograde tracing and immunohistochemical localization of choline acetyltransferase. Neuroscience 13: 627-643.

171. Rylett RJ, Schmidt BM (1993) Regulation of the synthesis of acetylcholine. Prog Brain Res 98: 161-166.

172. Sanchez-Vives MV, McCormick DA (2000) Cellular and network mechanisms of rhythmic recurrent activity in neocortex. Nat Neurosci 3: 1027-1034.

173. Sarter M, Parikh V (2005) Choline transporters, cholinergic transmission and cognition. Nat Rev Neurosci 6: 48-56.

174. Schliebs R, Arendt T (2006) The significance of the cholinergic system in the brain during aging and in Alzheimer's disease. J Neural Transm 113: 1625-1644.

175. Semba K (2000) Multiple output pathways of the basal forebrain: organization, chemical heterogeneity, and roles in vigilance. Behav Brain Res 115: 117-141.

176. Sesack SR, Deutch AY, Roth RH, Bunney BS (1989) Topographical organization of the efferent projections of the medial prefrontal cortex in the rat: an anterograde tract-tracing study with Phaseolus vulgaris leucoagglutinin. J Comp Neurol 290: 213-242.

177. Shepherd C, McCann H, Halliday GM (2009) Variations in the neuropathology of familial Alzheimer's disease. Acta Neuropathol 118: 37-52.

178. Shipp S (2007) Structure and function of the cerebral cortex. Curr Biol 17: R443-R449.

179. Shu Y, Hasenstaub A, Badoual M, Bal T, McCormick DA (2003) Barrages of synaptic activity control the gain and sensitivity of cortical neurons. J Neurosci 23: 10388-10401.

180. Silver R, Lesauter J (2008) Circadian and homeostatic factors in arousal. Ann N Y Acad Sci 1129: 263-274.

181. Sim JA, Allen TG (1998) Morphological and membrane properties of rat magnocellular basal forebrain neurons maintained in culture. J Neurophysiol 80: 1653-1669.

182. Simon MI, Strathmann MP, Gautam N (1991) Diversity of G proteins in signal transduction. Science 252: 802-808.

183. Smith CB, Bowen DM (1976) Soluble proteins in normal and diseased human brain. J Neurochem 27: 1521-1528.

184. Somogyi P, Hodgson AJ, Smith AD, Nunzi MG, Gorio A, Wu JY (1984) Different populations of GABAergic neurons in the visual cortex and hippocampus of cat contain somatostatin- or cholecystokinin-immunoreactive material. J Neurosci 4: 2590-2603.

185. Steriade M (1993) Sleep oscillations in corticothalamic neuronal networks and their development into self-sustained paroxysmal activity. Rom J Neurol Psychiatry 31: 151-161.

186. Steriade M (1999) Brainstem activation of thalamocortical systems. Brain Res Bull 50: 391-392.

187. Szentgyorgyi V, Balatoni B, Toth A, Detari L (2006) Effect of cortical spreading depression on basal forebrain neurons. Exp Brain Res 169: 261-265.

188. Szymusiak R, Alam N, McGinty D (2000) Discharge patterns of neurons in cholinergic regions of the basal forebrain during waking and sleep. Behav Brain Res 115: 171-182.

189. Szymusiak R, McGinty D (1986) Sleep-related neuronal discharge in the basal forebrain of cats. Brain Res 370: 82-92.

190. Takamori S, Moriyama Y (2003) [Vesicular glutamate transporter and glutamatergic signaling]. Tanpakushitsu Kakusan Koso 48: 1816-1823.

191. Takamori S, Riedel D, Jahn R (2000) Immunoisolation of GABA-specific synaptic vesicles defines a functionally distinct subset of synaptic vesicles. J Neurosci 20: 4904-4911.

192. Tamamaki N, Yanagawa Y, Tomioka R, Miyazaki J, Obata K, Kaneko T (2003) Green fluorescent protein expression and colocalization with calretinin,

parvalbumin, and somatostatin in the GAD67-GFP knock-in mouse. J Comp Neurol 467: 60-79.

193. Timofeev I, Grenier F, Steriade M (2001) Disfacilitation and active inhibition in the neocortex during the natural sleep-wake cycle: an intracellular study. Proc Natl Acad Sci U S A 98: 1924-1929.

194. Tinsley CJ (2009) Creating abstract topographic representations: implications for coding, learning and reasoning. Biosystems 96: 251-258.

195. Toth A, Gyengesi E, Zaborszky L, Detari L (2008) Interaction of slow cortical rhythm with somatosensory information processing in urethane-anesthetized rats. Brain Res 1226: 99-110.

196. Toth A, Hajnik T, Zaborszky L, Detari L (2007) Effect of basal forebrain neuropeptide Y administration on sleep and spontaneous behavior in freely moving rats. Brain Res Bull 72: 293-301.

197. Toth A, Zaborszky L, Detari L (2005) EEG effect of basal forebrain neuropeptide Y administration in urethane anaesthetized rats. Brain Res Bull 66: 37-42.

198. Traub RD, Whittington MA, Colling SB, Buzsaki G, Jefferys JG (1996) Analysis of gamma rhythms in the rat hippocampus in vitro and in vivo. J Physiol 493 (Pt 2): 471-484.

199. Tseng KY, Kasanetz F, Kargieman L, Riquelme LA, Murer MG (2001) Cortical slow oscillatory activity is reflected in the membrane potential and spike trains of striatal neurons in rats with chronic nigrostriatal lesions. J Neurosci 21: 6430-6439.

200. Tsuboi Y, Dickson DW (2005) Dementia with Lewy bodies and Parkinson's disease with dementia: are they different? Parkinsonism Relat Disord 11 Suppl 1: S47-S51.

201. Tucek S (1985) Regulation of acetylcholine synthesis in the brain. J Neurochem 44: 11-24.

202. Tucek S (1990) The synthesis of acetylcholine: twenty years of progress. Prog Brain Res 84: 467-477.

203. Uusisaari M, Obata K, Knopfel T (2007) Morphological and electrophysiological properties of GABAergic and non-GABAergic cells in the deep cerebellar nuclei. J Neurophysiol 97: 901-911.

204. Valassi E, Scacchi M, Cavagnini F (2008) Neuroendocrine control of food intake. Nutr Metab Cardiovasc Dis 18: 158-168.

205. Vanderwolf CH, Harvey GC, Leung LW (1987) Transcallosal evoked potentials in relation to behavior in the rat: effects of atropine, p-chlorophenylalanine, reserpine, scopolamine and trifluoperazine. Behav Brain Res 25: 31-48.

206. Varga C, Hartig W, Grosche J, Keijser J, Luiten PG, Seeger J, Brauer K, Harkany T (2003) Rabbit forebrain cholinergic system: morphological characterization of nuclei and distribution of cholinergic terminals in the cerebral cortex and hippocampus. J Comp Neurol 460: 597-611.

207. Venter JC (1983) Muscarinic cholinergic receptor structure. Receptor size, membrane orientation, and absence of major phylogenetic structural diversity. J Biol Chem 258: 4842-4848.

208. Vertes RP (2004) Differential projections of the infralimbic and prelimbic cortex in the rat. Synapse 51: 32-58.

209. Vincent SR, McIntosh CH, Buchan AM, Brown JC (1985) Central somatostatin systems revealed with monoclonal antibodies. J Comp Neurol 238: 169-186.

210. Vogels OJ, Broere CA, ter Laak HJ, ten Donkelaar HJ, Nieuwenhuys R, Schulte BP (1990) Cell loss and shrinkage in the nucleus basalis Meynert complex in Alzheimer's disease. Neurobiol Aging 11: 3-13.

211. Wang CC, Shyu BC (2004) Differential projections from the mediodorsal and centrolateral thalamic nuclei to the frontal cortex in rats. Brain Res 995: 226-235.

212. Washburn MS, Moises HC (1992) Electrophysiological and morphological properties of rat basolateral amygdaloid neurons in vitro. J Neurosci 12: 4066-4079.

213. Whitehouse PJ, Price DL, Struble RG, Clark AW, Coyle JT, Delon MR (1982a) Alzheimer's disease and senile dementia: loss of neurons in the basal forebrain. Science 215: 1237-1239.

214. Whitehouse PJ, Struble RG, Clark AW, Price DL (1982b) Alzheimer disease: plaques, tangles, and the basal forebrain. Ann Neurol 12: 494.

215. Wilson CJ, Kawaguchi Y (1996) The origins of two-state spontaneous membrane potential fluctuations of neostriatal spiny neurons. J Neurosci 16: 2397-2410.

216. Woolf NJ, Butcher LL (1985) Cholinergic systems in the rat brain: II. Projections to the interpeduncular nucleus. Brain Res Bull 14: 63-83.

217. Woolf NJ, Butcher LL (1986) Cholinergic systems in the rat brain: III. Projections from the pontomesencephalic tegmentum to the thalamus, tectum, basal ganglia, and basal forebrain. Brain Res Bull 16: 603-637.

218. Woolf NJ, Eckenstein F, Butcher LL (1984) Cholinergic systems in the rat brain: I. projections to the limbic telencephalon. Brain Res Bull 13: 751-784.

219. Wu CK, Hersh LB, Geula C (2000) Cyto- and chemoarchitecture of basal forebrain cholinergic neurons in the common marmoset (Callithrix jacchus). Exp Neurol 165: 306-326.

220. Wu M, Zaborszky L, Hajszan T, van den Pol AN, Alreja M (2004) Hypocretin/orexin innervation and excitation of identified septohippocampal cholinergic neurons. J Neurosci 24: 3527-3536.

221. Xie SX, Ewbank DC, Chittams J, Karlawish JH, Arnold SE, Clark CM (2009) Rate of decline in Alzheimer disease measured by a Dementia Severity Rating Scale. Alzheimer Dis Assoc Disord 23: 268-274.

222. Yan Z, Feng J (2004) Alzheimer's disease: interactions between cholinergic functions and beta-amyloid. Curr Alzheimer Res 1: 241-248.

223. Yufu F, Egashira T, Yamanaka Y (1994) Age-related changes of cholinergic markers in the rat brain. Jpn J Pharmacol 66: 247-255.

224. Yuste R, MacLean JN, Smith J, Lansner A (2005) The cortex as a central pattern generator. Nat Rev Neurosci 6: 477-483.

225. Zaborszky L (1989) Afferent connections of the forebrain cholinergic projection neurons, with special reference to monoaminergic and peptidergic fibers. EXS 57: 12-32.

226. Zaborszky L, Buhl DL, Pobalashingham S, Bjaalie JG, Nadasdy Z (2005) Three-dimensional chemoarchitecture of the basal forebrain: spatially specific association of cholinergic and calcium binding protein-containing neurons. Neuroscience 136: 697-713.

227. Zaborszky L, Carlsen J, Brashear HR, Heimer L (1986) Cholinergic and GABAergic afferents to the olfactory bulb in the rat with special emphasis on the projection neurons in the nucleus of the horizontal limb of the diagonal band. J Comp Neurol 243: 488-509.

228. Zaborszky L, Cullinan WE (1992) Projections from the nucleus accumbens to cholinergic neurons of the ventral pallidum: a correlated light and electron microscopic double-immunolabeling study in rat. Brain Res 570: 92-101.

229. Zaborszky L, Cullinan WE (1996) Direct catecholaminergic-cholinergic interactions in the basal forebrain. I. Dopamine-beta-hydroxylase- and tyrosine hydroxylase input to cholinergic neurons. J Comp Neurol 374: 535-554.

230. Zaborszky L, Duque A (2000) Local synaptic connections of basal forebrain neurons. Behav Brain Res 115: 143-158.

231. Zaborszky L, Duque A (2003) Sleep-wake mechanisms and basal forebrain circuitry. Front Biosci 8: d1146-d1169.

232. Zaborszky L, Gaykema RP, Swanson DJ, Cullinan WE (1997) Cortical input to the basal forebrain. Neuroscience 79: 1051-1078.

233. Zaborszky L, Hoemke L, Mohlberg H, Schleicher A, Amunts K, Zilles K (2008) Stereotaxic probabilistic maps of the magnocellular cell groups in human basal forebrain. Neuroimage 42: 1127-1141.

234. Zaborszky L, Leranth C, Makara GB, Palkovits M (1975) Quantitative studies on the supraoptic nucleus in the rat. II. Afferent fiber connections. Exp Brain Res 22: 525-540.

235. Zaborszky L, Pang K, Somogyi J, Nadasdy Z, Kallo I (1999) The basal forebrain corticopetal system revisited. Ann N Y Acad Sci 877: 339-367.

236. Zarow C, Lyness SA, Mortimer JA, Chui HC (2003) Neuronal loss is greater in the locus coeruleus than nucleus basalis and substantia nigra in Alzheimer and Parkinson diseases. Arch Neurol 60: 337-341.